

THE GLOBAL COASTAL OCEAN

INTERDISCIPLINARY
REGIONAL STUDIES AND SYNTHESSES

Edited by

ALLAN R. ROBINSON

Harvard University

and

KENNETH H. BRINK

Woods Hole Oceanographic Institution

THE SEA

**Ideas and Observations on Progress in the Study
of the Seas**

Volume 14

Harvard University Press
Cambridge, MA and London

THE SEA

Ideas and Observations on Progress in the Study of the Seas

EDITORIAL BOARD

ALLAN R. ROBINSON, *Editor-in-Chief, Harvard University*

EDWARD A. BOYLE, *Massachusetts Institute of Technology*

KENNETH H. BRINK, *Woods Hole Oceanographic Institution*

KLAUS F. HASSELMANN, *Max-Planck-Institut für Meteorologie*

JAMES J. MCCARTHY, *Harvard University*

I. NICHOLAS MCCAVE, *University of Cambridge*

BRIAN J. ROTHSCHILD, *University of Massachusetts, Dartmouth*

Copyright ©2005 The President and Fellows of Harvard College

All rights reserved

Printed in the United States of America.

Published with the financial assistance of UNESCO/IOC.

Library of Congress Cataloging-in-Publication Data

Robinson, Allan R.

The Sea: Ideas and Observations on Progress in the Study of Seas

Volume 14. Interdisciplinary Regional Studies and Syntheses

Allan R. Robinson and Kenneth H. Brink

Includes bibliographic information and index.

1. Oceanography 2. Submarine geology

ISBN: 0-674-01527-4

Library of Congress catalog card number: TK

Chapter 32. THE PHYSICAL, SEDIMENTARY AND ECOLOGICAL STRUCTURE AND VARIABILITY OF SHELF AREAS IN THE MEDITERRANEAN SEA (27,S)

N. PINARDI AND M. ZAVATARELLI

University of Bologna, Corso di Scienze Ambientali, Ravenna, Italy

E. ARNERI

ISMAR-CNR, Ancona, Italy

A. CRISE

Istituto nazionale di oceanografia e geofisica sperimentale, Trieste, Italy

M. RAVAIOLI

ISMAR-CNR, Bologna, Italy

Contents

1. Introduction
 2. The shelf scales of the Mediterranean
 3. Sedimentary structures in the shelf areas
 4. The physical shelf regimes and the meteorological forcing
 5. Open ocean-shelf areas coupling
 6. Pelagic ecosystem functioning in the Mediterranean Sea shelf areas
 7. Exploitation of fisheries resources in the shelf areas
 8. Final remarks
- Bibliography

1. Introduction

The article reviews the most recent findings on the interdisciplinary characteristics of the Mediterranean Sea shelf areas, from the Northern to the southern shelf regions. First of all a classification of the shelves is carried out in terms of shelf extension, sedimentary and physical flow field properties. Secondly, the ecosystem functioning in the pelagic compartment is described as a function of the hydrodynamic regimes, as well as in relationship to land derived river inputs, if present.

The shelf ecosystem is analysed up to the level of fish stocks and recruitment, making connections with lower trophic level dynamics and physical conditions.

The aim is to start a phenomenological and methodological synthesis toward the understanding of the coupled physical, sedimentary and ecological processes in the Mediterranean shelf areas. In order to do so, the physical, sedimentary and ecological subsystems are reviewed for several shelf system study cases. The main aim is to discuss in these subsystems the coupling between physical-chemical-biological and sedimentary processes at the level of ecosystem functionality in the Mediterranean Sea coastal areas. The main time scale of interest is the seasonal that captures the largest changes in amplitude for all the system state variables.

Six different shelf regimes are chosen to describe the characteristics of the processes present in the Mediterranean shelves. We selected two northern shelves, the Gulf of Lions and the Northern Adriatic Sea and three in the south, the Algerian, Egyptian and Israeli shelves. In addition, we describe the Sicily Strait that represents an extended shelf area without any relevant river input and with distinct characteristics from the other sites since it is a large channel area that allows the exchange of water masses between the Eastern and Western Mediterranean sub-basins.

2. The shelf scales of the Mediterranean

The shelf areas of the world ocean as well as the Mediterranean are characterized first of all by their morphological extension, the connection with the land derived inputs and the open ocean currents. The land-derived inputs are determined by the flow rate or river runoff that is strongly forced by precipitation. Thus the shelf extension and the precipitation regimes are the background environmental factors that will allow a first classification of the Mediterranean shelf areas. In the following we will describe the shelf extension and the hydrological cycle of the Mediterranean Sea with the aim of classifying the main characteristics of the Mediterranean shelf areas on the basis of these two basic environmental field variables.

2.1 *Shelves of the basin*

The Mediterranean shelf areas are represented by a bathymetric chart in Fig. 1a. In this picture the 200 meters isobath has been chosen to define the seaward boundary of the continental shelf. The geographical names are shown in Fig.1b for future reference. Analysing Fig. 1a the impression is that the Mediterranean shelf areas are mainly narrow bands around deep basins. However, Manzella (1992) reports a shelf relative extension of 20% in Mediterranean against 7.6% for the World Ocean which is confirmed by our new computations. Thus shelf dynamics is relatively more important in the Mediterranean than in the rest of the world ocean.

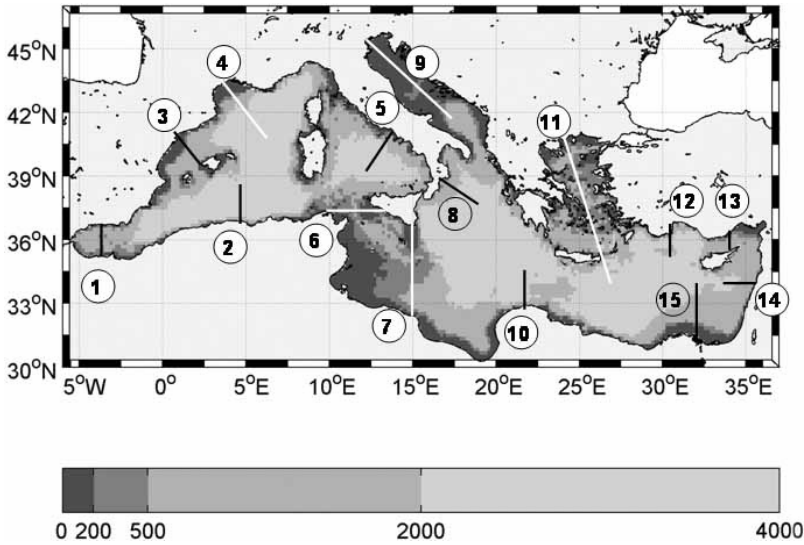


Figure 32.1a Shelf areas are indicated by different grey colors indicated in the palette. The numbers indicate 15 transects that are used to compute the topographic slopes in Table 1.

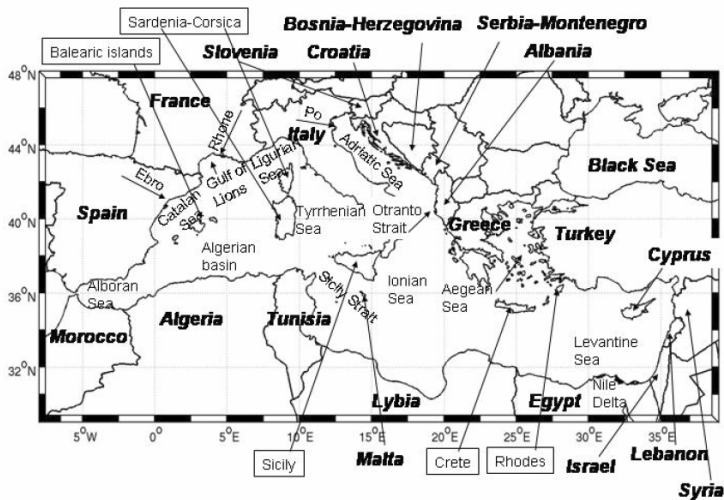


Figure 32.1b The coastlines and political geography of the Mediterranean Sea together with the major Sea names.

Taking as a reference Fig. 1a, it is evident that the major differences in shelf extension are between the northern and southern shores. The narrow and steep shelves of the Moroccan, Algerian and Libyan coasts contrast with the relatively extended shelves of the northern regions. There are exceptions to this north-south rule: for the northern coasts, narrow shelves are found along part of the Turkish coasts, in the Aegean Sea, in the Ligurian Strait and the northern Alboran Sea. In the

southern coasts, extended shelves are found in the Tunisian shelf and near the Nile Delta. However, the Tunisian shelves are part of the Sicily Strait, which is an exception to many rules, as we will discuss later. Other very narrow shelves are along the eastern sides of the Mediterranean sub-basins, such as the Israeli and Syrian coasts, as well as the eastern part of the Aegean, the Adriatic Sea and the Tyrrhenian Sea.

The island's shelves are exceptions to a north-south rule. Most of them, are connected to the mainland by the 500 meters isobath. The islands shelves are different mainly between the western and eastern Mediterranean sub-basins. Eastern islands are dominated by narrow shelves (Crete and Cyprus) while more extended shelves are found in the western Mediterranean islands (Mallorca, Corsica and Sardinia). Moreover for the island of Sardinia, shelves are more extended on the western than the eastern side.

We continue our classification of the shelf areas by looking at the different topographic gradients of the shelves. We calculated such gradients along fifteen transects indicated in Fig. 1a and results are presented in Table 1.

TABLE 32.1

The topographic gradients along the 15 transects depicted in Fig. 1a in (km/km) and the approximate distance from the coast of the sea-ward limit of the continental shelf, chosen to be the 200 meters contour isobath. Some transects connect two continental boundaries and then two different shelf extensions and gradients are calculated and the transect number is repeated.

| Transect name | Shelf gradient (km/km) | Shelf extension from coasts in km | Comments |
|----------------|---------------------------|--------------------------------------|---|
| 1-Morocco | 1.7E-01 | 20-30 | |
| 1-Spain | 4.2E-02 | 10-20 | |
| 2-Algeria | 5.2E-01 | 10-20 | |
| 3-Spain | 6.2E-02 | 50-60 | |
| 3-Mallorca | 5.4E-02 | 10-20 | |
| 4-France | 7.4E-02 | 70-80 | |
| 5-Italy | 1.0E-01 | 10-20 | |
| 6-Tunisia | 4.7E-02 | 110-120 | This shelf area contains a 'deep pit' |
| 6-Italy | 4.9E-02 | 30-40 | |
| 7-Libya | 1.1E-01 | 10-20 | |
| 7-Italy | 1.5E-02 | 140-150 | |
| 8-Italy | 1.7E-01 | 10-20 | |
| 9-Italy | 7.0E-03 | 330-340 | This shelf area is considered without the middle Adriatic |
| 9-Italy | 1.1E-02 | 520-530 | This shelf area contains the pits of the middle Adriatic |
| 10-Libya/Egypt | 3.2E-01 | 10-20 | |
| 11-Greece | 8.0E-02 | 40-50 | |
| 12-Turkey | 1.8E-01 | 10-20 | |
| 13-Turkey | 1.8E-01 | 10-20 | |
| 13-Cyprus | not determined | < 10 | |
| 14-Israel | not determined | < 10 | |
| 15-Egypt | 4.7E-02 | 70-80 | |

The gradient values are calculated with a grid spacing of 10 km along the transects and then an average value is obtained for each shelf transect. Most regions of Table 1 have shelves extending only for 10–30 km from land (12 shelves out of 20 contained in the 15 transects) with gradients exceeding 0.01 (km/km). The wide shelf areas extend from 30 to 150 km offshore and they are all directly connected to major river runoffs (Spanish-Catalan coast, the Gulf of Lions region, the Adriatic, the Northern Aegean Sea, the Nile coastal area) except for the Sicily Strait. The Adriatic Sea is an exception since its shelf can be considered to extend for about 500 km along the longitudinal axis of the basin with an interruption due to the presence of the Middle Adriatic depressions (about 250 meters deep and located in Fig. 2 at about 320 km from the northern end of the Adriatic). The shelf break practically occurs between the Middle and the Southern Adriatic, as we will see later.

In Fig. 2 we show some of the transects of Fig. 1a that are chosen as study cases for the present investigation. The narrow shelves of the Israeli and Algerian coasts are similar in shape to each other (for this reason, we have shown only transect 2, the Algerian transect), while the extended shelves are different and supposedly they are affected by very different physical, sedimentological and ecosystem processes.

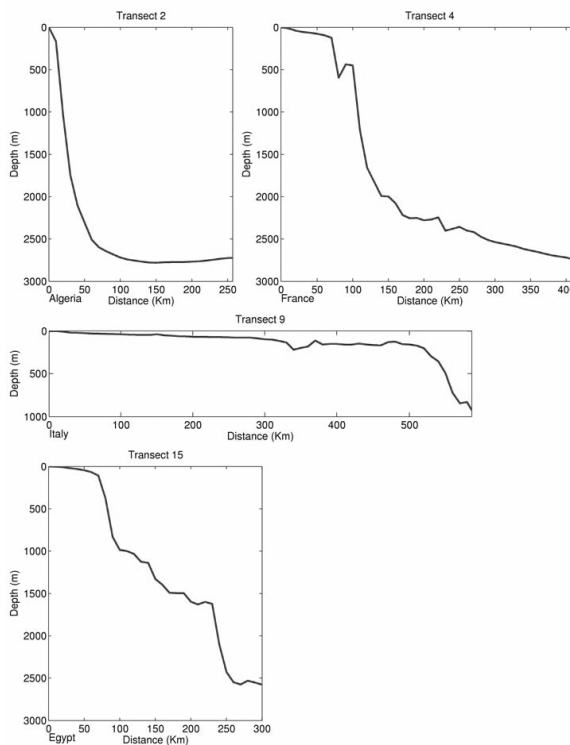


Figure 32.2 The topographic slope along the four transects: 2 (Algerian), 4 (Gulf of Lions), 9 (Adriatic) and 15 (Egypt).

The concept of narrow shelves has been recently reviewed by Sanchez-Arcilla and Simpson (2002). They postulate that ‘narrow shelves may be regarded as regions constrained by two “boundary layers” (one in the near-shore and the other on the slope) that merge and control processes across the continental shelf’. They also add that ‘in narrow shelves, therefore, the near-shore and slope processes effectively couple these regions to the shelf dynamics, while in the wide shelf areas the three areas will behave in a more uncoupled manner’. Sanchez-Arcilla and Simmons (2002) note that the nonlinear coupling between near-shore and slope processes can be large when the local Rossby number becomes larger than a threshold value, let’s say:

$$Ro = \frac{U}{f_o L} > 0.1$$

where L is the shelf width, f_o is the Coriolis parameter and U is the along slope current amplitude.

Supposing that everywhere in the Mediterranean the along slope currents are of the order of $20-30 \frac{cm}{s}$, $f_o \approx 1 \cdot 10^{-4} s^{-1}$, the critical shelf width for strong nonlinear coupling between near-shore and slope processes is:

$$L < 10 \frac{U}{f_o} = [20-30] km \quad (1)$$

Thus all the narrow shelves described in Table 1 with extensions less than 20–30 km are narrow from both a morphological and a dynamical point of view. Sanchez-Arcilla and Simpson (2002) classified the Ebro river shelf area as a mixture of narrow and extended shelves. Our transect 3, shown in Fig. 1a and Table 1, falls between the two chosen by Sanchez-Arcilla and Simpson (2002) and it is defined an ‘extended shelf area’.

To conclude this section we show in Fig. 3 the Sicily Strait transects 6 and 7 since they are very peculiar. The westernmost transect contains two deep troughs that allow the intermediate waters of the Eastern Mediterranean to propagate westward. In addition, on the Tunisian side of the Strait the shelf break is interrupted by a distinct trough that is occupied by the current flowing eastward, carrying waters of Atlantic origin. Thus the continental shelf areas of Tunisia and Sicily in the transect 6 are well separated and different in character even though they are both extended. The easternmost transect of Fig. 3 shows the steep continental shelf break and narrow shelf on the Libyan side, which partially confirms the rule that southern shelves are steeper than northern ones also in the Sicily Strait. The Italian side of the same transect has an extended shelf area partially connected to the Malta island shelf. In conclusion, the Sicily Strait offers a complex shelf area scenario, with the continental shelf interrupted by deep troughs and a unique, very extended shelf area on the Tunisian side of the Strait.

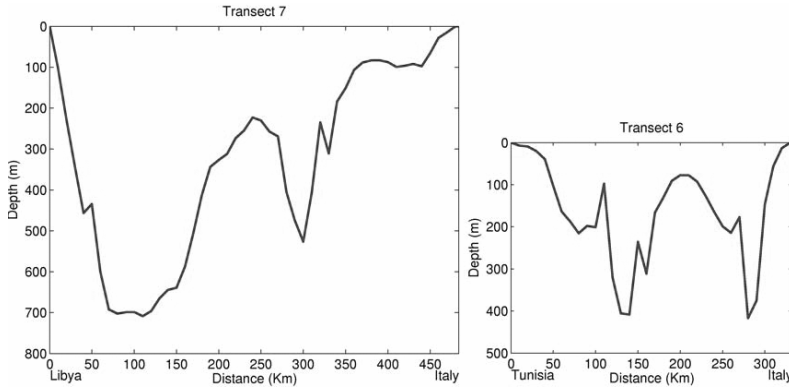


Figure 32.3 The topography along transects 7 (left panel) and 6 (right panel) delimiting the Sicily Strait.

2.2 Hydrological cycle of the basin

As noted before, most of the extended shelf areas have relevant river runoff inputs. Thus, to initially characterize the shelf areas, we need to concentrate on the hydrological cycle of the Mediterranean basin. The difference between the northern and southern shelf characteristics will be expressed here in terms of precipitation regimes over the Mediterranean wide area. The precipitation regime over land in turn determines the river runoff and by consequence the shelf sedimentary structure and composition. The area in which precipitation is analyzed encompasses the river catchments excluding the Nile catchment that extends further south of 25°N, in the tropical African wind belt.

The hydrological cycle in the Mediterranean area has been studied extensively in the eighties (Peixoto et al., 1982) and a very recent study has revisited the hydrological balance of the Mediterranean from recent meteorological data sets (Mariotti et al., 2002, hereafter called MSZL).

MSZL revisited the various components of the hydrological cycle focusing on the ocean-atmosphere branch. In Fig. 4 we show the large latitudinal gradient in precipitation from the NCEP 50 years re-analysis data set (Kalnay et al., 1996). The precipitation latitudinal gradient is more evident during the summer months while during winter the precipitation maxima are centred on the sea, always embedded in a positive northward gradient.

MSZL computed a new evaporation (E) minus precipitation (P) budget from the NCEP re-analyses, giving a range of $E - P = [603 - 699] \frac{mm}{yr}$ for the entire

Mediterranean Sea. This is somewhat lower than published before from the data in the sixties and seventies, due to decadal variability connected to NAO. MSZL discuss the precipitation-NAO teleconnection and find significant correlations between the precipitation regime over the Mediterranean and the NAO index, as we will discuss later.

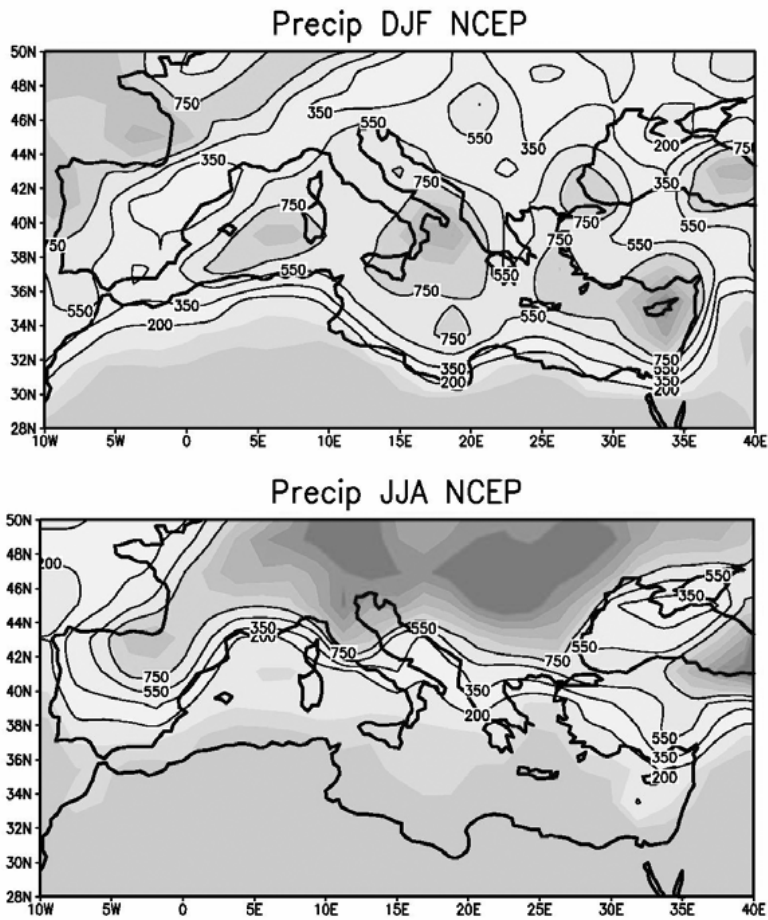


Figure 32.4 The climatological precipitation over the Mediterranean area computed by MSZL from the NCEP re-analysis data set. Upper panel: the December-January-February -DJF mean, lower panel: the June -July -August -JJA mean (units mm yr^{-1}).

The Runoff (R) time mean budget for the Mediterranean is connected to the precipitation regime and it can be deduced considering the following steady state balance:

$$R = E - P - G - B \quad (2)$$

where G is the net Gibraltar inflow and B is the Black Sea inflow and R the total runoff in the basin. Considering $B = 75 \frac{\text{mm}}{\text{yr}}$ (corresponding to a net inflow of $6 \cdot 10^3 \frac{\text{m}^3}{\text{s}}$ assuming an area of $2.5 \cdot 10^{12} \text{m}^2$ as in MSZL) and $G = 500 \frac{\text{mm}}{\text{yr}}$ (or $G = 0.04 Sv$) we obtain the range

$$R = [28 - 124] \frac{mm}{yr} \quad (3a)$$

or

$$R = [2200 - 9800] \frac{m^3}{s} \quad (3b)$$

for the two extreme values of E-P range estimated by MSZL.

MSZL does not include a detailed breakdown of the land hydrological budget in terms of river runoff but they take a basin mean runoff value of 100 mm/yr or equivalently $8 \cdot 10^3 \frac{m^3}{s}$ which is well within our estimate (3b). This contribution is

about 10% of the value of precipitation and evaporation but it is important during spring, becoming relatively comparable to the E-P budget. It is interesting to note that the traditional value for the runoff given by Anati and Gat (1989) is quite

larger, of the order of $14 \cdot 10^3 \frac{m^3}{s}$ but the source of these estimates is unknown.

Recently, Struglia et al. (2004) revisited the river discharges into the Mediterranean Sea, utilizing different historical data sets. Keeping in mind all the possible shortcomings of these data sets, their total annual discharge estimate is

$8 \cdot 110^3 \frac{m^3}{s}$ which is within the limits of our indirect calculation. Boukthir and

Barnier (2000) give a value of $11 \cdot 10^3 \frac{m^3}{s}$ using a different data set. Thus we can

say that the uncertainty in the river discharge coming from the best existing data sets is of several thousands of $\frac{m^3}{s}$.

The distribution of runoff for the climatology (January and May) is given in Fig. 5. All the northern rivers have a late winter-spring and autumn maximum discharge regime connected to the ice-snow melting cycle and the precipitation maxima during autumn (not shown). The pattern of runoff magnifies the north-south gradient already seen in the precipitation pattern but the quality of data for the runoff is more questionable. In our data set, all the African and the Middle East rivers are absent. Struglia et al. (2004) show instead that the Northern African

rivers plus the Middle East rivers can account for $2.4 \cdot 10^3 \frac{m^3}{s}$ about 25% of the

total runoff. They however include a Nile runoff ($1.2 \cdot 10^3 \frac{m^3}{s}$) that is much larger

than the one we show in Table 2 based upon more recent data. They also document a much smaller influence of Adriatic rivers except the Po, because they do not consider the Croatian rivers and Albanian rivers that could account for a large part of the fresh water discharge in the Adriatic Sea (Raicich, 1996).

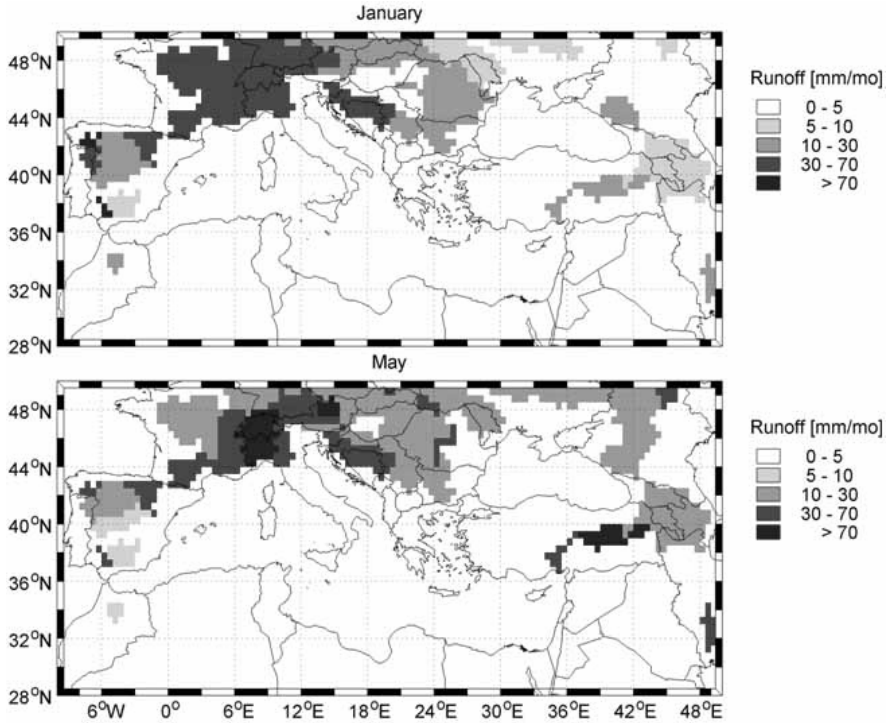


Figure 32.5 January and May mean observed runoff values from <http://www.gdrc.sr.unh.edu> (units mm mo^{-1}).

The annual mean runoffs by the major rivers and areas are reported in Table 2 for future reference. We use the largest estimate of the Adriatic river runoff by Raicich (1996) but our conclusions will not be changed by using a smaller estimate. The overall runoff budget (3b) can be made up for its largest part by summing solely the major rivers localized along the northern coasts (the Ebro, the Rhone, the Po, the other Adriatic rivers, the northern Aegean rivers). This result is also confirmed by Struglia et al. (2004): they show that European continental discharges can account for over 75% of the annual runoff budget.

A particular attention has to be put in the Nile runoff that has been totally regulated by the Aswan dam and it is now lower than other river runoffs. The sedimentary remnants of the present interglacial period Nile runoff form the present day extended Egyptian continental shelf. The same sedimentary remnants could be also present in the Tunisian shelf where there is evidence that, between 9 and 7 thousand years ago, there was higher precipitation due to stronger teleconnections with the Arctic Oscillation Index (Arz et al., 2003), which supposedly gave rise to high runoff along the northern African coastal areas.

TABLE 32.2
The major Mediterranean rivers and areas runoff values
(major is considered to be a runoff greater than $100 \frac{m^3}{s}$).

| River | Mean annual runoff (m^3/s) | Reference |
|-----------------------------|--------------------------------|---|
| Ebro | 150 | Cruzado et al., 2002 |
| Rhone | 1690 | http://www.grdc.sr.unh.edu |
| Po | 1585 | Raicich (1994) |
| All other Adriatic rivers | 4091 | Raicich(1994) |
| Northern Aegean rivers | 515 | Kourafalou et al. (2003) |
| Nile | 110 | Hamza(2003) |
| All other Nile Delta runoff | 430 | Hamza(2003) |
| Total | 8571 | |

Struglia et al. (2004) document the seasonal changes in the annual mean runoff that amount to $5 \cdot 10^3 \frac{m^3}{s}$ with minimum values reached during July-August-September for all the rivers except the Nile, which is now totally regulated. This large seasonal variability is a major forcing of the Mediterranean coastal areas, which has profound influences on the shelf dynamics.

If we consider the NAO-precipitation correlation and variability, MSZL estimate that the E-P budget could vary on a decadal frequency by $100 \frac{mm}{yr}$ which is of

the same order of magnitude of the mean runoff value deduced before from the steady state budget calculation (3a). The NAO index (Hurrell, 1995) exhibits a large negative correlation with precipitation over the Mediterranean region on interannual and decadal time scales (MSZL compute a correlation coefficient of -0.84). This means that the decadal/interannual variability of the sedimentary and ecosystem dynamics in the shelf areas of the Mediterranean, dominated by runoff regimes, can be as large as the seasonal variability. On interannual time scales, Josey (2003) computes that changes in the E-P budget can be one order of magnitude less than the decadal changes. These E-P changes are mainly due to precipitation variability, which in turn will affect the river runoff.

Another remarkable result about precipitation variability is that a systematic increase in winter droughts, all over Italy has been documented by Brunetti et al. (2000). The proportion of dry days has increased by almost 50% with respect to the previous 30 years average (see Fig. 5 of Brunetti et al., 2000). The change has been abrupt from the beginning of the 80's until the end of 2000. This means that the river regimes have also changed, especially for large river catchment systems such the Ebro, Rhone and Po.

Struglia et al. (2004) discuss directly the runoff variability correlated with the NAO index. It is found that several rivers are significantly anti-correlated with NAO winter index and they loose the anti-correlation going toward spring and

summer. They also argue that this anti-correlation is strictly related to the anti-correlation of precipitation with NAO. Struglia et al. (2004) compute then the changes in discharge due to the constant increase of the NAO index from the middle of the '70s to the '90s computing a decrease in total discharge in the basin of about $1.7 \cdot 10^3 \frac{m^3}{s}$ which is 17% percent of the winter mean budget and that is concentrated on the Rhone, Ebro and Po rivers.

In conclusion, the atmospheric precipitation distribution determines the runoff budget of the basin that is determined for 75% or more of the total amount by the northern river discharges and the remaining by the runoff on the southern shores. Together with the shelf extension, this characterizes the overall structure of the Mediterranean shelf areas that mainly consists of narrow shelf areas without river runoff in the southern shores and extended shelf areas with runoff in the northern regions.

The river runoff spatial distribution could be also partially responsible for the surface chlorophyll latitudinal gradient: the northern shores are fertilized by the nutrient inputs (see section 6) and local chlorophyll maxima are established in every near-shore coastal area under river runoff influence (ROFI- areas or Region of Fresh Water Influence). As it can be seen in Fig. 6, the northern shores show higher chlorophyll concentrations with respect to the southern shores and local maxima appear near the northern river outflows. The other two local maxima, on the Tunisian and Egyptian shelves, are mainly connected to non-photosynthetic suspended matter.

Crispi et al. (2001) studied the longitudinal/latitudinal gradient in chlorophyll with a box model that demonstrated the importance of river loads in the maintenance of the chlorophyll gradient of Fig. 6. In particular, they point out that the western basin is generally more productive because it has larger nutrient inputs due to the presence of both the Ebro and Rhone river runoffs and the Gibraltar inflow. We argue here that this demonstrates an extremely active role played by the shelf regions of the basin on the biochemical fluxes of the basin, driving the large scale north-south gradients at the same level of importance of the Gibraltar inflow.

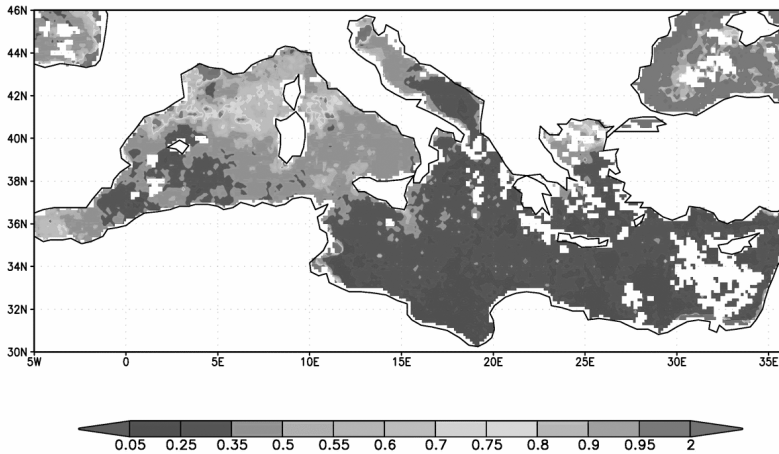


Figure 32.6 The SeaWiFS surface chlorophyll analysed for the winter of year 2000 (white areas are cloud covered).

3. Sedimentary structures in the shelf areas

Sediment processes on the shelf are heavily influenced by topographic structures such as slopes and canyons and by river runoff. Seasonal variations in the atmospheric forcing influence the marine currents on the shelf that are responsible for transferring the suspended particulate to the sediments. The sedimentation rate and the sediment composition depend on all these environmental factors. In this section, we will take a detailed look at sedimentary structures in the shelf areas identified here as case studies. In the western Mediterranean, we will consider the Algerian and Gulf of Lions continental shelves; in the central Mediterranean, the Adriatic and Sicilian shelves and in the eastern Mediterranean, the Nile Delta zone and the Israeli coasts.

3.1 *Gulf of Lions*

The continental margin of the North West Mediterranean is characterised by a relatively extended continental shelf (see section 2) with a well-defined edge at a depth of 100–200 m. The shelf is eroded by numerous undersea canyons. The principal sources of sediments are the main rivers, the Rhône and Ebro, and the atmosphere. The biogenic productivity of surface waters also plays a major role.

Holocene deposits in the Gulf of Lions can be divided into three separate zones according to their thickness. The first zone extends from the Rhône delta to the Têt (western side of the Gulf) and is characterised by large sediment accumulations with a thickness between 30 and 50 m (Got and Aloisi, 1990). The second zone covers a large part of the middle shelf and the thickness drops from 30 m to 5 m. The third zone occupies the outer shelf at a depth between 90 and 200 m and is characterised by thin Holocene deposits and outcrops of relict sand representing the coastline during the last phase of eustatic lowering, remoulded during the first phase of rising sea level (Figure 7a, Durrieu de Madron et al., 2000).

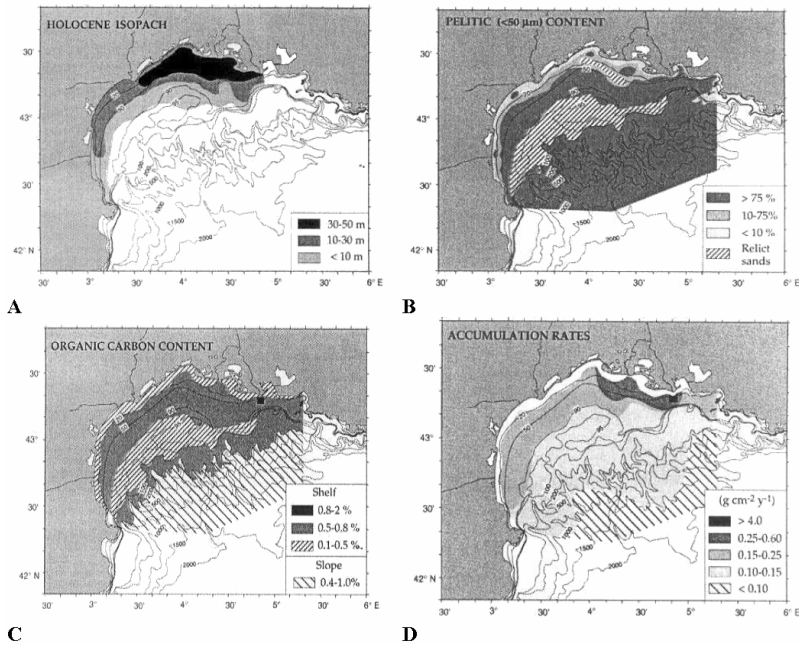


Figure 32.7 a Thickness of the Holocene sediments in the Gulf of Lions (Got and Aloisi, 1990). b Pelitic content in Holocene sediments in the Gulf of Lions (Got and Aloisi, 1990; Gensous et al., 1993). c Organic carbon content in Holocene sediments in the Gulf of Lions (Durrieu de Madron et al., 2000). d Accumulation rates in the Holocene sediments of the Gulf of Lions (Buscail and Germain, 1997; Durrieu de Madron et al., 2000; Zuo et al., 1991 and 1997).

3.1.1 Grain size

The grain size of the inner shelf sands decreases seawards, with the muds of the middle shelf occurring at a depth of about 20–30 m. There is, in fact, a correlation between grain size and the attenuated effect of wave motion seawards (Jago and Barousseau, 1981). The only exceptions are the prodelta deposits accumulating at river mouths and consisting predominantly of silty mud. These sediment accumulations are due to the fact that precipitation is large in the autumn and spring leading to a significant flow of terrigenous sediments into coastal marine environments. In this coastal environment, there is a high seasonal variation of geochemical parameters and discontinuities in the typical prodelta sediment sequence are due to physical-chemical rather than sedimentological variations. In the case of the river Têt, the surface layers of the prodelta deposits are silty (60 μm median) and poor in carbonates (5%) and organic carbon (0.5%). The sediment water content in the surface layer is high (45–50%), compared to about 30% in underlying layers. The grain size of the silt is graduated as a result of hydrodynamic effects, but a relationship between the intense bioturbation produced by a crustacean (Thalassinidean) and an increase in the coarser particle fraction has also been noted. In the spring, when this crustacean is excavating tunnels, the finer particles are eliminated in the overlying water, while the coarser particles accumulate in the tunnels (Buscail et

al., 1995). Deposits on the outer shelf and slope are predominantly pelitic (Figure 7b).

3.1.2 Organic carbon

The organic carbon content varies according to the type of sediments. It is generally low in the sandy deposits of the inner shelf (< 0.3%) and the relict sands (0.25–0.5%) (Buscail et al., 1995; Durrieu de Madron et al., 2000). In the muddy littoral deposits (between 40 and 100 meters depth) values remain low (0.4–0.6%) and drop to 0.3% in deep waters. The highest values are found in the muddy prodelta deposits with values between 1–2.2% (Figure 7c and Table 3).

TABLE 32.3

Figures indicating the organic carbon content in the delta zone of the principal rivers in the Gulf of Lions according to various authors.

| River | Organic carbon (%) | Notes | Reference |
|--------------|--------------------|---|--------------------------------|
| Aude | 1.1–1.4 | | Buscail et al., 1995 |
| Rhône | 1.1–1.6 | | Buscail et al., 1995 |
| | 1–2 | | Durrieu de Madron et al., 2000 |
| Têt | 2.17 | | Zuo et al., 1997 |
| | 0.5 | in autumn the deposits are enriched with organic carbon (2.5%), pelite (92%) and fine bioclastic carbonates (20%) | Buscail et al., 1995 |

The same variations occur for other trace elements, confirming that more than 90% of particulate matter coming from the rivers is deposited in the prodelta, shelf and slope zones, with only a small quantity transported into the basin through the canyons.

These hydrodynamically active prodelta environments demonstrate that carbon degradation predominates over burial. Land and sea sources are important, but 80% of the organic carbon flow is degraded at the interface on the continental shelf (Buscail et al., 1990).

3.1.3 Sedimentation and accumulation rates

It is difficult to determine the sedimentation rate because there are low gradients in the Pb activity profile of core samples taken at river mouths due to the rapid sediment deposition and mixing (Zuo et al., 1997). The sediments consist of silt, silty shale and shale and a linear dependence can be noted (with a correlation coefficient of $R=0.87$) between the sedimentation rate and depth. The sedimentation rate in the prodelta zone is very high and near the mouth of the river Rhône may reach a few centimetres per year ($5-9 \frac{\text{cm}}{\text{yr}}$). The same trend can be observed in the area of the Ebro and Têt rivers, although the sedimentation and mixing rates are lower as a result of the lower sediment transport (sedimentation rate in the Têt prodelta is estimated to be $0.1 \frac{\text{cm}}{\text{yr}}$, Courp and Monaco, 1990).

In the shelf zone, the sedimentation rate is between (10–60cm)/(100 years) (Zuo et al., 1991). The sedimentation rate enables the sediment accumulation to be estimated. For an area of 15340 km², the sediment accumulation is about 10 · 10⁶ ton/year. This estimate does not include prodelta areas. In prodelta areas, considering an area of 150 km², a sedimentation rate of 5–9 $\frac{\text{cm}}{\text{yr}}$ (see above) and a mean density of 1.60 $\frac{\text{g}}{\text{cm}^3}$, the accumulation rate amounts to 2–3 · 10⁶ ton/year (Zuo et al., 1997).

According to Durrieu de Madron et al. (2000) the mean accumulation rate at the Rhône mouth amounts to 40 $\frac{\text{g}}{\text{cm}^2 \text{ yr}}$. This value decreases rapidly seawards. In the distal part of the Rhône prodelta (20 km from the coast), the mean value is 0.4 $\frac{\text{g}}{\text{cm}^2 \text{ yr}}$. The values are even lower for the rest of the shelf with a mean of 0.15 $\frac{\text{g}}{\text{cm}^2 \text{ yr}}$. Figure 7d and Table 4 gives the accumulation rates from a number of authors. The discrepancies between the values in Table 4 are due to the fact that Zuo et al. consider the last 100 years, while Got and Aloisi consider the whole Holocene period (10,000 years), but the general sediment transport and deposition pattern is confirmed by both authors.

TABLE 32.4
Sedimentation rate and flows in the North West Mediterranean
according to various authors.

| Area | Sed. rate (cm/100years) | Flow (g/cm ²)/100years | Accumulation (10 ⁶ ton) | Reference |
|---|----------------------------|---------------------------------------|---------------------------------------|---------------------------|
| Gulf of Lions (15340 km²) | 7–41 | 5–31 | 10±4 | Zuo et al., 1991 and 1997 |
| NW Mediterranean (280000 km²): | | | | Zuo et al., 1997 |
| Shelf (10%) | 6 (2–12) | 4 | 11 | |
| Slope and basin | 1–2 | 0.9 | 23 | |
| Tot. | | | 34±15 | |
| NW Mediterranean (280000 km²): | | | | Got and Aloisi, 1990 |
| Shelf (10%) | | | | |
| Holocene deposits: (2.6 · 10 ⁻¹¹ m ³) | | | 44 | |
| Slope and basin | | | 20 | |
| Tot. | | | 64 | |

It is interesting to note that the Gulf of Lions, occupying just 5% of the total surface of the North West Mediterranean, represents about 30% of total sedimentation.

3.2 The Algerian continental shelf

The Algerian continental shelf is narrow (see section 2). In the bays and gulfs, the shelf extends for 10–20 km, such as in the Gulf of Oran, the Gulf of Arzew and the Gulf of Bône, where the edge of the shelf is located at a depth of 120 - 150 m.

Climatic and geodynamic variations during the Pliocene and Quaternary led to the temporal and spatial superimposition of two types of marine sediments; 1) autochthonous biogenic carbonate sediments deposited mainly during wet periods with abundant land plant cover and scarce rill erosion of continental zones; 2) allochthonous terrigenous sediments deposited during semi-arid periods such as the current African climate as a result of rill erosion of continental zones with scarce plant cover (Pauc, 1991). The carbonate sediments consist of silt and biogenic calcareous sands, composed mainly of bioclastic fragments, calcareous algae, bryozoans, pelecypods and gastropods (Caulet, 1972).

In the Gulf of Arzew, biogenic carbonates are distributed in the western part from Cape Carbon to the sea off Mostaganem. Towards the west, this facies is largely buried under more recent sediments (Figure 8a). Current terrigenous sediments come mainly from the River Chèliff, which drains silty and shaly debris. The finest fraction of these sediments ($<2\mu\text{m}$) is distributed towards the west under the influence of currents; the silty fraction ($>10\mu\text{m}$), is, on the other hand, distributed along the coastal belt at a depth of 40 m. The total organic carbon (TOC) content amounts to between 0.2 and 1.2% with the highest values occurring in the pelitic fraction (Figure 8b).

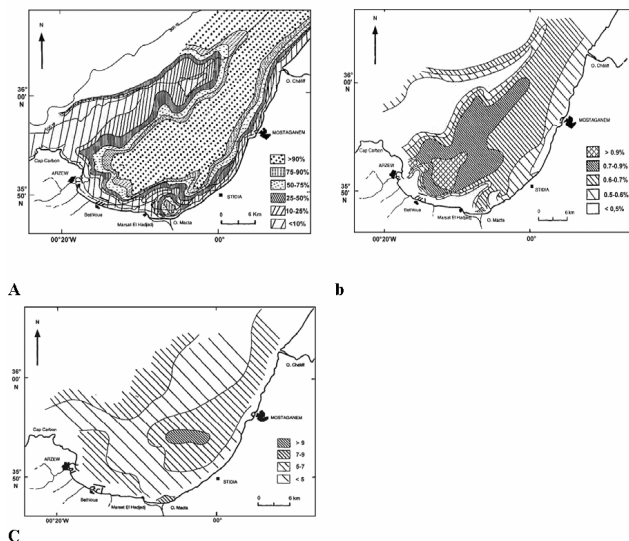


Figure 32.8 A) Pelite distribution in surface sediments in the Gulf of Arzew (South West Mediterranean) (Buscail et al., 1999). B) Total organic carbon distribution in surface sediments in the Gulf of Arzew (South West Mediterranean) (Buscail et al., 1999). C) Carbon/nitrogen (C/N) ratio distribution in surface sediments in the Gulf of Arzew (South West Mediterranean) (Buscail et al., 1999). Reprinted with permission.

The nitrogen content varies between 0.05 and 0.35% with the highest values occurring near the port of Arzew, and the lowest in the coarser sediments near Cape Carbon. The C/N ratio varies from 5 to 7 (figure 8c). In the fine fraction (<40 μ m) the ratio is slightly higher (Buscaïl et al., 1999). This ratio is indicative of the origin and the degree of evolution of organic material present in the sediment. Values of C/N < 6, found in these areas, indicate the presence of organic material of essentially marine origin (Monoley et al., 1991; Müller and Suess, 1979), although interpretation of the C/N ratio is somewhat delicate as nitrogen is more sensitive than carbon to degradation and a high ratio may thus also indicate the presence of degraded or already highly mineralised organic debris.

The same distribution, with the same facies, also occurs in the Bay of Algeri (Maouche, 1987). The TOC content (0.3–1.5), nitrogen values and C/N ratio are similar to those found in the Gulf of Arzew.

3.3 *Adriatic Sea*

The Adriatic itself is an epicontinental sea, in other words, a semi-closed basin within a continent. The eastern Adriatic coast is generally high and rocky, while the western coast is low and largely sandy. The northern part of the basin, by convention bounded to the south by the transect approximately at 43.5°N (see Fig. 9), is shallow, with a mean depth of 35 m and a slight slope (0.35 m km⁻¹) towards the south east (see section 2). The middle Adriatic is moderately deep [basin] (on average 140 m) with two depressions dropping down to 260 m. South of the depressions is the morphological elevation of the Pelagosa sill (see Fig. 9), oriented in a northeast – southwest direction and formed during the Quaternary. This represents really the shelf break for the Adriatic Sea. The south Adriatic extends south of the latitude of 42° N to the threshold of the Strait of Otranto and is characterised by a large depression more than 1,200 m deep (Fig. 9). Exchange of waters with the Mediterranean Sea occurs through the Strait of Otranto with a threshold of 800m.

Sediment dynamics forces a distribution of the coarser sediments close to the coasts and the formation of a band of fine sediment accumulation approximately parallel to the coast further offshore (Wang and Pinardi, 2002). Outward from the coasts, there are outcrops of relict sands from the Versilia transgression (Flandrian) covering a large part of the shelf with an irregular morphology inherited from the sub-aerial environment of the last ice age. A large number of rivers flow into the Adriatic, transporting suspended material. Of particular importance are the river Po in the northern basin and the group of Albanian rivers in the southern basin.

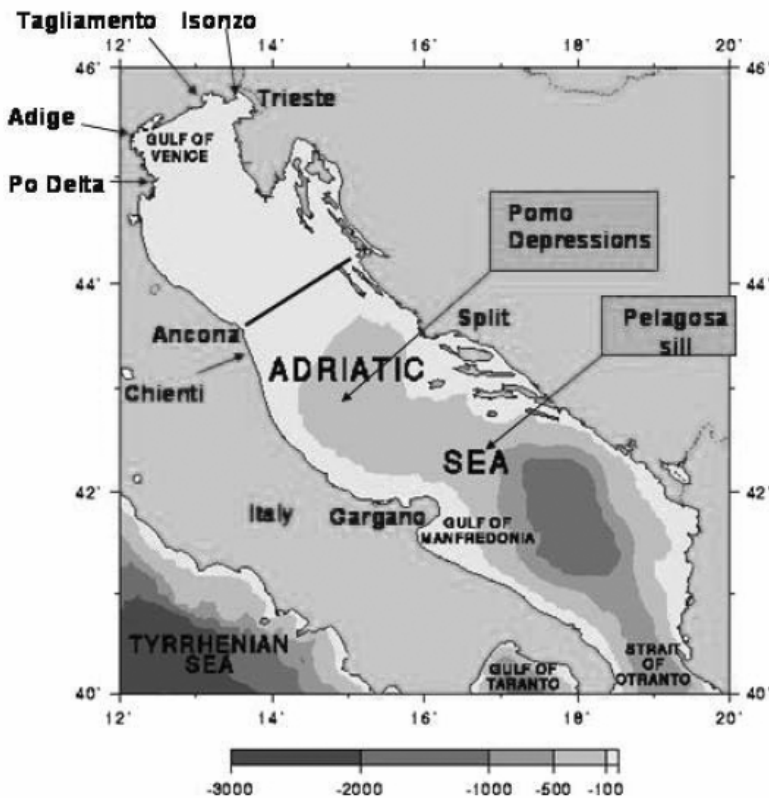


Figure 32.9 The Adriatic Sea geometry and bathymetry. The transect indicate the approximate limit of the Northern Adriatic Sea.

3.3.1 Sedimentation and accumulation rates

In the area between the Gulf of Trieste and the Middle Adriatic, three zones can be identified on the basis of recent data on sedimentation rates ($\frac{cm}{yr}$) and accumulation rates ($\frac{g}{cm^2 yr}$), obtained using ^{137}Cs and ^{210}Pb (Table 5). For the southern Adriatic and in the western-central zone, Frignani and Langone (1991) and Frignani et al. (1996) report accumulation rates of $0.06 \frac{g}{cm^2 yr}$. The three northern and middle Adriatic areas are described below.

TABLE 32.5
Accumulation and sedimentation rates in the Adriatic Sea

| Area | Accumulation rates ($\frac{g}{cm^2 yr}$) | Sedimentation rate ($\frac{cm}{yr}$) | References |
|-------------------------------|--|--|--|
| Trieste-Adige Delta | | | |
| Isonzo mouth | | 8.2 | Frignani et al., 1990 |
| Tagliamento mouth | | 2.1 | Delfanti et al., 1994 |
| Gulf of Venice (15–20 m deep) | 0.45–1 | | Alvisi et al., 2000 |
| Adige prodelta (15–20 m deep) | 0.5>1.2 | | |
| Adige (20 m deep) | 0.8 | | Frignani et al., 1990 |
| Delta Po-Ancona | | | |
| Po di Levante-Po di Pila | | | |
| Depth: 7 m | 0.86–1.86 | | Frignani et al., 1990; 1989 |
| 20 m | 0.77 | | |
| 27 m | 0.22–0.48 | | |
| > 30 m | 0.3–0.4 | | |
| Depth: 5 m | 1.6 | | Alvisi et al., 2000 |
| 10 m | 0.3 | | |
| Punta Maestra (20 m deep) | | 2 | Frignani et al., 1990; 1989 |
| Po di Goro | | | |
| Depth: 14 m | 0.84 | | |
| 18 m | 1.8 | | |
| 21 m | 1.0 | | |
| 23 m | 0.37 | | |
| 24 m | 0.39–1.20 | | |
| Depth: 10 m | 0.8–1.5 | | Alvisi et al., 2000 |
| 20 m | 0.3–1.4 | | |
| <30 m | 0.4–1 | | |
| | 0.77 | | Frignani et al., 1996 |
| Porto Garibaldi | | | |
| Depth: 13 m | 0.26 | | Frignani et al., 1987 |
| 26 m | 0.39 | | Guerzoni et al., 1984 |
| Depth: 10–20 m | 0.3 | | Alvisi et al., 2000 |
| 20–30 m | 0.4 | | |
| Fiumi Uniti mouth (20 m deep) | 0.27 | | Frignani et al., 1987 Guerzoni et al., 1984 |
| Bevano mouth | | | |
| Depth: 14 m | 0.4 | | |
| 21 m | 0.31 | | |
| Rubicone mouth | | | |
| Depth: 9 m | 0.22 | | Giordani et al., 1992 |
| 12 m | 0.24 | | |
| 20 m | 0.22 | | |
| 24 m | 0.26 | | |
| 41 m | 0.28 | | |
| Depth: 10 m | 0.2–0.4 | | Alvisi et al., 2000 |
| <20 m | 0.2 | | |
| | 0.3 | | Frignani and Langone 1991 |
| Ancona-Gargano | | | |
| Chienti mouth | | | |
| Depth: 28 m | 0.52–0.8 | | |
| 62 m | 0.17 | | |
| 90 m | 0.07–0.08 | | |

TABLE 32.5 (*cont.*)
Accumulation and sedimentation rates in the Adriatic Sea

| | | |
|--------------------------------|------|--|
| Middle Adriatic deep | | Frignani et al., 1987 |
| Depth: 176 m | | Sorgente et al., 1996 |
| >200 m | 0.05 | |
| | 0.04 | |
| Central Adriatic | 0.12 | Frignani and Langone 1991; Frignani et al. 1996 |
| Southern Adriatic Basin | | |
| South Adriatic Pit | 0.06 | |

3.3.2 Northern Adriatic: Trieste—Adige Delta

Near the mouth of the river Isonzo (Fig. 9), the sedimentation rate is seasonally high, in fact, short lived radionuclide dating shows a speed of $8.2 \frac{cm}{yr}$ (Frignani et al., 1990). Near the Tagliamento (Fig. 9), there is a high seasonal sedimentation rate ($2.1 \frac{cm}{yr}$) (Alvisi et al., 2000; Delfanti et al., 1994) together with a low accumulation rate on century scale. It can be hypothesised that the difference is due to the erosive action of the currents. Off the mouth of the river Adige (Fig. 9), the accumulation rate amounts to $0.8 \frac{g}{cm^2 yr}$ (Frignani et al., 1990). Radiometric analysis indicates an absence of sedimentation in the sandy belt off the coast.

3.3.3 Po Delta—Ancona area

In the area off the Po Delta, there are high accumulation and sedimentation rates as the inflow of material from the hinterland is very high. Data in the literature (Frignani et al., 1989; 1990) confirm that the sedimentation rate decreases as the water becomes deeper. The sedimentation rate values drop rapidly moving from around the Po delta in the southward direction due to the current action that advects sediments along the coasts, away from the delta. South of the Po Delta, the values are lower and more or less constant (Frignani and Langone, 1991; Frignani et al., 1996). Off the coast of Emilia Romagna, the accumulation rate is below $0.5 \frac{g}{cm^2 yr}$ (Frignani et al., 1990; Guerzoni et al., 1984; Giordani et al., 1992). Recent studies of sediment resuspension and deposition due to the Po river delta runoff have established that the specific combination of wave and currents climate in the Adriatic determines the sediment deposition as a function of grain size along the western Adriatic coastlines (Wang and Pinardi, 2003).

3.3.4 Ancona-Gargano area

The area is characterised by extreme spatial and temporal variations in sedimentation. The greatest variability occurs in a land-sea direction and many parameters vary in bands parallel to the coast (Sorgente et al., 1996; Sorgente, 2002).

Off the mouth of the river Chienti, one of the rivers with the greatest solid flow in this section of coast ($2.2 \cdot 10^6 \frac{\text{ton}}{\text{yr}}$), accumulation rates decrease gradually as water depth increases, with a high seasonal sedimentation rate at some points. The characteristics at stations sampled in the Middle Adriatic depressions are similar, with shaly sedimentation from currents arriving from the north transporting fine material from the Padana Plain. Sedimentation rates amount to about $0.05 \frac{\text{g}}{\text{cm}^2 \text{yr}}$ at a depth of 176 m and $0.04 \frac{\text{g}}{\text{cm}^2 \text{yr}}$ at a depth of more than 200 m (Frignani et al., 1987; Sorgente et al., 1996).

3.3.5 Organic carbon

Data gathered during recent surveys indicate that the highest organic carbon values are found near the mouth of the Po river and in the Middle Adriatic depressions (Giordani et al., 2002 - Table 6). The Adriatic Sea is characterised by a nutrient concentration and primary productivity trend decreasing in the land-sea and north-south directions, in accordance with inflow from the land and hydrodynamic patterns. The quantity of organic carbon reaching the water-sediment interface amounts to 42–56% of primary productivity in the shallower zones of the northern shelf and about 25% further out in the deeper sea. On the southern shelf, values vary between 26% and 3%, from zones nearest the coast to the deeper areas. The majority of the organic material characterising the Adriatic sediments is of land origin, but the autochthonous biogenic fraction increases proceeding southwards. The C/N ratio, whose southward decrease reflects these variations, can be used as an indicator of the degree of preservation of sediments (Faganeli et al., 1994).

TABLE 32.6

Primary productivity and organic carbon data for a number of stations in the Adriatic Sea (Giordani et al., 2002, modified).

| Area | Station | Depth (m) | Primary productivity ($\text{gC m}^2 \text{year}^{-1}$) | OrgC (%) | C/N (at. ratio) |
|-----------------------------|--------------------------|-----------|---|----------|-----------------|
| North Adriatic | S3 (44°20.07'-12°39.95') | 30 | 216 | 0.85 | 6.7 |
| | S6 (43°42.20'-13°38.50') | 41 | | 0.93 | 7.9 |
| Middle Adriatic Depressions | P1 (42°51.00'-14°45.00') | 246 | 60 | 0.87 | 7.2 |
| Southern Adriatic Pit | A1 (41°50.74'-17°44.71') | 1196 | 97 | 0.65 | 7.9 |
| Strait of Otranto | O2 (39°49.72'-18°57.48') | 870 | 66 | 0.46 | 6.8 |
| Ionian sea | I1 (38°29.10'-17°59.27') | 2360 | 62 | 0.55 | 6.3 |

In areas with high sediment accumulation rates ($>0.1 \frac{\text{g}}{\text{cm}^2 \text{yr}}$), more than 50% of carbon produced is not oxidised and accumulates in the sediments, while in areas with a lower rate, only about 1% is conserved (Canfield, 1993). The Middle

Adriatic depression is a special case as, in addition to normal accumulation in the water column, there is also strong lateral transport from the more productive northern shelf (Hopkins et al., 1999).

3.4 The Sicilian-Tunisian Platform

The Strait of Sicily is characterised by various depositional environments (Fig. 10; Argnani, 1992; Bowles et al., 1992). The southern Sicilian shelf is characterised by the inflow of terrigenous material from the Atlantic Ionian Stream-AIS branch (see section 4) that forms a wedge of well-stratified sands and silty shale varying in thickness from about 5–6 metres near the coasts to almost zero at the edge of the shelf (Colantoni et al., 1985). An exception is the Adventure Bank (Fig. 10) characterised by a virtually flat surface with a mean depth of about 80–90 metres. It is isolated from the inflow of terrigenous material by the strong currents and deposition is therefore authigenic: 1) heterometric carbonate sands consisting mainly of the remains of organisms (bryozoans, red algae, serpulidae, foraminiferida, gastropods and corals) living in the extensive eelgrass and seaweed meadows and 2) fragments of biogenic concretions (coraligen) (Colantoni et al., 1985).

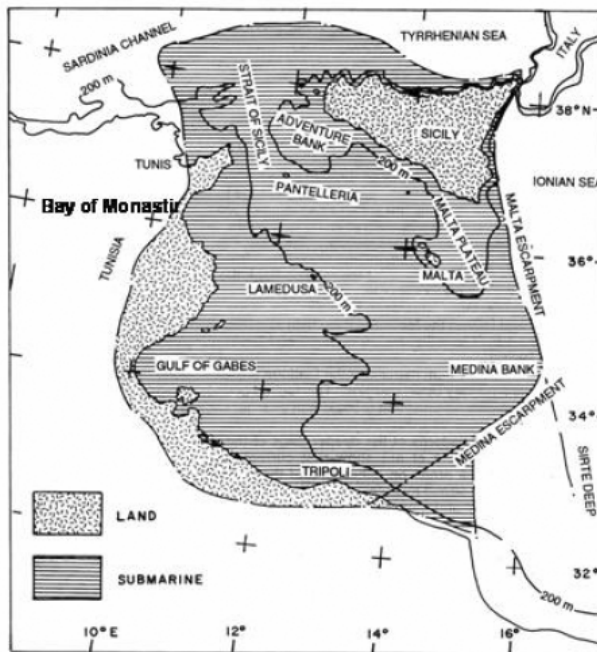


Figure 32.10 General map showing the location of the Sicilian-Tunisian Platform (from Max and Colantoni, 1992). Reprinted with permission

In the Lampedusa Bank the sediments are very similar to those of the Adventure Bank, but with a higher percentage of sandy fraction. The calcium carbonate content is very high (>90%) (Tonarelli et al., 1992).

In marked contrast to the surface deposits of the Adventure and Lampedusa Banks, the Malta Plateau sediments are finer and consist largely of shaly silt with low carbonate content (about half). The carbonate sediments, consisting of α -ganogenic and algal debris, are limited to waters shallower than 75 metres. In deeper waters of the Malta plateau, pelagic, hemipelagic and terrigenous debris, probably eolian in origin, represent the main clastic depositional components (Tonarelli et al., 1992).

The Tunisian continental shelf is the most extended in the Mediterranean Sea as a whole. Recently the littoral between Tunis and the Gulf of Gabes has suffered from eutrophication and, as a result, build-up of algae has gradually lead to the deposit of sediments rich in organic material. Information about the whole shelf is difficult to find but data are available for the Bay of Monastir, which is south of Tunis (Fig. 11).

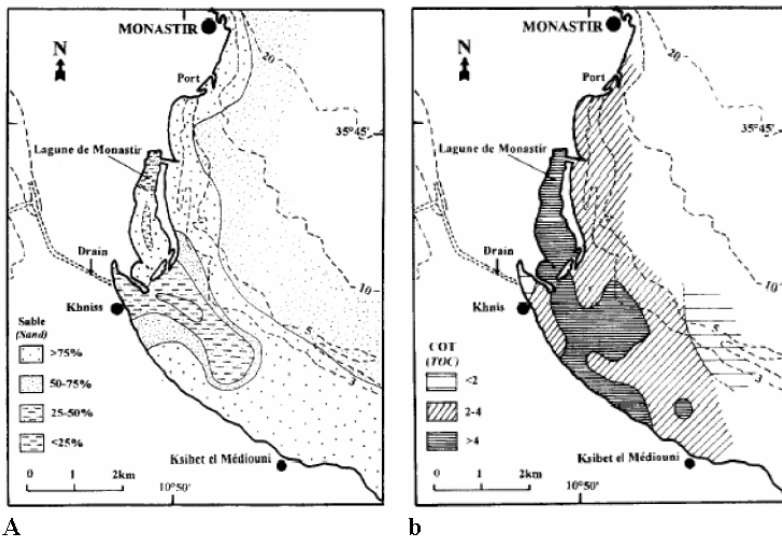


Figure 32.11 A) Percentage of sand ($>63\mu\text{m}$) in the surface sediments (from Sassi et al., 1998). B) Lateral distribution of organic carbon content (TOC) in the surface sediments (from Sassi et al., 1998). Reprinted with permission.

In this Bay, the sediments are largely sandy, while in the coastal zone of Khnis, the pelitic fraction predominates as a result of the high inflow of fine sediments from the drainage canal (Fig. 11a). The river runoff and waste-waters flow is directed into a drainage canal discharging in the Khnis zone. The whole area is characterised by currents of low amplitude (see section 4) due largely to the shallow water depth (Sassi et al., 1998).

There is a high organic carbon content (TOC) in the surface sediments, with values between 2–6%. The highest percentages ($>4\%$) can be found in the Khnis area, confirming the high levels of organic pollution. In the rest of the coastal strip, they vary between 2–4%, attenuating beyond the 3m isobath (1% at a depth of greater than 5m). The nitrogen (N) content is also high (0.5–1%), reaching the

highest levels in the zones richest in organic carbon. The C/N ratio is indicative of the nature of the organic material present in the recent sediments and the degree of mineralisation. In this zone, the ratio is less than 6 beyond the 3m isobath and reflects the silty marine origin (algae, eelgrass, plankton, etc) of the organic material, while the values of between 5 and 10 in the innermost areas indicate a composite origin, predominantly marine, but with a continental component. Locally (mouth of the drainage canal and Monastir lagoon) there are values of more than 10 (fig. 11b).

3.5 The Nile Delta zone

In the Nile Delta, the predominant sediments are terrigenous debris, shale and dark grey silt. The dark grey colour of the sediments is largely due to the high percentage of finely scattered organic debris and crystalline pyrite aggregates. There are few calcareous skeletal remains (foraminiferida, pteropods and heteropods) probably due to a dilution effect caused by the high percentage of clastic sediments. Mineralogical analysis indicates that the majority of the silts and sands are made up of mica and quartz (Herman, 1972). Construction of the Aswan Dam in 1964 drastically altered the water flow and the sedimentation pattern along the entire coast, considerably reducing the sedimentation rate.

In the absence of large quantities of sediment inflow from the Nile, wave and current action has caused heavy coastal erosion. However, in the Manzala lagoon (Fig. 12), accumulation rates are currently high (1.2 cm/yr), greater than those occurring during the Holocene period (0.7 cm/yr). This is due to the high input of water and sediment from the dense network of irrigation canals flowing into the lagoon (Benninger et al., 1998) and the high subsidence rates in the basin.

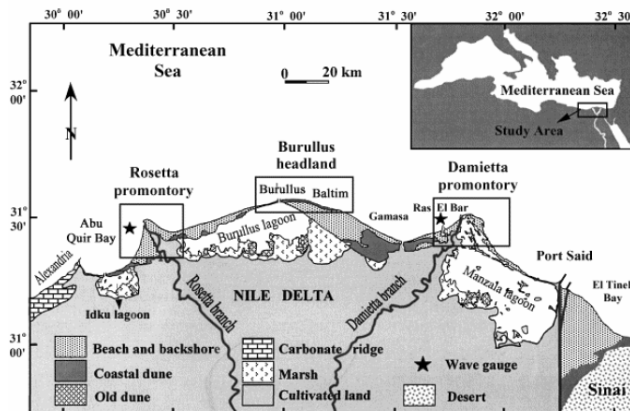


Figure 32.12 Map of the main promontories in the Nile delta area (Rosetta, Burullus and Damietta) and the geomorphologic units present (from Frihy et al., 2003). Reprinted with permission.

In the western side of the delta area (Figure 12), the recent building of protective structures (1990–2000) near the principal promontories (Rosetta, Burullus and

Damietta) has reduced and modified coastal erosion. Previously erosion was concentrated in the most projecting part of the promontories with regression values of up to 88 m/yr (Rosetta promontory) and sediment was largely transported by currents running parallel to the coast in an easterly direction. Now erosion is distributed more uniformly along the coast with local areas of accumulation where the coast is growing by up to 37 m/yr (Frihy et al., 2003).

3.6 *The Israeli continental shelf*

On the basis of current and wind direction measurements (Emery and Neev, 1960; Golik, 1997) and the characteristics of the sediment (Pomerancblum, 1966; Rosignol, 1969), numerous authors consider that the sandy sediments deposited along the coasts of Sinai and Israel derive largely from the Nile outflow. More recent studies carried out after construction of the Aswan dam (1964) which considerably reduced the contribution of sediment from the Nile, showed that the contribution of Israeli rivers is also significant in this area (Stanley et al., 1997; 1998).

The Israeli continental shelf extends for a maximum of 60 km in the Gaza area, shrinking to 25 km off the coast corresponding to the border with Lebanon. It consists largely of Pliocene-Quaternary sediments transported by the Nile and the sedimentation rates drop as the distance from the Nile increases (Ross and Uchupi, 1977; Almagor, 1993). Currents parallel to the coast are the main sediment transport agent in the South East Mediterranean from Sinai to the Bay of Haifa. North of Haifa, near the border with Lebanon, transport along the coast is less significant and the sandy fraction consists almost entirely of biogenic debris (Golik, 1997).

Marine sediments on the inner shelf south of Haifa consist of quartz, biogenic and detrital carbonates (5–10%), small percentages of heavy minerals and feldspars and shaly minerals. Sands are widespread in areas near the coast to a depth of 25 m, while shaly silt occurs at a depth of > 30 m. The shaly fraction represents more than 50% of the sediment at a depth of > 50 m.

Mineralogical study of the shaly fraction suggests that only 30–40% derives from inflow from the Nile. It is calculated that about 5–10% consists of grains transported by sandstorms and that the net contribution from Israeli rivers amounts to about 50% (Sandler and Herut, 2000).

4. **The physical shelf regimes and the meteorological forcing**

4.1 *Hydrodynamic regimes classification at the large scales*

The general circulation of the basin has been studied extensively in the past twenty years and it is now becoming very well mapped by observational data sets and reproduced by numerical simulations. One recent overview of the general circulation is given by Theocharis et al. (1998). The circulation can be subdivided into three main components: the large scale vertical circulation or thermohaline circulation, the sub-basin scale together with the Gibraltar-Atlantic water current system and the mesoscales.

As we have seen before, the Mediterranean is a concentration basin, i.e. water losses exceed water gains from precipitation and runoff. In addition, the net heat

budget of the basin is negative (Bethoux, 1979), so that the vertical thermohaline circulation is negative or anti-estuarine, with waters exiting the Mediterranean at depths and entering from the Atlantic at the surface (Bryden and Kinder, 1991). The general characteristics of the thermohaline circulation are schematized in Fig. 13. This circulation is characterized by multi-decadal time scales and it is propelled by the water mass transformation processes that occur in the open ocean areas of the Northern Mediterranean. Both deep and intermediate waters form in the regions offshore the Gulf of Lions, the southern Adriatic and the northern Levantine basin, forced by intense heat losses during late winter (February-March) and influenced by the presence of large scale cyclonic circulations driven by wind stress curl. The new feature of such a conveyor belt is the introduction of the Aegean Sea as a source of deep waters for the Ionian Sea abyssal plains. This event has occurred at the end of the eighties and first half of the nineties and it has been documented as the Eastern Mediterranean Transient (EMT, Roether et al., 1996). Recently, Manca et al. (2003) have found that the Aegean has stopped the production of deep waters and that the Adriatic Sea has started to be again the unique site of production of the deep waters for the Eastern Mediterranean.

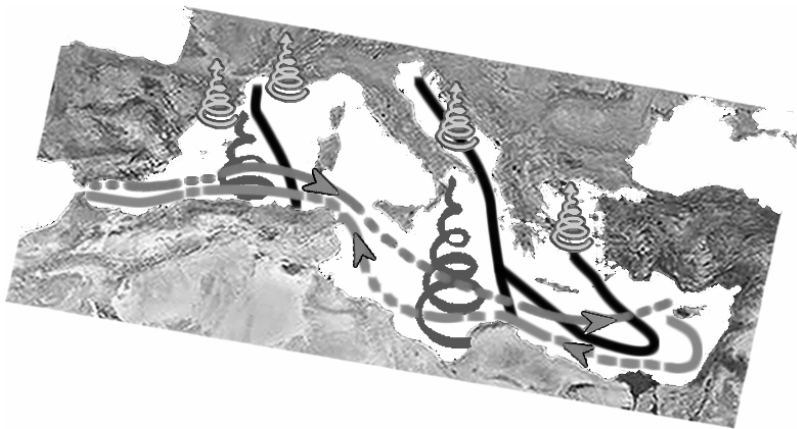


Figure 32.13 The three conveyor belts of the Mediterranean Sea. The first, dashed and in the zonal direction, is the surface-intermediate water masses circulation that is forced by Gibraltar and the Levantine Intermediate Water (LIW) formation processes occurring in the Northern Levantine basin. The second is the meridional vertical circulation in the Eastern Mediterranean, that is forced by deep water formation in the Southern Adriatic and Aegean Seas. The third is the meridional circulation in the western Mediterranean, forced by open ocean deep water convection in the Gulf of Lions. The spirals indicate the preferential site for strong heat losses from the ocean to the atmosphere during winter time.

The knowledge of the sub-basin scale circulation is relatively new (Robinson et al., 1991): it has several time scales and an important one is the steady state component. The latter consists of cyclonic and anticyclonic permanent gyres that are wind and thermal fluxes driven, superimposed to and interacting with the Gibraltar inflow system (Pinardi and Masetti, 2000). In Fig. 14 we show the time mean sea surface height (SSH) from a long term simulation of an ocean general circulation model devised for dynamical studies (Demirov and Pinardi, 2002): it shows the northern regions of the basin occupied by cyclonic gyres (the Gulf of Lions

gyre, the Tyrrhenian gyre, the southern Adriatic gyre and the Rhodes gyre) and the southern regions interested by anticyclonic gyres and generally high values of SSH. This circulation bears a resemblance to the double gyre circulation of the middle-latitude oceanic regions with reduced space scales and amplitude, due to the limited meridional extension of the basin, the different wind stress strength and the peculiar forcing of Gibraltar.

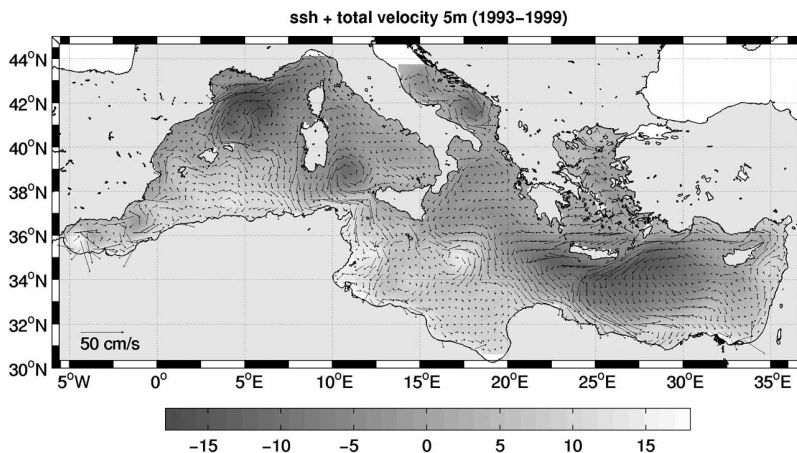


Figure 32.14 The mean sea surface height (ssh) from a 1993–1999 model simulation together with the surface velocity field. The grey bar is in cm and the basin average ssh is set equal to zero.

The time mean anticyclonic gyres of the circulation, while they are evident in theoretical studies of the wind driven circulation without Gibraltar inflow (Pinardi and Navarra, 1993, Molcard et al., 2001), are notably changed by interaction with the Gibraltar-Atlantic current system. The final result is that anticyclonic motion is either limited to a narrow band encompassing the continental slopes and shelves of the south-eastern Mediterranean (see for example the anticyclonic gyre centered at 28° E and 31.5° N or centered around 35° E and 35° N) or present in extended areas of the Algerian basin, the Sicily Strait and the southern Ionian Sea. These extended anticyclonic areas are normally occupied by mesoscales and non-permanent anticyclonic gyre structures so that the time mean circulation results in a weak downwelling area.

The sub-basin scale cyclonic (anticyclonic) gyres imply that at their centers upwelling (downwelling) motion prevails while at their borders the contrary occurs. This means that for cyclonic permanent gyres that impinge on the continental slope and sometimes on the shelf, there is an induced downwelling tendency on the shelf. In Fig. 15 we show the SSH again with the schematic of the upwelling/downwelling motion as deduced from the SSH slope. In general we see that downwelling motion prevails near the shelf areas, thus inducing the conclusion that the average sub-basin scale circulation induces open ocean upwelling and shelf areas downwelling. This has a profound influence on the shelf scale ecosystem dynamics, as we will discuss later. The only large shelf upwelling centers are asso-

ciated with wind driven permanent or seasonal upwellings as in the case of the Sicilian and eastern Aegean coastal areas.

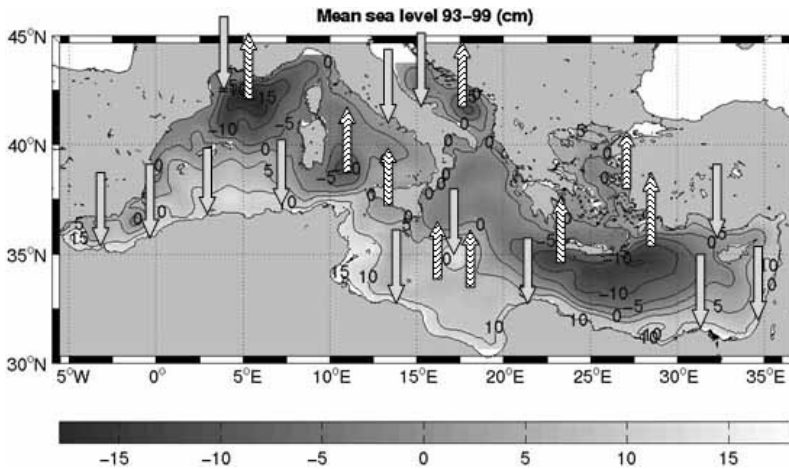
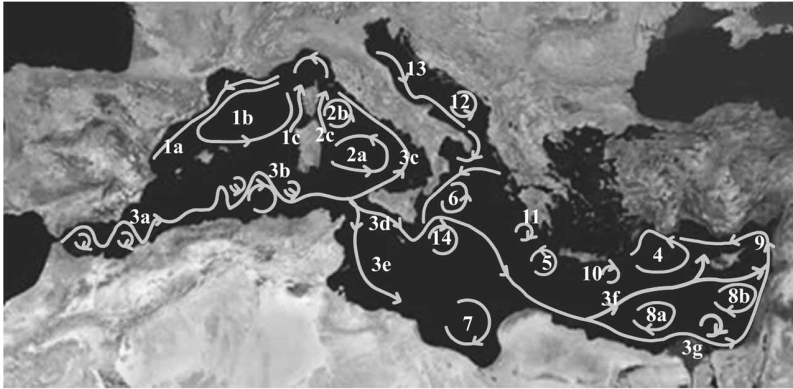


Figure 32.15 The time mean sea surface height of Fig. 32. 14 shown here only with amplitude contours. Arrows indicate the large scale vertical motion direction. The arrows start and point to the specific areas where the motion has the largest amplitude.

The sub-basin scale structures have amplitudes that are seasonally varying mainly due to the large wind stress variability. Coupled to such a seasonal variability there is also a large signal of interannual variability (Molcard et al., 2001, Korres et al., 2000). This implies that the general circulation structure can be quite different each year from the long term mean shown in Fig. 14 and 15. The more realistic schematic of the sub-basin scale structures, which considers interannual structures is presented in Fig. 16. The striking feature of this new picture is that the number of sub-basin scale features has increased and the size of the gyres has decreased.

The Gibraltar forced flow field is now decomposed in several sub-basin current systems, notably the Algerian current in the western Mediterranean, the Atlantic-Ionian Stream in the Ionian Sea and the Mid-Mediterranean jet in the Levantine basin. On the right side of the Gibraltar-Atlantic current system looking downstream (in the eastward direction), the prevailing motion is anticyclonic: we note the anticyclonic Algerian current eddies, the Mersa-Matruh and Shikmona gyres. The anticyclonic tendency in the southern Mediterranean is increased with respect to the steady state mean by the presence of sub-basin scale structures that vary at interannual time scales. Specifically, interannual atmospheric forcing helps to form anticyclonic gyres on the southern flank of the Gibraltar-Atlantic flow system (Korres et al., 2000) and in addition, flow instabilities would favor the formation of anticyclonic gyres on this side of the current system. This process will increase the amplitude of the open ocean downwelling areas thus increasing the north-south oligotrophic gradient suggested by Fig. 6.



- | | |
|---|--|
| 1a Liguro-Provençal-Catalan current (LPC) | 4 Rhodes Gyre |
| 1b Gulf of Lyon Gyre | 5 Western Cretan cyclone |
| 1c Western Corsica Current | 6 Western Ionian cyclonic Gyre |
| 2 Northward Tyrrhenian current and gyres: | 7 Syrte Gyre |
| 2a Northward current and Southern Tyrrhenian Gyre | 8 Anticyclonic system of the South-eastern Levantine basin |
| 2b Northern Tyrrhenian Gyre | 8a Mersa-Matruh Gyre system |
| 2c Eastern Corsica Current | 8b Shikmona Gyre system |
| 3 Gibraltar-Atlantic current system | 9 Asia Minor current |
| 3a Alboran basin Gyres and meanders | 10 Iera-Petra Gyre |
| 3b Algerian current gyres, eddies and meanders | 11 Pelops Gyre |
| 3c Tyrrhenian bifurcation/current | 12 Southern Adriatic cyclonic Gyre |
| 3d Atlantic-Ionian Stream | 13 Western Adriatic Coastal Current |
| 3e African MAW (Modified Atlantic Water) Current | 14 Western Ionian anticyclonic Gyre |
| 3f Mid-Mediterranean Jet | |
| 3g Southern Levantine current | |

Figure 32.16 Schematic of the surface circulation from recent observational data and model simulations. Names of structures and currents are listed.

The last circulation scale, the mesoscales, has by definition a shorter time scale than the one associated with the thermohaline circulation and the subbasin scale flow field structures. However current amplitudes are large and eddies are pervasive in the basin (Robinson et al., 1996). The mesoscales have been studied in the past in several subregions of the Mediterranean Sea (Robinson et al., 1987, Hecht et al., 1987, Millot, 1987, Paschini et al., 1993). The eddy-mean flow interaction mechanisms have not been studied yet but there is evidence from satellite altimetry of westward eddy propagation and a seasonal cycle in the eddy kinetic energy (Ayoub et al., 1998). In the Adriatic, evidence suggests that eddies are most frequent during spring and summer, when the atmospheric forcing relaxes and energy is converted from larger to smaller spatial scales (Artegiani et al., 1997).

4.2 Hydrodynamic regimes classification at the shelf scale

In this section we will overview the known circulation structures for the six study case areas: the Gulf of Lions, the Algerian shelf, the Sicily Strait, the Adriatic Sea, the Nile Delta and the Israeli shelf.

4.2.1 The circulation in the Gulf of Lions shelf

As introduced before, the northern shelves are, by and large, Regions Of Freshwater Influence (ROFI) that have been recently classified by Simpson (1997) and the Gulf of Lions is no exception to that.

The current system of this region is dominated on the slope boundary by the Liguro-Provençal-Catalan current (LPC) that flows along the Liguro Provençal and Catalan coast (see Fig. 16). The LPC is 30–50 km wide and it is formed upstream by the convergence of the Western Corsica Current (WCC in Fig. 16) and Eastern Corsica Current (ECC in Fig. 16). The current flows along the edge of the continental shelf, but it can form meanders penetrating the shelf (Auclair *et al.*, 2001; Flexas *et al.*, 2002, Echevin *et al.*, 2003). Millot (1990a) estimated that in the Gulf of Lions the exchanged water with the open sea due to the LPC is 1000 times larger than the Rhône runoff (Table 2).

The LPC carries Modified Atlantic Waters (MAW, Astraldi and Gasparini, 1992) westward during summer that have a significant subsurface salinity minima. In the Gulf of Lions, Winter Intermediate Waters (WIW) can form that are very cold ($T < 12$ °C) and then leave the shelf, forming lenses in the deep ocean at around 600 m depth. The seasonal water mass structure along transect 4 of Fig. 1a is shown in Fig. 17. The shelf cool and fresh waters in March contrast with the warmer and saltier water in the open sea, where the vertical homogenization and open ocean upwelling is evident down to the depth of 500 meters. It is interesting to notice the mixing between shelf and open ocean waters occurring between the depths of 100 and 500 meters, probably due to the WIW leaving the shelf. The summer picture shows a smaller contrast in temperature between shelf and open ocean waters but larger differences in salinity. The shelf, fresher waters now extend further in the open ocean and the subsurface Modified Atlantic Water signal is evident. During summer the LPC is clearly deeper, around 200 meters depth and hugging the escarpment (visible from the downwelling slope of the 38.2 isohaline in Fig. 17).

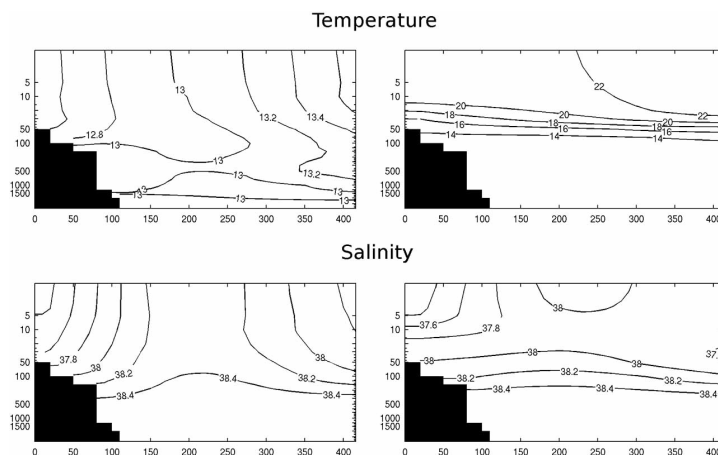


Figure 32.17 The climatological March (left panels) and August (right panels) temperature (upper panels) and salinity (lower panels) distributions along the transect 4 of Fig. 1a. The climatological data are taken from the Medar (2002) data set.

The dynamical nature of the LPC is still under debate but it is evident from Fig. 14 that it is the intensified border of the Gulf of Lions gyre. Its strength and position is influenced by the wind stress curl structure over the region (Herbaut et al., 1996, Korres et al., 2000) and by the frictional dissipation mechanisms against the continental escarpment (Pinardi and Navarra, 1993).

An important topographic feature of the shelf escarpment are the canyons (see section 3) and the so-called Rhône fan that has been indicated as a favorable site for the occurrence of open ocean deep convection (Madec et al., 1991). The LPC forms a deep meander over the Rhone fan (shifting inside the shelf) that produces an offshore cyclonic eddy that could be the preconditioning site for deep water homogenization to occur (Madec et al., 1991).

The westward transport of the LPC on the shelf around 5° E is about 2 Sv (Echevin et al., 2003) with a seasonal cycle of ± 0.2 Sv. Meanders of 30 km and 110 km wavelength form along the slope, propagating westward with 10 cm/s (see Fig. 18). The mesoscale variability has energy peaked at 3.5 and 7 days (Alberola et al., 1995). On the westward side of the Gulf of Lions shelf, relatively large anti-cyclonic eddies can form that trap waters on the shelf and then dissipate by moving westward (Echevin et al., 2003). The shelf is dominated by transient mesoscale variability induced both by the LPC meandering and directly by the wind.

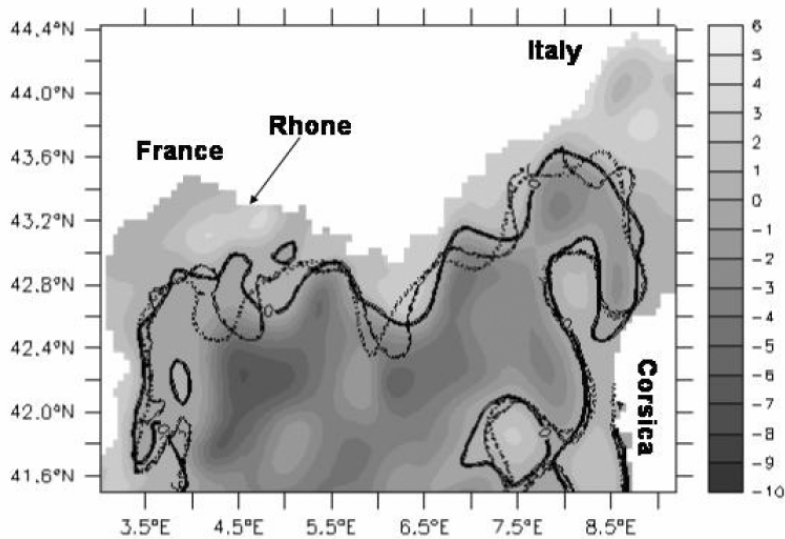


Figure 32.18 Meanders of the LPC depicted from a high resolution model of the north-western Mediterranean (reprinted with permission from Echevin et al, 2003).

The Rhône river plume moves cyclonically on the shelf and extends up to the westward side of the Gulf. During the winter, the shelf waters remain confined on the shelf while during the summer the Rhône plume and the shelf waters in general can extend offshore (Echevin et al., 2003).

4.2.2 The circulation near the Algerian shelf

The Algerian shelf current system is dominated by the dynamics of the Algerian current that is part of the Gibraltar-Atlantic water flow system described previously. Due to the shelf narrowness (see Fig. 2 and Table 1) the open ocean/slope currents intrude on the shelf. Here the slope current is formed by the Algerian current jets that show amplitudes of 50–60 cm/s. These are the largest current values in the Mediterranean basin and the critical shelf extension computed in (1) becomes larger, indicating that the shelf here is totally dominated by slope current intrusions up to the near-shore boundary layer.

The Algerian current forms large meanders and forms well known eddies due to mixed barotropic and baroclinic instabilities of the current. The largest and most persistent eddies are anticyclones (Fig. 19): they separate from the coast after their birth and follow a north-eastward path at the beginning of their life. After they get far enough from the coasts, they propagate backward, in the westward direction. The meandering Algerian current transports Atlantic Water (AW) into the Mediterranean Sea and the waters appear as filaments around the intense eddy field (not shown here).

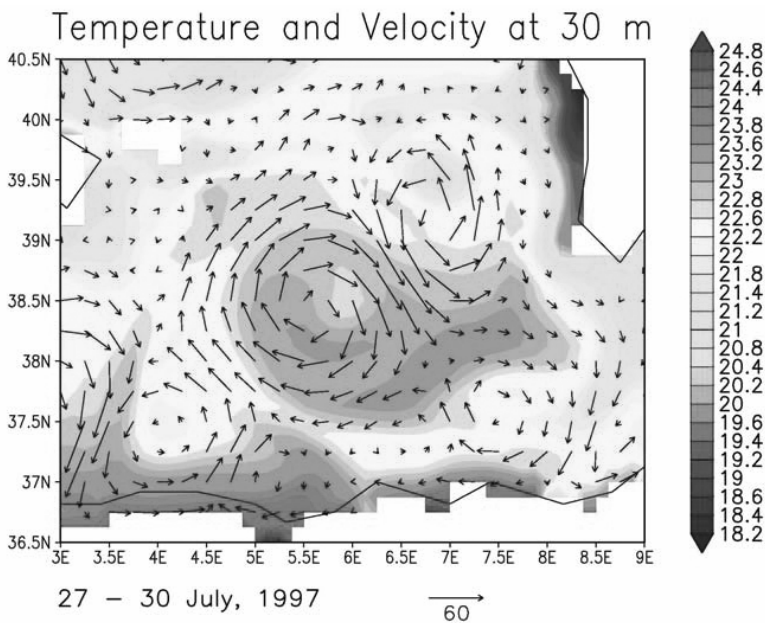


Figure 32.19 The 30 m currents and temperature field from a model simulation for the period 27–30 July 1997 in the Algerian basin.

Smaller scale cyclones are also found (Fig. 19) but they are more evanescent in time and it is difficult to observe them from satellite sea surface imagery. Thus their effects on the overall dynamics of the open ocean areas is quite unknown and in particular their effect on the shelf areas. Millot et al. (1990b, 1997) describes the dynamics of the mesoscale eddies of this region in great details.

This intense mesoscale field produces mushrooms of coastal waters that are pushed offshore by dipoles of cyclonic/anticyclonic eddies (Fig. 19 where warmer coastal waters are meandering outwards from the coasts). On the other hand, anticyclonic eddies, when they are still close to the coasts, might advect nutrient rich open ocean waters on the shelf, allowing for enhanced primary productivity (see also section 6). These blooms are episodic and relatively low in biomass. This process, due to the upwelling occurring at the anticyclones borders impinging on the shelf, has not been fully studied yet.

4.2.3 The circulation in the Sicily Strait shelves

The circulation in the Sicily Strait has been recently mapped by Robinson et al. (1999) and Sammari et al. (1999) and it has been simulated in details by Sorgente et al. (2003) and Drago et al. (2003). Recently an overview of the variability has been published by Lermusiaux and Robinson (2001). The Sicily Strait currents form a two layer system with 1–2 Sv transport in each layer and strong seasonal variability (Manzella et al., 1988, Astraldi et al., 1996). The surface flow field is directed eastward and the subsurface is westward, carrying Modified Levantine Intermediate Waters-MLIW. Here we will concentrate on the entrance of the Gibraltar-Atlantic current system in the Strait (transect 6 in Fig. 2), on the Tunisian shelf and the shelf between Sicily and Malta (part of transect 7 in Fig. 2).

Herbaut et al. (1996) have described for the first time the bifurcation of the Gibraltar-Atlantic flow system before entering the Sicilian Strait. Three branches form (Fig. 16), one going northeastward into the Tyrrhenian Sea, the other entering the central part of transect 6 and the third propagating close to the Tunisian coasts, on the shelf.

The seasonal climatology of transect 6 is shown in Fig. 20. The low salinity isolines mark the entrance of the Algerian current in the Strait from the surface down to 50 meters and on the Tunisian side of the transect. By contrast, a sharp halocline divides the surface waters from the intermediate, salty waters coming from the eastern basin. The wintertime temperature distribution shows interleaving layers of different temperature and the Italian side of the transect is warmer than the Tunisian. Below 100 m., the Italian side of the transect is occupied by a warm, salty water patch that might correspond to a vein of MLIW progressing westward. The summer picture is very different, the MAW layer is now subsurface, between 30 and 50 meters depth and waters have warmed up substantially (up to 10 °C at the surface) also down to 50–100 meters.

Fig. 21 shows the most recent simulation of the circulation in this area by Sorgente et al. (2003). This picture contains the salient structures of the circulation described in the literature. Robinson et al. (1999) called the segment of the Gibraltar-Atlantic current system entering the central Sicily Strait the Ionian-Atlantic Stream (AIS, Fig. 16) while the current on the Tunisian shelf area has been called by Sorgente et al. (2003) the African MAW current. The AIS flows near the Sicilian coasts, forms two large meanders (especially during the summer months, see Fig. 21b) and exits in the deep Ionian Sea between Malta and Sicily. On the northward side of the AIS upwelling centers form due to the upwelling favorable winds always present in this area. The AIS itself forces upwelling on its northern side and it does so especially during the summer time, when it reaches maximum amplitude. The African MAW current shows smaller wavelength meanders along the shelf

slope and its amplitude is seasonal. In the Gulf of Gabes area (Fig. 21) the MAW mixes strongly with adjacent waters and increases its salinity from winter to summer. It is interesting to notice (not confirmed yet by observations) that the simulation shows a reversal of the along slope African MAW current in the region between 14° and 17° E, going from summer to winter, probably due to the extension in summer of the anticyclonic Syrte gyre (Fig. 16). Due to this summer reversal, upwelling centers may develop along the Libyan shelf.

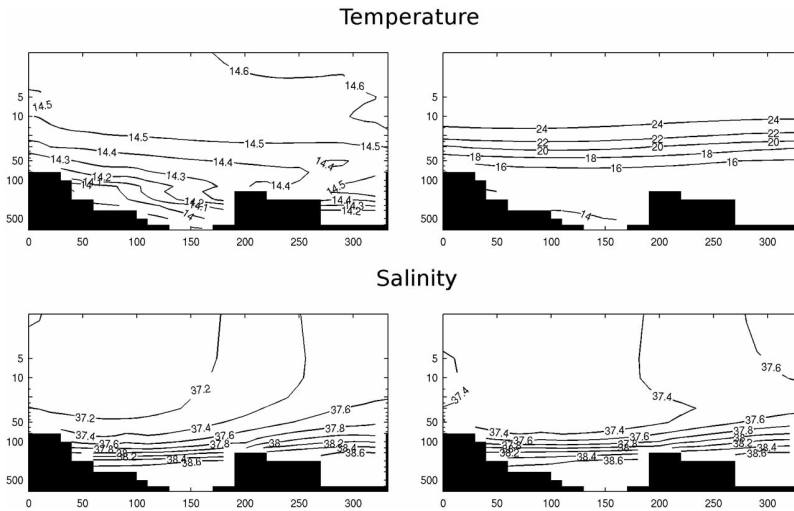


Figure 32.20 The climatological March (left panels) and August (right panels) temperature (upper panels) and salinity (lower panels) distributions along the transect 6 of Fig. 1a. The left side of the transect corresponds to the Tunisian shelf, the left to the Italian shelf. The climatological data are taken from the Medar (2002) data set.

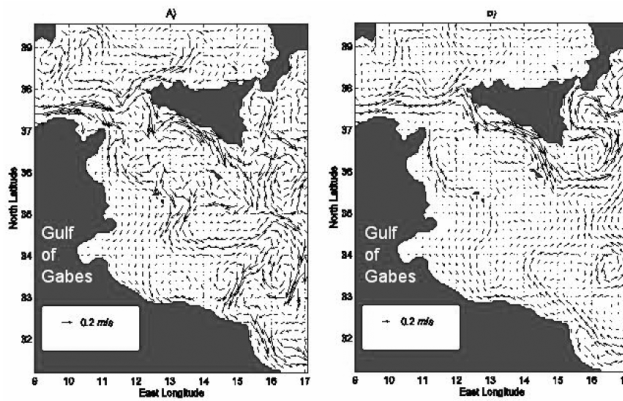


Figure 32.21 Surface circulation for (a) February and (b) August from Sorgente et al. (2003) simulations. Reprinted with permission.

As we said in section 2, Malta and Sicily are connected by an extended shelf (see Fig. 1a) called the Malta channel by Drago et al. (2003) where the Sicily upwelling center can extend 100 km offshore from the Sicily coast. The dynamics of this area is dominated by the latitudinal excursion and the amplitude changes of the AIS. This current structure determines the extreme productivity of these shelf waters where spawning and nursing grounds are found for most fish species of the area (see section 7).

4.2.4 The circulation in the Adriatic shelf areas

The circulation of the North and Middle Adriatic Sea has been described recently from observations and numerical simulations (Cushman-Roisin et al., 2001, Zavatarelli et al., 2002, Zavatarelli and Pinardi, 2003). The actual shelf break for the Adriatic Sea is commonly considered to be at the Pelagosa sill (see Fig. 9) but for this discussion we will concentrate only on the shallower part of the Adriatic Sea, down to Ancona (see Fig. 9).

The Adriatic Sea shelf area is controlled by air-sea fluxes and inflow of heat and salt at the shelf break. It is clearly a ROFI area influenced not only by the Po river but also by all the northern Adriatic rivers discharging along the Italian side of this area (see Fig. 9). The fluxes of heat and water combine in the so-called buoyancy budget that is very nearly zero averaged over the whole Adriatic Sea, due to the contrasting contribution of the heat and fresh water fluxes in this area. The buoyancy flux is written in fact:

$$B = \frac{\alpha_T g}{C_p} Q - \beta g S (E - P - \frac{R}{A}) \quad (4)$$

where Q is the net heat flux at the air sea interface (Maggiore et al., 1998), C_p is the specific heat, α_T is the coefficient of thermal expansion, β is the coefficient of haline expansion, g is gravity, S is the surface salinity, E the evaporation, P the precipitation and R the runoff ($\frac{m^3}{s}$) divided by the cross-sectional area, A , at the river mouth.

In the Adriatic, Q is negative on a mean annual basis ($-22 \frac{W}{m^2}$ from Artegiani et al., 1997) and also $(E - P - \frac{R}{A})$ is negative, mainly due to R . This gives rise to a balancing effect in (4). This means that the basin would be forced by the heat flux to work as an anti-estuarine marginal sea, forming deep waters, while the water budget would impose an estuarine circulation, as for a dilution basin. The dynamics of the Adriatic shelf is dominated by the balance between these two competing mechanisms in (4).

The overall water mass structure of the Northern and Middle Adriatic basin is dominated by the seasonal cycle in the heat fluxes and the runoff as it can be seen from Fig. 22. The water masses are totally renewed every year in the Northern Adriatic while the Middle Adriatic receives or renews locally its deep waters (be-

tween 200 and 250 meters depth) every few years only (Zavatarelli et al, 1998, Cushman-Roisin et al, 2001). The deep waters of the Northern Adriatic are the heaviest waters in the Mediterranean ($\sigma_T \geq 29.5$) and they slide southward, toward the Middle and the Southern Adriatic, entraining local waters and losing their signature. The signature of the cold waters is present in Fig. 22 where the isotherms bulge southward at the bottom of the transect. To be noted is the inverse vertical temperature gradient with waters cooler at the surface than at depths. This is allowed by the fresher surface waters that maintain a stable vertical density gradient. During summer, due to the spring discharge the water are fresher at the northern end of the Adriatic Sea while they maintain the same salinity in the middle Adriatic Sea. The large seasonal thermocline forms every year, between 10 and 30 meters depth, isolating the deep, cold waters present in the Middle Adriatic Pit (located at about 350 km along the transect of Fig. 22).

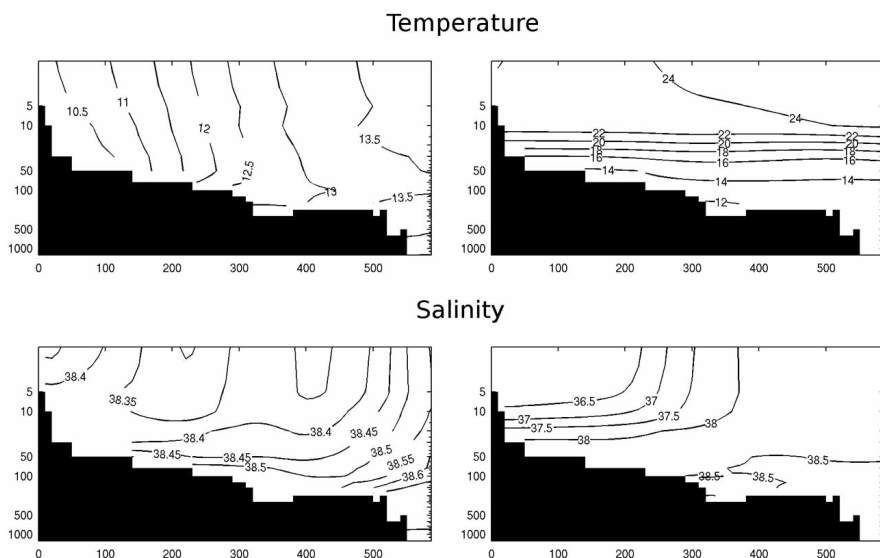


Figure 32.22 The climatological March (left panels) and August (right panels) temperature (upper panels) and salinity (lower panels) distributions along the transect 9 of Fig. 1a. The left side of the transect corresponds to the Northern Adriatic. The climatological data are taken from the Medar (2002) data set.

The other important driving mechanism for this area is given by the wind stress that has two very important regimes: the Bora or easterly wind and the Sirocco or southerly wind. The Bora is channeled through the Dinaric Alps and it forms intense jets that have positive and negative curls (Pullen et al., 2003). This induces strong changes in the vorticity sign of the circulation and sometimes reversal of the cyclonic circulation of the basin occurs in portions of the basin, especially the shallow, northern parts. The Scirocco, on the other hand, is forcing high sea level in the Northern Adriatic and could reverse the sign of the currents along the Italian coastlines (Poulain et al., 2003).

The circulation is generally cyclonic in the northern shelf areas and it is composed of a western boundary intensified current, called the Western Adriatic Coastal Current (WACC). The latest observational evidence of the Adriatic Sea circulation structure is given by Poulain (2001). In Fig. 23 we show the result of the simulation from Zavatarelli and Pinardi (2003), which synthesize the evidence for the changes in the seasonal circulation. During winter the circulation is dominated by the WACC and the overall scales are large. We note however, that the northward current on the eastern side of the shelf (along the Istrian coasts) tends to separate from the coasts, cutting the cyclonic circulation north of the Po River from the circulation south of it. We call this the cyclonic cut-off. During summer, the circulation is still cyclonic along the Italian coasts but a very large countercurrent (called the Istrian Coastal Counter-Current (ICCC), Supic et al., 2000) forms on the eastern side of the northern Adriatic. During summer, the cyclonic cut-off of the circulation has branched into two currents: one is southward of its winter position, toward the Middle Adriatic Sea, leaving a larger area dominated by mesoscales. The anticyclonic circulation north of the cyclonic cut-off can be also wind induced, if the Bora jet occurring normally above the Istrian peninsula is shifted southward or it is highly sheared. In conclusion we can say that the Adriatic shelf circulation is dominated by wind stress curl and thermohaline forcings, changing structure and direction of currents at least seasonally.

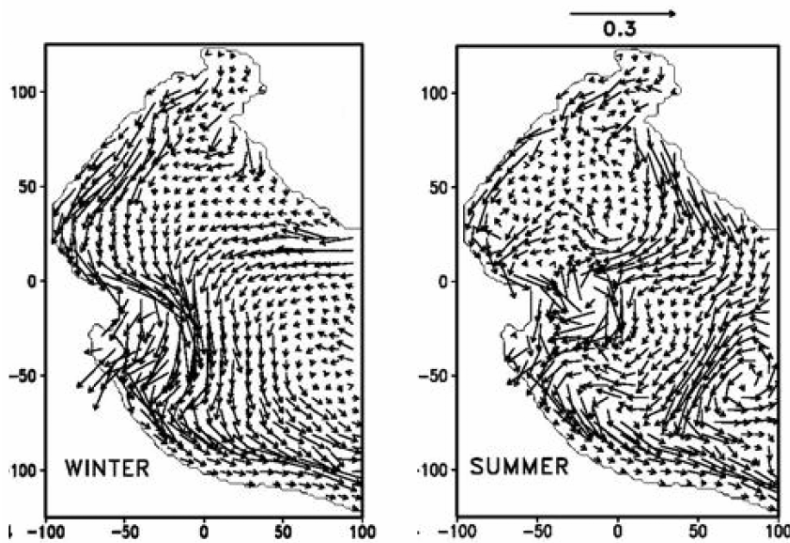


Figure 32.23 Northern Adriatic shelf circulation from model simulations (Zavatarelli and Pinardi, 2003). The reference arrow is in m/s.

4.2.5 The circulation in the south-eastern Levantine: the Nile Delta and Israeli shelf areas

The Egyptian and Israeli shelf areas are opposite in extension (see Table 1) but the latter is strongly interconnected by the open ocean flow field to the Egyptian

slope current regime and then to the sediment and biochemical fluxes of that region. Thus they will be examined together in terms of the open ocean/slope currents.

For the near coast flow field the information on the Nile Delta coastal area is very scarce. It is evident that the Egyptian shelf is still a ROFI area (Hamza et al., 2003) but very different from pre-Aswan dam period. The damming completely changed the Nile runoff from 1968 onward, the annual total discharge averaging only one-tenth of the average value for the period prior to 1964 (see Table 2) and having the maximum discharge in winter. On the other hand, the Israeli shelf is very narrow both by morphology and by dynamical considerations. The runoff by the local rivers can account for a conspicuous part of the sedimentation rate of the Israeli shelf (see section 3) but nothing is known about the influence on the local hydrodynamics.

The climatological distribution of temperature and salinity for the two months of March and August is shown in Fig. 24. First of all, the salinity distribution shows that the Nile signal is present on the Egyptian shelf and it extends as far as several hundred kilometers from the coasts. The Levantine Intermediate Water layer is present both in winter and summer and hugs the shelf escarpment between 100 and 300 meters depth, thus influencing the shelf slope area. It is interesting to notice that during summer the Modified Atlantic Water is present on the shelf by a subsurface salinity minimum between 30 and 100 meters. The isotherms and isohalines are quite flat but a dominant downwelling structure can be recognized in the distributions near the shelf break.

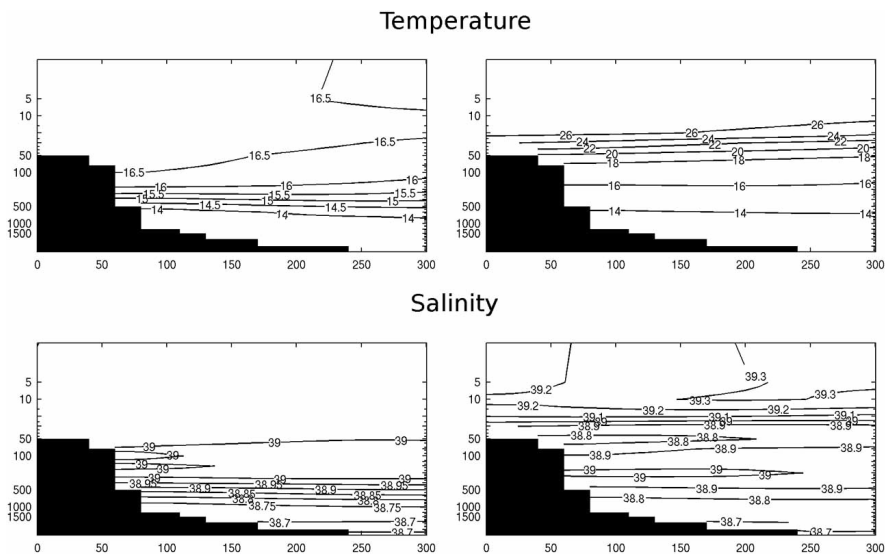


Figure 32.24 The climatological March (left panels) and August (right panels) temperature (upper panels) and salinity (lower panels) distributions along the transect 15 of Fig. 1a. The left side of the transect corresponds to the Egyptian coast. The climatological data are taken from the Medar (2002) data set.

The open ocean flow field in the southeastern Levantine has been mapped first by the MC cruises (Hecht et al., 1987) and then by the POEM experiment (the POEM group, 1992). It has been also recently simulated by a high numerical resolution seasonal model of the Levantine basin by Korres and Lascaratos (2003). These simulations offer a unique opportunity to see the possible current regimes on the Egyptian shelf areas and slope. The simulations are reproduced in Fig. 25 for the winter month of february. The slope current field is always in the eastward direction but intense meandering is occurring upstream of the Nile Delta shelf area, around the Mersa-Matruh anticyclonic gyre (see Fig.16). The Nile Delta slope current is formed by the convergence of a southward branch of the Mid-Mediterranean Jet (MMJ) and the slope eastward current, called the southern Levantine current in Fig. 16, always present along the African coasts. On the shelf, it seems that anticyclonic circulation is possible, in the near-shore area. From the circulation picture of Fig. 25 it is evident that the Nile Delta area behaves as an extended shelf area where the slope current and the near coast currents do not interact strongly.

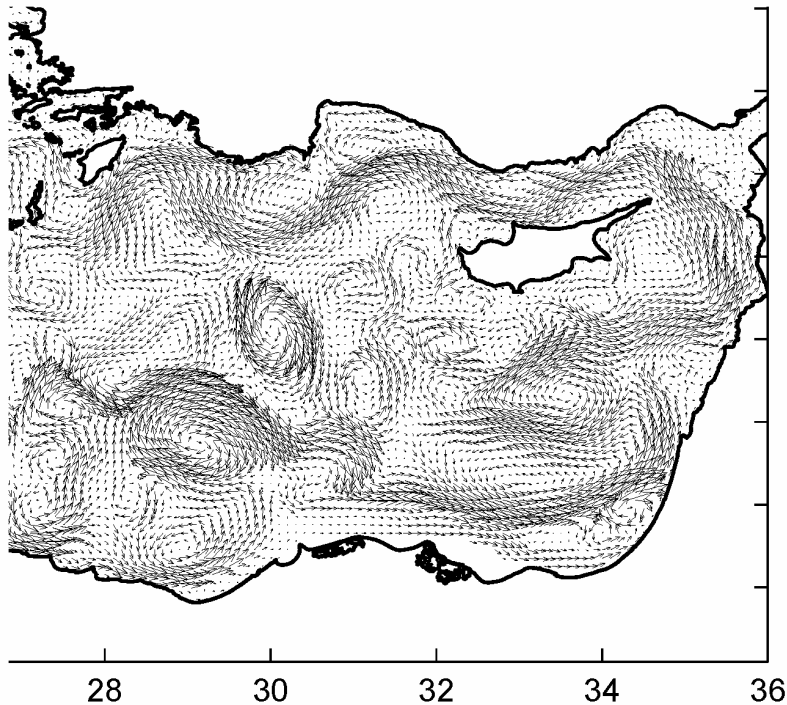


Figure 32.25 Circulation of the southeastern Levantine basin from a model simulation (from Korres and Lascaratos, 2003)

The Israeli slope currents are northward but large meandering occurs also there, together with eddy detachment (Brenner, 2003). The large anticyclonic eddy in the open ocean areas of Fig. 25, in front of the Israeli coasts, is the Shikmona gyre (see

Fig. 16) that has been documented by many authors (Hecht et al., 1988, Brenner, 1991). It is possible that, due to the nonlinear dynamics of such eddy formation processes, convergence and divergence areas would appear in near shore areas, with local upwelling and downwelling centers. During summer, the shelf areas are much warmer than the open sea and the mesoscale activity is at the minimum. Current meter data on the shelf (Brenner, 2003) show that the shelf currents are all the year long northward except for September where local reversals may occur, when the slope current is farthest from the continental shelf edge.

4.3 Meteorological forcing of the circulation

The meteorological forcing of the Mediterranean Sea is particularly complex and presents a strong seasonal variability. The atmosphere forces the ocean and its coastal areas by transferring momentum, heat and water across the sea surface. The heat and water fluxes combine in the buoyancy flux that has been written in equation (4)

The water flux has been discussed in section 2.2 and we know that on the long-term mean it is positive. The heat flux in the Mediterranean Sea is known to have a negative long-term mean equal approximately to $-7\frac{W}{m^2}$ (Garrett, 1983, Castellari et al., 1998). The structure of the heat flux is consistent with large heat losses during the winter that overcome the heat gains during summer. The areas with largest heat losses are the Gulf of Lions gyre, the Rhodes gyre, the northern Aegean Sea and the Adriatic Sea, where deep and intermediate waters form (heat losses greater than $1000\frac{W}{m^2}$ have been recorded in the Gulf of Lions, Schott and Leaman, 1991).

Roussenov et al. (1995) and Korres et al. (2000) noted that the southern Mediterranean shelf areas are sites of intense air-sea interactions during winter, due to the relatively large temperature differences between ocean and atmosphere. During summer, the upwelling areas in the southern Sicily and Turkish coasts of the Aegean Sea are sites of intense heat gain due to the relatively low temperatures of the water.

In order to quantify the effect of shelf areas on the total heat budget of the basin, we calculated the heat flux with and without shelf areas (defined as the part of the basin with depth less than 200 m) from a 21-year simulation of the circulation with the model described by Pinardi et al. (2003). The results are presented in Table 7: they show that the shelf areas account for about 20% of the basin mean heat losses and their contribution is extremely variable with the years. The overall negative contribution to the mean heat budget due to the shelf areas reinforces the concept that the Mediterranean shelf areas are predominantly downwelling sites where the heat exchange with the atmosphere is large and it contributes to the negative heat budget of the basin. The model used in the computations of Table 7 does not contain the Northern Adriatic, thus this important contribution is neglected. However, this would make the results presented here even more consistent with the interpretation given above since the annual mean heat flux over the Northern Adriatic is negative.

TABLE 32.7

The basin mean heat flux over the basin in units of $\frac{W}{m^2}$.

The heat flux has been computer from a model simulation that does not include the northern Adriatic Sea shelf area (seen in fig. 14 by the absence of arrows above 43° N) in the overall basin mean.

| Year | Basin mean heat flux | Basin mean without shelf | Difference | Percentage of change |
|-------|-------------------------|-----------------------------|------------|----------------------|
| 1979 | 9.6 | 10.2 | -0.5 | 6. |
| 1980 | 8.7 | 8.8 | -0.1 | 1. |
| 1981 | 0.5 | 0.6 | -0.1 | 24. |
| 1982 | -8.2 | -8.5 | 0.3 | 4. |
| 1983 | 4.2 | 4.5 | -0.3 | 8. |
| 1984 | 2.4 | 2.2 | 0.2 | 8. |
| 1985 | 2.5 | 2.3 | 0.2 | 7. |
| 1986 | -5.9 | -6.2 | 0.3 | 6. |
| 1987 | -2.4 | -3.3 | 0.9 | 39. |
| 1988 | -4.0 | -4.6 | 0.6 | 16. |
| 1989 | 9.8 | 9.9 | -0.1 | 2. |
| 1990 | 1.4 | 1.2 | 0.3 | 19. |
| 1991 | -9.9 | -10.5 | 0.6 | 7. |
| 1992 | -5.0 | -6.0 | 1.0 | 20. |
| 1993 | 15.9 | 15.9 | 0.0 | 1. |
| 1994 | 9.6 | 12.4 | -2.9 | 31. |
| 1995 | 4.5 | 7.4 | -2.9 | 65. |
| 1996 | -2.4 | -0.8 | -1.6 | 66. |
| 1997 | 4.7 | 6.1 | -1.4 | 30. |
| 1998 | -4.8 | -4.2 | -0.7 | 14. |
| 1999 | -3.1 | -3.7 | 0.6 | 21. |
| Total | 1.4 | 1.7 | -0.3 | 19 |

The momentum flux is given by the wind stress at the sea surface. In Fig. 26 we show one estimate of the wind stress for the period 1993–1999. The wind stress is dominated by the two intense structures of the Mistral in the Western Mediterranean and Etesian winds in the Eastern basin. These two structures are both present in the annual mean but they have larger amplitudes in winter for the Mistral and in summer for the Etesian. We should remark that this mean wind stress pattern is changing with a decadal time scale, following the NAO index phases. This change is documented in Demirov and Pinardi (2002) and Samuel et al. (1999) and it has profound influences on the circulation. Raicich et al. (2003) remark also that the Etesian winds are the lower branch of the African Hadley cell system that during summer extends its influence over the Mediterranean Sea.

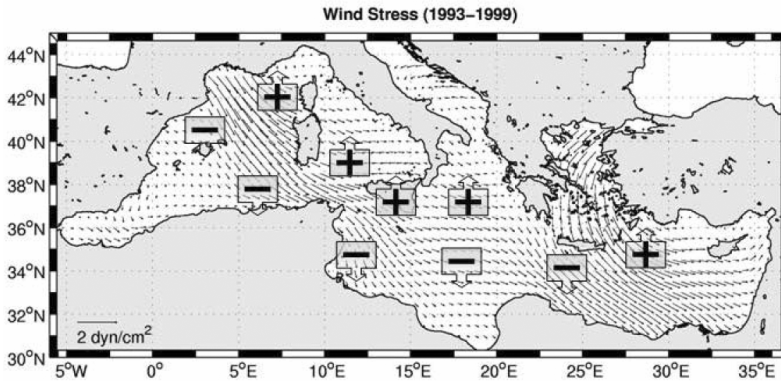


Figure 32.26 The average wind stress computed from four daily ECMWF operational surface wind analyses for the period 1993–1999. The boxes indicate the Ekman vertical velocity sign. Positive means upwelling, negative downwelling.

The other important wind systems (Sirocco and Libeccio, Bolle, 2002) are northward but they are less frequent and intermittent than the Mistral and the Etesian and they do not appear on the average. However, they can start intense upwelling along the Italian coasts of the Adriatic Sea (Poulain et al., 2003) and/or along the western coasts of the Ionian Sea.

Another important forcing on the open ocean as well as the shelf areas of the Mediterranean Sea is the curl of the wind stress. The curl of the wind stress has been described in great details in many other papers (Molcard et al., 2002, Demirov and Pinardi, 2002, Josey et al., 2000) and it is formed by dipoles of positive and negative vorticity input on the right and left sides of the winds looking downward in their direction. These dipoles are depicted in Fig. 26 and are responsible for forcing many of the permanent and semi-permanent cyclonic and anticyclonic gyres described in section 4.1. Thus the wind stress curl is important and is related to the vertical velocity, w_E at the base of the surface Ekman layer:

$$w_E = \hat{k} \cdot \nabla \times \left(\frac{\bar{\tau}}{\rho f} \right) = \frac{\partial}{\partial x} \left(\frac{\tau_y}{\rho f} \right) - \frac{\partial}{\partial y} \left(\frac{\tau_x}{\rho f} \right)$$

where $\bar{\tau} = (\tau_x, \tau_y)$ is the wind stress with its components, ρ is the density and f is the Coriolis parameter. In Fig. 27 we show the basin average wind stress curl over the Mediterranean Sea. The wind stress curl is generally positive over the basin, thus inducing a cyclonic vorticity input but it weakens and even reverses during summer, thus producing the enhancement of the anticyclonic circulation structures, permanent and semi-permanent. Note the very low cyclonic vorticity input in the 1989–1990–1991 years that is partly responsible for the changes in circulation that occurred in these years and that induced a strong anticyclonic vorticity in the flow field (Demirov and Pinardi, 2002). After 1993, the cyclonic input of vorticity in the basin almost tripled thus generating stronger slope currents such as the LPC and the Asia Minor Current (Fig. 16). This is clearly going to be important for the shelf area dynamics, which, especially for the narrow shelf areas, is profoundly affected by the slope current intensity.

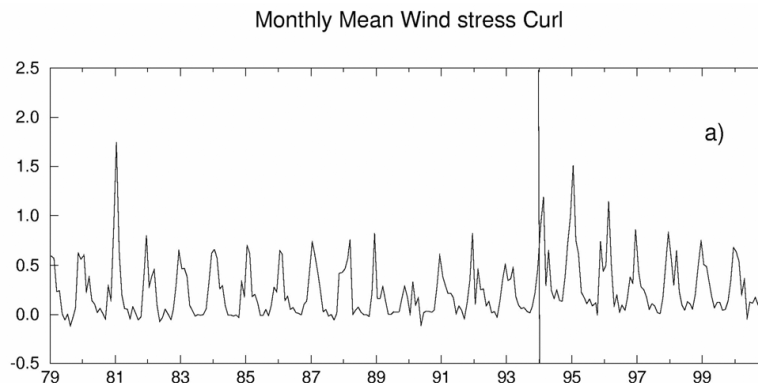


Figure 32.27 The area average wind stress curl for the 23 years from 1979 to 2001 calculated from ECMWF surface wind field. Units are dyne/cm^2 .

5. Open ocean-shelf areas coupling

5.1 *The Continental Shelf Pump*

Runoff from rivers annually delivers ~ 0.8 Pg of carbon to the Mediterranean margins, 45% of which is organic, primarily in dissolved form (Liu et al., 2000), leading some authors to assert that the continental margins are net heterotrophic systems (Smith and Mackenzie, 1987). However a recent study suggests that the margins as a whole are a weak net CO_2 sink of about 0.1 Pg yr^{-1} (Liu et al., 2000). The ocean shelves can act as net carbon sinks if they transfer a substantial part of the primary production organic carbon to the oceanic interior through the combination of physical and biological processes known as Continental Shelf Pump (CSP) (Tsunogai et al., 1999). In the Mediterranean, even if the Adriatic shelf has been recognized as the main candidate as an effective CSP site (G. Civitarese, pers. comm.) proper quantification and its relative importance is still far from being fully assessed.

There is another important aspect of the Mediterranean shelves that should also be considered for its biogeochemical implications. Although the shelf surface is proportionally large compared with the World Ocean, the shelves are much narrower. What makes the Mediterranean Sea peculiar under this aspect is that almost all well developed shelves are located on the northern side of the basin and dense waters formed on the shelves are prone to replenish and spread into the ocean interiors from the northern side of the basin, contributing in creating north-south gradients in the system.

Moreover, Adriatic and Aegean Seas are elongated inlets where the exchanges are confined to a relatively small open boundary. This means that the shelf water has a mean residence time that can be long (time scales of months-years). This long lasting permanence allows the editing of the quality and quantity of organic matter and major chemical constituents in the water column along its seaward transit through production, decomposition, and other biotic and abiotic modifications. Biochemical (bacterial production and decomposition, photochemical modification), benthic-pelagic coupling and physically-mediated processes (adsorption,

flocculation, settling) perturb the original biochemical signature of the land derived organic materials that arrive to their ultimate long term storing compartments heavily transformed.

As an example, the relevance of this complex suite of biogeochemical processes has been testified in a recent study carried out in the Ionian Sea (Seritti et al, 2003) where the slope in DOC/AOU profiles has been connected with the origin and age of the water masses (Adriatic vs Aegean). In general, the resulting composition of organic compounds and key elements in all their forms leaving the continental margins are dependent on a shelf-specific history and in turn, in the long run, affect the whole Mediterranean biogeochemical cycles.

5.2 *The deep ocean-shelf exchanges*

We have seen in section 2 and 4 that the mechanisms active in the deep ocean-coastal ocean interactions in Mediterranean are site-specific. However the common feature that allows some classification of the shelf dynamical regime can be found in the flow field that develops on the barrier constituted by the shelf slope. Along the shelf slope, the current field $\mathbf{v} = (u, v)$ is in geostrophic balance, that means that :

$$\bar{\mathbf{k}} \cdot \mathbf{v} \times \frac{\partial \mathbf{v}}{\partial z} = 0$$

where $\bar{\mathbf{k}}$ is the unit vector in the vertical direction (Brink, 1998). As Sanchez-Arcilla and Simpson (2003) pointed out, the slope currents will interact with the shelf areas if they break the geostrophic constraint. The advection of momentum is the term that is responsible of the departure from geostrophy, more than other ageostrophic terms. The relative importance of nonlinearity is usually estimated by means of the Rossby number,

$$Ro = \frac{U}{fL}$$

already defined in section 2. Ro is $O[10^{-3}]$ in Mediterranean if we take the open ocean flow scale variables, and thus the advection is small compared with the Coriolis term. However near the shelf break length scales become narrower and the geostrophic constraint can be broken by nonlinear advective processes. Several categories of non-linear processes control in the Mediterranean the open sea-shelf exchanges and they will be treated separately in the sections below.

5.2.1 **Slope and coastal currents spill-outs over the topographic obstacles**

The diverting of a general circulation current (also called slope current) into a shelf is commonly found in the Adriatic and Gulf of Lions areas. The pressure gradient induced by buoyancy fluxes in conjunction with the wind driven circulation (with variable intensity) explains the departure from geostrophy of the mean circulation. For sake of an example, we will discuss here the Adriatic case only.

Gacic et al. (1999) calculated from direct measurements that about 25% of the water entering Otranto Strait is able to pass over the Pelaguza sill (see Fig. 3.3) shelf break toward the Central Adriatic. These waters are carried by the large-scale northward Adriatic slope current that develops especially during autumn and winter (Artegiani et al., 1997), connected to the Otranto inflow. We call this an example of slope current spill out over the shelf break.

On the other hand, the WACC carries nutrients southward in a way that can be compared to a 'coastal current spill-out' out of the shelf break (located south of the Pelaguza sill). In fact the net seasonally integrated nutrient transport estimated at the Pelaguza transect is always directed seaward with a summer-to-winter variability that ranges from 7140–14780 Mmol DIN to 456–588 Mmol phosphate. Silicate seasonal variability closely follows DIN dynamics (11760–25780 Mmol)

These figure are subjected to changes according with the general circulation pattern of the region. The change of the thermohaline circulation in the Eastern Mediterranean (Roether et al, 1996), the EMT, has been found to have consequences on the Adriatic shelf dynamics. Due to the EMT, the Levantine Intermediate Water has been substituted with Cretan Intermediate Water and this has allowed the intrusion of alloctonous plankton species, typical of Levantine basin, up the northernmost part of the Adriatic (Gulf of Trieste).

Frontal instabilities Instabilities of the slope and coastal fronts are usually related to the strong baroclinic structure of these features and the quasi-geostrophic two-layer theory predicts that the scale of such instabilities is related to the wavelength of the fastest-growing meanders (Pedlosky, 1979) that is:

$$\lambda = 2\pi R_m$$

where R_m is the geometric mean of internal Rossby deformation radii in each of the two layers.

Slope current instabilities produce eddies that may detach from the slope. Long-lasting anticyclonic northwestward-prograding eddies found in the Algerian basin (Arnone and LaViolette, 1986 and section 4) are generated by baroclinic instability of the Algerian Current and they impinge on the shelf areas modifying the nutrient budgets. In section 4 we have discussed their effects on the shelf areas that produce open ocean-shelf exchanges and in section 6 we will discuss their effects on biogeochemical fluxes.

Baroclinic instabilities of the Western Adriatic Coastal Current-WACC, that is the most noticeable coastal current front in the whole Mediterranean Sea, are commonly found in images in the visible band and, seasonally, in the infrared band, but only after the Adriatic shelf break, located at the Pelaguza sill, the frontal instabilities can be effective in transferring shelf waters offshore.

Cold filaments have been observed in the Adriatic Sea, (Borzelli et al., 1999) and have been explained as a baroclinic extension of the Rossby adjustment on a sloping bottom. Filaments-type instabilities were also reported along the Spanish sector of the LPC (see Fig.4.4, Font et al., 1995).

Another frontal instability occurring in the Mediterranean shelf areas is related to the upwelling centers. Mesoscale structures are found in the Sicily Strait, where wind driven coastal upwelling generates cold filaments that intrude in the vein of

MAW entering the EMed through the Sicily Strait (Buongiorno Nardelli et al., 1999).

Coastal and slope currents, upwelling front instabilities deserve more studies to assess the effectiveness of this mechanism in determining the resulting lateral fluxes, despite the large number of observations already available. Although mesoscale processes are frequently described in the slope areas of the Mediterranean shelves, a quantitative assessment of their importance is not yet available.

Wind driven coastal upwellings Upwelling processes determine exchange of water masses and properties at the shelf break and thus open ocean-shelf interactions. Alongshore windstress induces cross-shore Ekman transport. The long-wave approximation (time scales longer than inertial period, small frictional effects, along-shore scales \gg cross-shore scales) allows finding a stationary solution of the depth integrated equations of motion, where surface and bottom Ekman transports balance the interior inviscid transport. This simplified view of the upwelling is modified by the space and time variability of the wind regime, which are prominent features of the Mediterranean area (if compared with the steady winds present in the open ocean, see Fig. 4.12). In this case spatial variability induces Ekman pumping while the short-term wind pulses can drive coastal upwelling also in the case of substantial cross-shore wind stress component (Brink, 1998).

Recurrent upwelling areas in the Mediterranean encompass the southern Sicily and Calabria coasts, Southern Spain and the eastern Adriatic and Aegean Sea coasts. In general, the Mediterranean wind driven coastal upwelling is believed to be not very efficient if compared with similar processes occurring in other parts of World Ocean and therefore its study in Mediterranean has been largely neglected. However, owing to the scarcity of macronutrients in the euphotic zone during most of the year, a reassessment of the upwelling areas importance for the nutrient basin budgets would be highly desirable.

5.2.2 Buoyancy forces: ROFI areas

Large Mediterranean ROFI areas where buoyancy input due to river runoff determines the coastal currents that eventually cross the shelf break are present in the Adriatic Sea (Po), Gulf of Lions (Rhône) and Catalan (Ebro) shelves. Typical transport can be calculated for the Mediterranean coastal currents assuming that buoyancy is balanced by inertial forces (and friction/mixing can be in first approximation disregarded because of small energy associated with tides). The transport in these wedge-like currents is:

$$Q = \frac{g' h_0^2}{2f}$$

where g' is the reduced gravity, and h_0 is the depth of the wedge (Hill, 1998). Entrainment in the current is an effective way to increase the transport/export of lower layer water and its properties.

The interactions with the wind show that in the case of downwelling favourable wind regime, the coastal current tend to adjust along the coast and maintain its integrity, while in the case of upwelling, the coastal current can be radically changed from its adjusted configuration.

5.2.3 Dense water formation downflows

Dense water formed in the Mediterranean shelves contributes to the ventilation of deep layers (Gulf of Lions and North Adriatic) of the Mediterranean. The down-sloping of dense water from the shelves offers another open-ocean shelf exchange mechanism that is extremely active in the Mediterranean Sea.

Generally, more attention has been paid to the open ocean dense water formation processes in the Mediterranean Sea but it is evident that the shelf deep waters contribute to the open ocean deep-water formation processes mainly because of their vicinity to the area of open ocean formation. In the Adriatic, the thermohaline characteristics of the dense water outflowing at the Otranto sill clearly require a contribution from the northern shelf waters.

Recently Aegean dense waters formed in the Cycladic Plateau have been found to be a major contributor to the Cretan Deep Water (CDW) masses that spilled over the Cretan sills into the abyssal plains, giving rise to the Eastern Mediterranean Transient-EMT.

Since the CDW is characterized by higher nutrient and lower oxygen concentrations than those normally measured at the same depths of the Cretan Sea, we can say that the deep ocean has been 'fertilized by the shelf areas'. The biogeochemical implications of this fertilization has been claimed as the putative origin of sporadic phytoplankton blooms reported in '90s in the Cretan Sea (A. Tselepidis, pers. comm.). Sediment trap experiments put in evidence that the Aegean deep waters exported about $2 \text{ mg m}^{-2}\text{d}^{-1}$ of organic carbon. The POC content in settling material was relatively high (3.5%-12%) indicating a significant organic input to the benthic system; during the period of highest stratification (June-September), near-bottom mean organic carbon fluxes amounted to $1.4 \text{ mg m}^{-2}\text{d}^{-1}$ on the Aegean side and $8.7 \text{ mg m}^{-2}\text{d}^{-1}$ on the Ionian side.

6. Pelagic ecosystem functioning in the Mediterranean Sea shelf areas

6.1 Background

Primary productivity estimates for the whole Mediterranean Sea range between 80 (Sournia, 1973) and $125 \text{ g C m}^{-2} \text{ y}^{-1}$ (Morel and Andr e, 1991; Antoine *et al.*, 1995). Estrada (1996) notes as these productivity estimates agree with the general view of the Mediterranean Sea as an oligotrophic ecosystem, this characteristic being maintained mainly (Hopkins, 1985), but not only (Crispi *et al.*, 2001), by the anti-estuarine thermohaline circulation of the basin and marked by a generalised phosphorus limitation (Berland *et al.*, 1980; Krom *et al.*, 1991; Thingstad and Rassoulzadegan, 1995; Thingstad *et al.*, 1998; Zohary and Robarts, 1998). The latter affects the structure and the functioning of the marine food web (Thingstad and Rassoulzadegan, 1999). In the Mediterranean pelagic system the food web is temporally and spatially dominated by the microbial food web where a large part of the carbon fluxes go through the small phytoplankton, protozoa and bacteria (Thingstad and Rassoulzadegan, 1999; Tanaka and Rassoulzadegan, 2002). The microbial food web is characterized also by phytoplankton-bacteria competition for inorganic nutrients (Thingstad and Rassoulzadegan, 1995; Thingstad *et al.*, 1997) and bacterial carbon production constitutes a significant proportion of the primary production (Turley *et al.*, 2000).

It is within this general ecosystem structure of oligotrophy, phosphorus limitation and microbial food web dominance that the coastal areas of the Mediterranean Sea are embedded.

It has been noted elsewhere in this chapter (see section 2), that in the Mediterranean Sea, two different kinds of coastal areas can be identified in dependence of the extension of the continental shelf (see fig. 1a and Table 1) and the dynamical control by the slope currents (eq. 1). Moreover, for the southern Mediterranean coastal areas, characterized mainly by narrow shelves and by absent (or non significant) river runoff contribution, the open ocean current regime (depicted in section 4) determines the shelf ecosystem productivity, since the upwelling of open ocean waters is the almost unique process providing nutrients to the euphotic zone. Therefore, the ecosystem functioning in the narrow shelf areas is expected to be mostly similar to the pelagic open ocean environment and characterized by a microbial food web dominance.

On the other hand, Mediterranean Sea coastal areas characterized by extended continental shelves have all significant runoff (Catalan shelf, Gulf of Lions area, Northern Adriatic), determining significant input of nutrient and organic matter. Thus they are less influenced by the open ocean pelagic ecosystem structure. The open ocean general circulation affects episodically, but still significantly (see section 5) such areas, in the form of current meanders or intrusions over the shelf. In particular, for extended shelf areas along the northern Mediterranean coastlines, the shelf dynamics is dominated by an overall downwelling vertical motion (see section 4), which does not allow for an internal (to the system) nutrient supply and therefore enhance the role of external nutrient inputs. It should be therefore expected the local ecosystem structure of the extended shelves to be dominated by the so-called "herbivorous" food web (Cushing, 1989), dominated by microphytoplankton (more specifically diatoms) and mesozooplankton.

Fig. 28 gives a schematic representation of the conditions leading to the development of the coastal and oceanic marine ecosystems. In dependence of the physical structure of the water column and of the prevailing limiting factor, the ecosystem structure is "rigidly" shaped into a coastal or open sea structure characterised respectively by the herbivorous and the microbial loop food chains. However, Legendre and Rassoulzadegan (1995) argue that the marine ecosystem might be shaped in a much wider spectrum of conditions (in dependence of changing environmental conditions) along a trophic continuum of which the two ecosystem structures mentioned above represent the two opposite extremes. We argue here that the opposite ends of the ecosystem structure are connected to the different seasons in the Mediterranean, so that the hypothesis of the trophic continuum can be achieved in a temporal sequence during the year. Vichi et al. (2003) shows this concept for the shelf areas of the Northern Adriatic (see section 6.2.3).

The trophic continuum can also be achieved spatially in extended shelf areas, due to the complex interplay of open-sea/coastal processes that take place there. In these shelves, there are sharp and highly variable (in space and time) ecological and biogeochemical horizontal and vertical gradients that could produce the continuum of ecosystem structures between the opposite ends of Fig. 28.

We shall try to demonstrate the above concept with examples from the Algerian coastal area, the Israeli coast, the Gulf of Lions and the northern Adriatic.

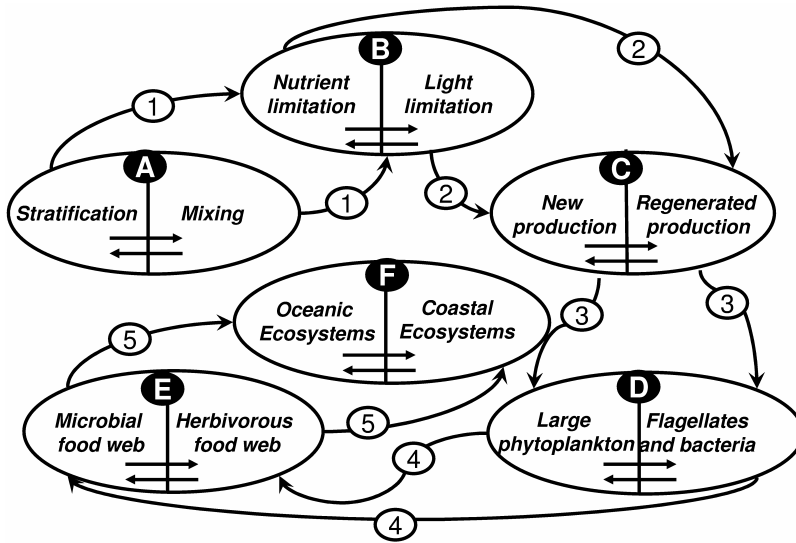


Figure 32.28 Representation of conditions leading to the establishment of a coastal or oceanic pelagic ecosystem. The sequence is a: the water column vertical structure; b: the factors limiting growth; c: the type of primary production; d: the type of organisms; e: the resulting food web; f: the type of ecosystem. Redrawn with modifications from Legendre and Rassoulzadegan (1995).

6.2 Study cases

6.2.1 The Gulf of Lions

Besides the wind, the two primary forcing elements for this region are the discharge of the Rhône River and the Liguro Provençal Catalan (LPC) Current described in 4.2.1. The Rhône annually averaged runoff and nutrient discharge is shown in Table 8 (after Moutin *et al.*, 1998):

The annually averaged vertical distribution of chlorophyll-*a*, phosphate and dissolved inorganic nitrogen concentration ($\Sigma\text{DIN} = \text{Nitrate} + \text{Nitrite concentration}$) along transect 4 of fig. 1a are shown in Fig. 29 in order to highlight differences between the coastal and the open sea domains. The Gulf of Lions appears as an area with a higher upper layers phytoplanktonic biomass (Fig. 29a), decreasing from the shelf to the offshore. The higher primary producers biomass is most probably due to the nutrient input from the Rhône ROFI area, which is particularly evident in the phosphate (Fig. 29b) and (to a lesser extent) in the dissolved inorganic nitrogen distribution (Fig. 29c). The Chlorophyll-*a* distribution also shows the signal of the summer subsurface chlorophyll maximum, a feature common to both the coastal and open sea areas. The slope of the dissolved nutrients iso-surfaces shows the open ocean upwelling, in the centre of the Lions Gyre, the downwelling at its borders, as expected.

TABLE 32.8
 Rhône River annually averaged runoff and P, N and Si discharge into
 the Gulf of Lions. From Moutin et al. (1998)

| Runoff | Total P | Total N | Total Si |
|-------------------|----------|---------|----------|
| m ³ /s | Kt/y | Kt/y | Kt/y |
| 1690 | 6.5–12.2 | 115–127 | 135–139 |

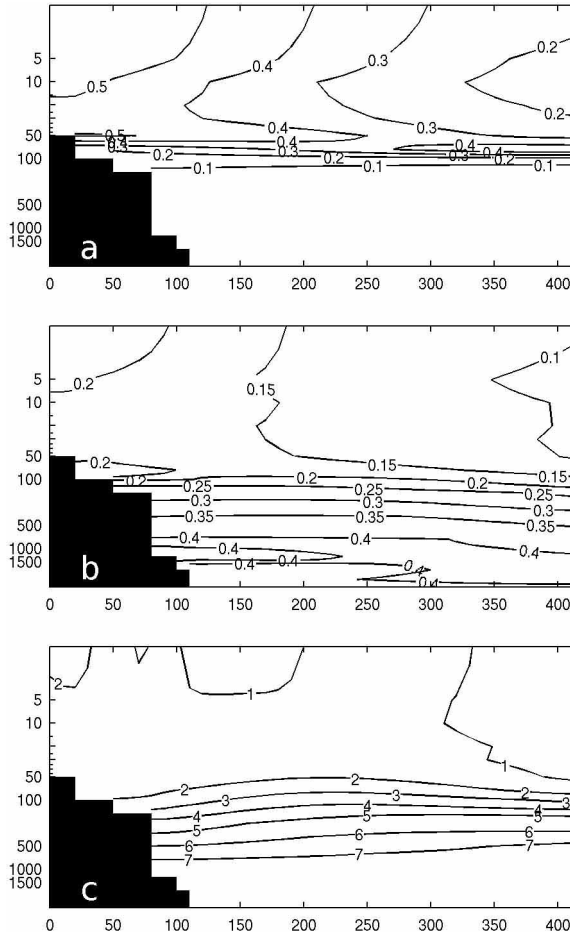


Figure 32.29 Annually averaged vertical distribution of: Chlorophyll-a (a), Phosphate (b) and ΣDIN (c) along section 4 of Fig. 32. 1a (Gulf of Lions). Units are mg m³ for Chlorophyll-a and mmol m³ for ΣDIN and Phosphate. Section starts from the Gulf of Lions (left) and extends into the Liguro-Provençal basin. The vertical scale is logarithmic and the horizontal scale is in km. Data are taken from the Medar (2002) database.

On the basis of primary production characteristics the Gulf of Lions can be divided into 4 distinct sub regions (Lefèvre et al., 1997): The Marseille Gulf, with

low primary productivity rates ($88 \text{ gC m}^{-2} \text{ y}^{-1}$); the Rhône river plume with high primary productivity rates ($300 \text{ to } 1550 \text{ gC m}^{-2} \text{ y}^{-1}$) a dilution zone with primary productivity rates ranging between $86 \text{ and } 142 \text{ gC m}^{-2} \text{ y}^{-1}$ and the shelf break region where the LPC is located, with low primary productivity rates, but with local phenomena of relatively high production (up to $500 \text{ gC m}^{-2} \text{ y}^{-1}$ in coincidence of frontal areas where the LPC and the dilution area waters meet). The seasonal production cycle has been investigated by Conan *et al.* (1998a, b) and characterised by three distinct periods: 1) a winter period with variable production, 2) a late winter surface phytoplankton bloom, 3) a summer period with average productivity rates and with a clear subsurface chlorophyll maximum. The Rhône plume spatial and temporal variability is highly dependent on local meteorological conditions (wind) and on the magnitude of the river outflow (Broche *et al.*, 1998). In the Rhône plume area Chlorophyll-concentrations are constant at about 1 mg m^{-3} without any marked seasonal variability (Morel and André, 1991); however, primary production (Minas and Minas, 1991) and nutrient concentration (Bianchi *et al.*, 1999) decline from the mouth of the river to offshore (Minas and Minas, 1991).

The phytoplanktonic population is constituted in almost equal proportions by pico-nanoplankton and microplankton (Owens *et al.*, 1989; Videau and Levanu, 1990; Woodward *et al.*, 1990). Moreover, in the transition zone between the plume and the offshore, a strong variation in the Bacterial-C/Phytoplankton-C ratio (Yoro *et al.*, 1997) and high concentrations of microzooplankton are observed (Gaudy, 1990). These findings are calling for an ecosystem structure with a significant microbial component and this seems also confirmed by the results of the study on the Rhône river plume microbial communities carried out by Naudin *et al.* (2001) that are indicating the occurrence in the plume of competition for nutrients between phytoplankton and bacteria.

Another feature typical of the Mediterranean pelagic ecosystem that is also present in the Gulf of Lions is the occurrence of phosphorus limitation. Diaz *et al.* (2001) found very strong evidence (fig. 30) for phosphorus limitation (N:P ratios higher than the Redfield value and even higher than the value proposed by McGill, 1969 for Mediterranean water) all over the Gulf, in the plume region and in the dilution area, intermittently affected by the river discharge and by the LPC. Although they did not carry out any measurement of the bacteria activity they could not rule out the possible role of bacteria competition for inorganic P in establishing the Phosphorus limitation condition.

In conclusions, the Gulf of Lyons extended shelf area is an example of heterogeneous environmental conditions, between open ocean and ROFI, where the ecosystem functioning is particularly homogeneous in spite of the large differences in primary production biomass and rates. In all parts of the shelf in fact, phosphorus limitation dominates and bacterial food web is an important component of the ecosystem, together with a mixture of micro and nanophytoplankton communities.

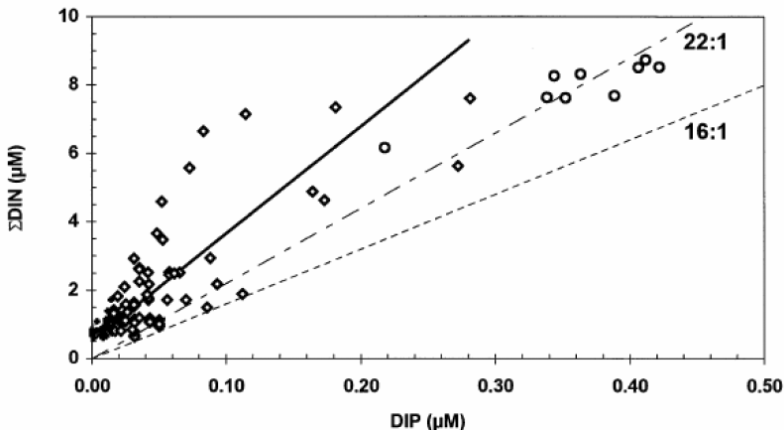


Figure 32.30 Σ DIN versus Phosphate (DIP) relationship. (○) 0–150 m layer. (◇) 200–400 m layer. Solid line represent the linear regression of data in the 0–150 m layer. Dashed and dashed-dotted lines indicate the 16:1 and 22:1 ratios respectively. From Diaz et al. (2001). Reprinted with permission.

6.2.2 The Algerian Coastal area

The Annually averaged vertical distribution of chlorophyll-a Phosphate and Σ DIN along transect 2 of Fig. 1a is shown in Fig. 31. The distribution of such properties confirm that in the case of narrow shelves, the open ocean nutrient and primary production characteristics extend over the shelf. In Fig. 31 the coastal areas as well as the open ocean have a noticeable subsurface Chlorophyll-a maximum (Fig. 31a). The largest difference between the near shelf areas and the open ocean can be noted in the intensity of the subsurface chlorophyll maximum (30–50 m depth) that is marked by higher concentrations in the vicinity of the Algerian coast.

The nutrient distribution (Figs 31b, c) is uniformly low between the shelf and the open ocean and the values are similar to the one present in the open ocean area in front of the Gulf of Lions. However, the Σ DIN concentrations are larger in the Algerian basin than in the Gulf of Lions area, hinting to a larger phosphorous limitation mechanism at work in this region.

As we said in section 4.2.2, the circulation feature strongly affecting this narrow shelf is the Algerian current (Millot, 1985, see also Fig. 16), which flows on the slope and the anticyclonic eddies that may induce coastal upwelling phenomena (Millot et al., 1990b). These processes are not shown in Fig. 31 since it is a climatological picture. A detailed study on the trophic characteristics of the Algerian current under all the physical features summarized above was carried out by Mörán *et al.* (2001). Their results point to a strong coupling of the marine ecosystem functioning (autotrophic and heterotrophic production) with the mesoscale dynamics. They show that the presence of mesoscales can induce nutrient increase in the upper layers and a consequent increase of primary producer biomass and production rates (Fig. 32). The primary production rates were found slightly higher (but comparable) to the values given for the open western Mediterranean waters. The bacterial biomass accounted for a significant source of carbon for the higher trophic levels. These two findings provide a further confirmation that in reduced

extension shelf areas the coastal ecosystem functioning is strongly constrained by the ecological characteristics of the open sea waters.

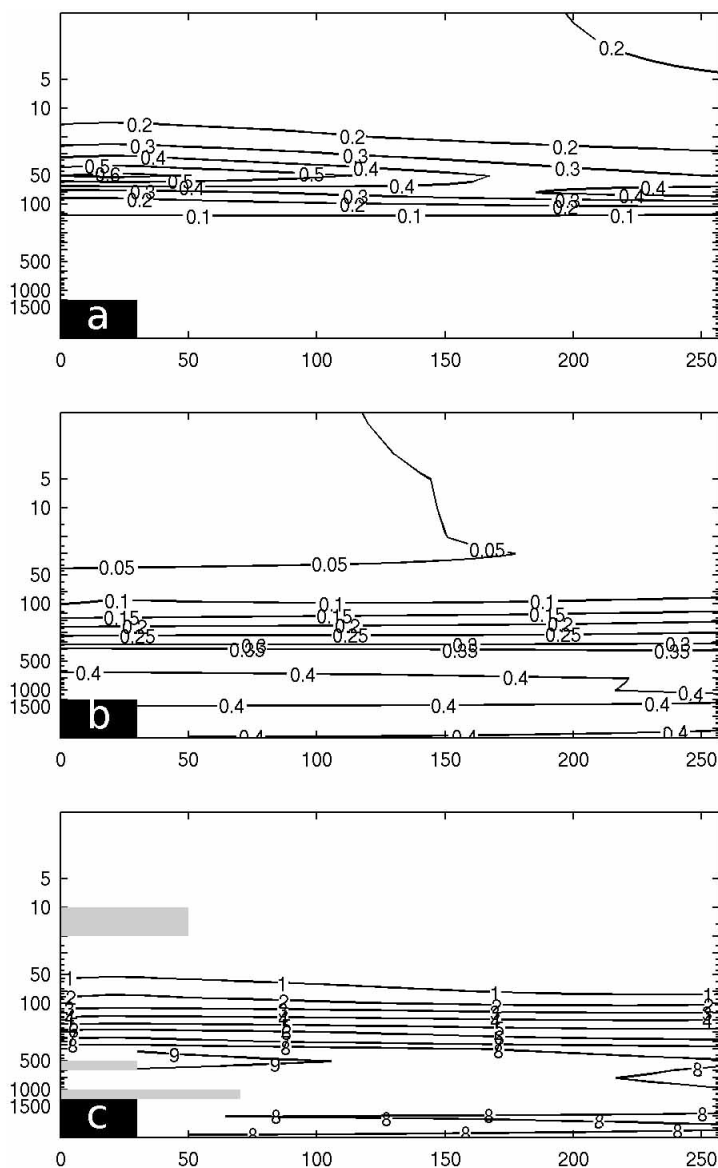


Figure 32.31 Annually averaged vertical distribution of: Chlorophyll-a (a), Phosphate (b) and Σ DIN (c) along section 2 of Fig. 32. 1a (Algerian current region). Units are mg m⁻³ for Chlorophyll-a and mmol m⁻³ for Σ DIN and Phosphate. Section starts from the Algerian coast (left) and extends into the Algerian basin. The vertical scale is logarithmic and the horizontal scale is in km. Data are taken from the Medar (2002) database. Grey shaded areas denote lack of data.

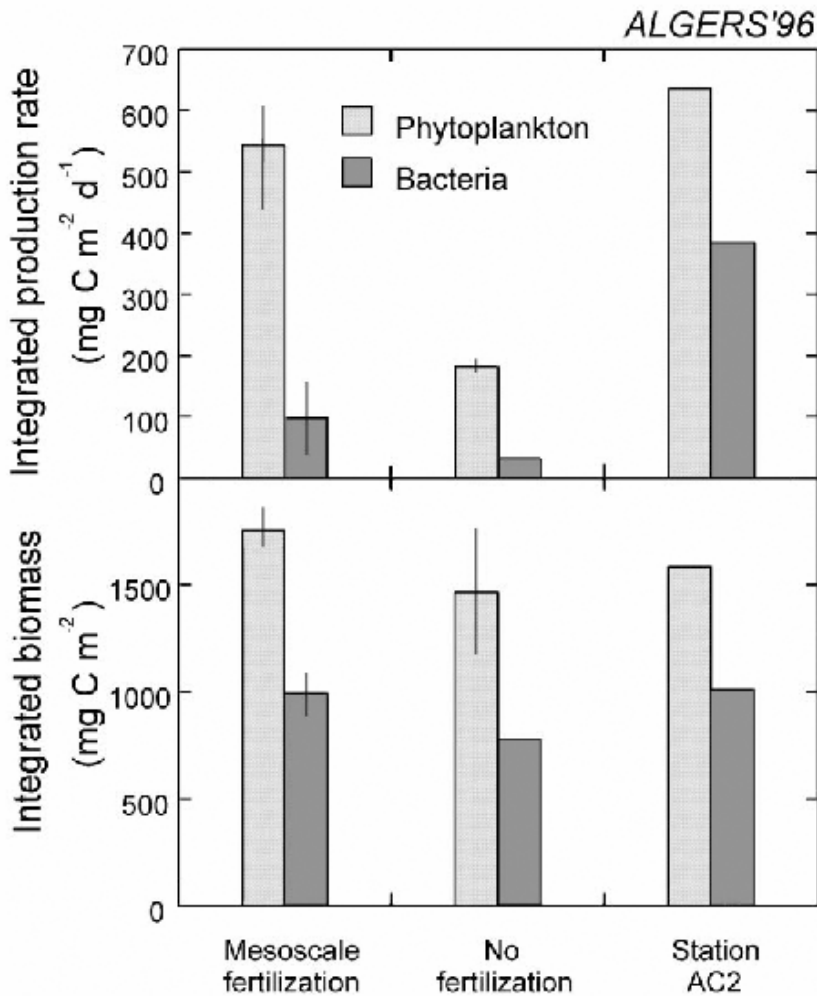


Figure 32.32 Averaged integrated values of phytoplanktonic and heterotrophic bacterial biomass and production under different hydrodynamic conditions in the Algerian basin: with and without mesoscale mechanism of fertilization. (Mòran et al., 2000). Station AC2 is a fixed station in the Algerian basin. Reprinted with permission.

6.2.3 The Sicily Strait area

The productivity of this area is not very well known and is generally considered moderate to low, which is somehow in contrast with the development of an intensive fishery, as we will discuss in section 7. In Fig. 33 we show the distribution of the chlorophyll, phosphorous and total inorganic nitrogen along the two transects across the Strait, called 6 and 7 in Fig. 1a. Both transects are characterized by a subsurface chlorophyll maximum but the amplitude of the maximum is reduced between the western and eastern transect, following the general oligotrophic gradient of the basin. The subsurface chlorophyll maximum is generally spread across

the transect 6 while along transect 7 the absolute maximum is present in the shelf region between Malta and Sicily (Fig. 33d). On the other hand, the chlorophyll abundance seems to spread toward the surface on the Tunisian side of the west-ernmost transect of the Strait bringing further evidence of the connection between Algerian current nutrient enrichment and local production.

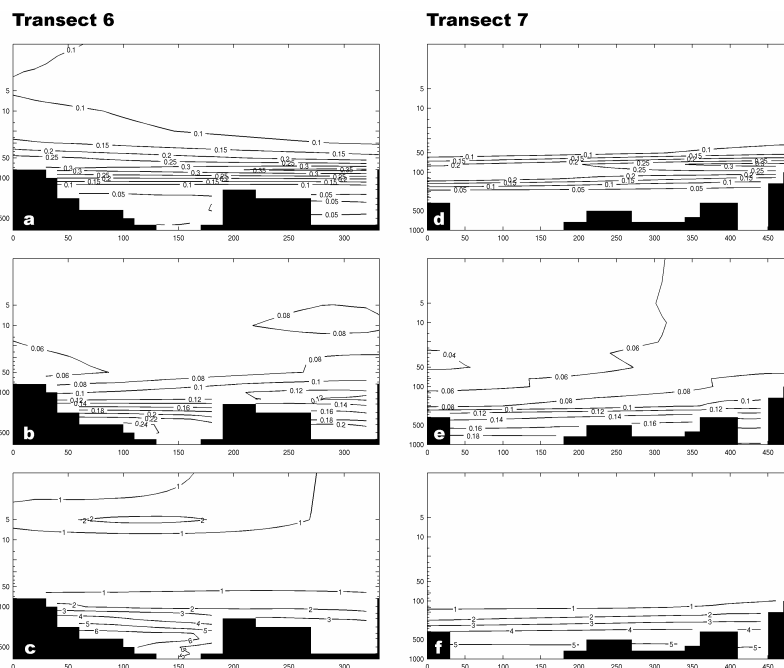


Figure 32.33 Annually averaged vertical distribution of: Chlorophyll-a (a,d), Phosphate (b,e) and Σ DIN (c,f) along transects (6,7) of Fig. 32. 1a (Strait of Sicily region). Units are mg m^{-3} for Chlorophyll-a and mmol m^{-3} for Σ DIN and Phosphate. Section starts from the Tunisian coast (left) and extends to the Sicilian coasts. The vertical scale is logarithmic and the horizontal scale is in km. Data are taken from the Medar (2002) database.

The nutrient concentrations diminish of about 50% in the surface waters going across the Strait in the eastward direction and by 20% in the waters below 100 meters. However, the N:P ratio seems to remain constant in the Strait hinting to an internal regulatory effect on the nutrient ratios in accordance with the absence of river inputs in this area.

It is believed that the Modified Atlantic Waters arriving in this area could be one source of enrichment (Maurin, 1977) as well as upwelling and downwelling zones associated with the Atlantic Ionian Stream-AIS structures that dominate the current flow regime of this area. Agostini and Bakun (2002) describe the general upwelling and downwelling motion generated by the upwelling favourable winds in this area. The Sicilian side of the Strait is the site of powerful upwelling that should increase the productivity of this area. From our transects, it seems however that the subsurface maximum value changes only 10–20% going from the Tunisian to the Sicilian side of the Strait transects. Thus the AIS fertilisation effect may be much larger than the wind upwelling in this region.

6.2.4 The northern Adriatic

As we have seen in section 4.2.3 and 3.3, the northern Adriatic is the northernmost part of the Adriatic Sea strongly affected by riverine fresh water and nutrient inputs. The main river discharging in the northern basin is the Po but smaller rivers are giving a significant contribution of fresh water and nutrients (Degobbi and Gilmartin; 1990, Raicich, 1996. See Table 9).

TABLE 32.9
Northern Adriatic annually averaged runoff and P, N and Si discharge. From Degobbi and Gilmartin (1990) and Raicich (1996).

| | Runoff m ³ /s | Total P Kt/y | Total N Kt/y | Total Si Kt/y |
|---|-----------------------------|-----------------|-----------------|------------------|
| Po river | 1585 | 15 | 162 | 168 |
| All other rivers in the northern Adriatic | 2728 | 28 | 272 | 234 |

The role played by the Po river runoff in forcing the marine ecosystem characteristics is highlighted in Fig. 34. Surface layers in the northern Adriatic are marked by higher concentrations of chlorophyll-a (Fig. 34a) and nutrient concentration (Fig. 34b, c). The signal of the subsurface chlorophyll maximum is particularly evident at depths of about 20–50 m. Note the very small concentration of phosphorous that is four times smaller than the one found in the Gulf of Lions shelf area (Fig. 29) and it is closer to the open ocean values (see Fig. 31). The total nitrogen is however only a factor of two less than in the open ocean bringing us to the conclusion that phosphorous limitation is less severe here than in the open waters. The nutrient isolines are downwelling from the shelf break toward the northern shelf making the process of enrichment from the open ocean not very plausible.

The surface phytoplankton seasonal cycle of the northern, middle and southern Adriatic Sea from satellite observations is shown in Fig. 35. The higher phytoplankton biomass in the northern Adriatic Sea is evident, while the seasonal cycle is characterised by three distinct periods of phytoplankton growth: winter, summer and late autumn, all connected to the Po runoff discharge cycle.

The Po river low salinity and nutrient rich waters are advected south along the WACC (see section 4). The offshore current extension is marked by a strong (salinity dependent) density front. Inflow of higher salinity, nutrient depleted water into the basin occurs along the eastern coast. The magnitude of the southerly inflow is modulated by the strength and intensity of the cyclonic gyres characterizing the circulation (Artegiani et al., 1997, Zavatarelli et al., 2002) as well as the presence of the counter current developing in summertime along the eastern coast of the Northern Adriatic (Supić *et al.*, 2000).

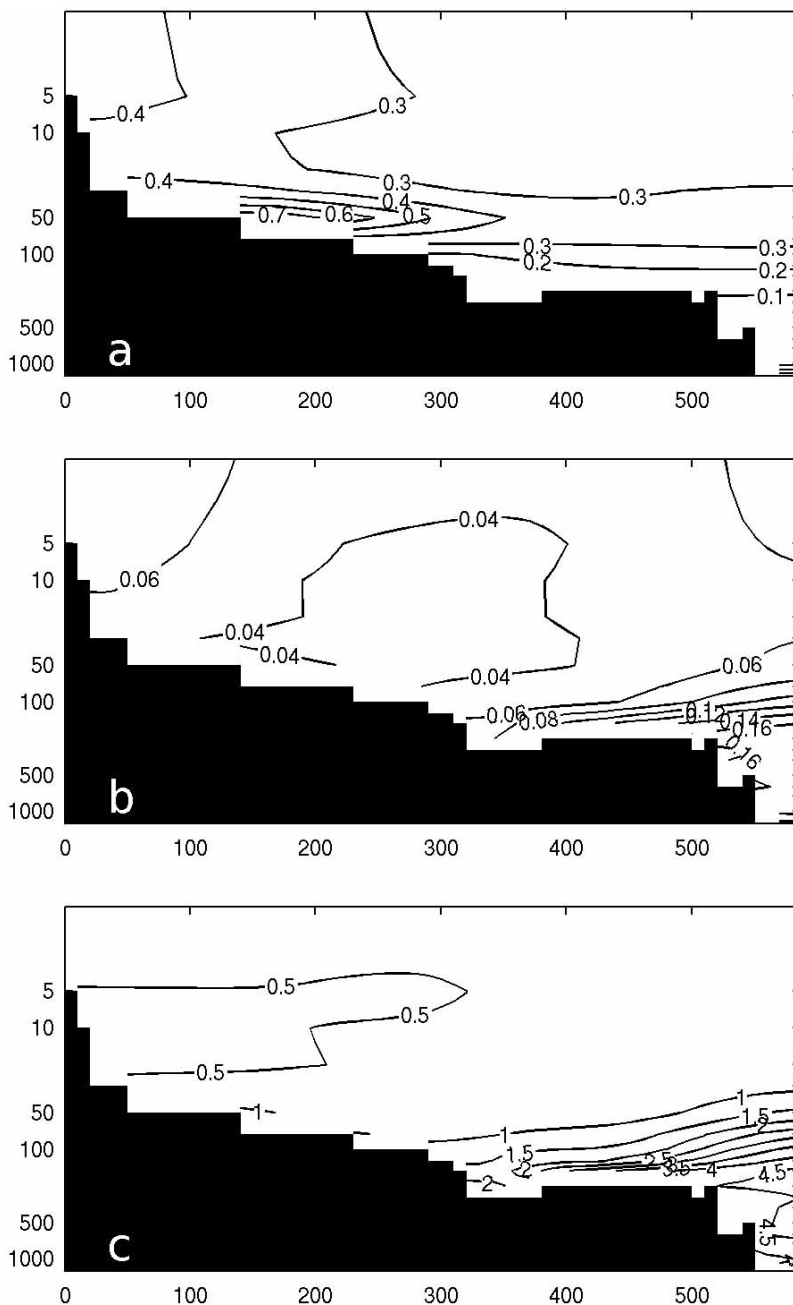


Figure 32.34 Annually averaged vertical distribution of: Chlorophyll-a (a), Phosphate (b) and ΣDIN (c) along section 9 of Fig. 32. 1a (Adriatic Sea). Units are mg m^{-3} for Chlorophyll-a and mmol m^{-3} for ΣDIN and Phosphate. Section starts from the northern Adriatic coast (left) and extends into the Middle Adriatic Sea. The vertical scale is logarithmic and the horizontal scale is in km. Data are taken from the Medar (2002) database.

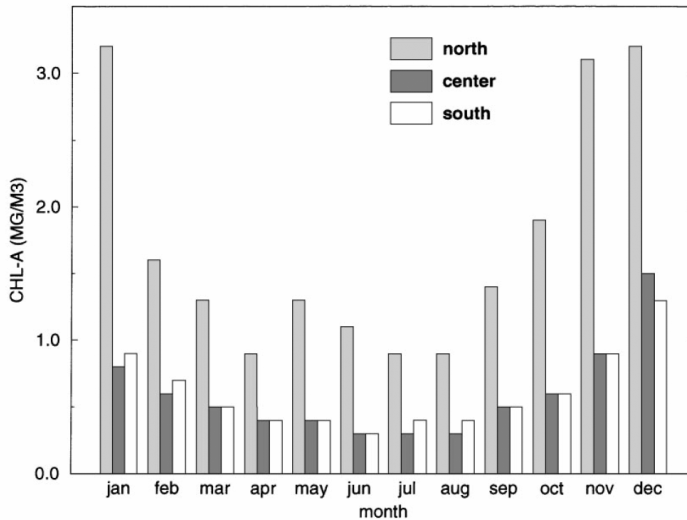
CZCS SURFACE CHLOROPHYLL

Figure 32.35 Monthly averaged surface chlorophyll-a concentration (mg m^{-3}) for the northern (north), middle (centre) and southern (south) Adriatic Sea. From Zavatarelli *et al.* (2000). Reprinted with permission.

It is well known that the western coasts of the northern Adriatic basin suffer from eutrophication phenomena leading to the development of anoxic conditions during the summer season (Vollenweider *et al.*, 1992). The higher biomass production in the western coastal areas is well reflected by the Chlorophyll-a concentration and primary production data reported by Fonda Umani (1996) for the eastern and the western part of the basin (Table 10).

The average phytoplankton biomass in the western part of the basin is about three times higher than in the eastern part and this applies also to the primary production maximum values measured. On the basis of that Fonda Umani (1996) identified two areas: An “open sea” area with low biomass and a western coastal zone with higher biomass separated by a very sharp trophic gradient roughly coincident with the frontal system separating the western coastal current from the offshore water. However, it can be noticed from Table 10, that minimum values in both areas are comparable. This points to a strong variability of the trophic conditions (with shift from the meso-eutrophic to the oligotrophic state) in the area mostly affected by river nutrient input. In fact, potential for phosphorus limitation in the northern Adriatic western coastal area was reported by Zavatarelli *et al.* (1998) in their analysis of the climatological nutrient and biomass seasonal distribution in the Adriatic Sea.

TABLE 32.10

Chlorophyll-a mean values and maximum and minimum of Primary production (^{14}C method) in the western and eastern North Adriatic. From Fonda Umani (1996).

| | Western basin | Eastern basin |
|--|---------------|---------------|
| Chlorophyll-a mg/m^3 | 2.87 | 0.9 |
| PP ($\text{mgC}/(\text{m}^3\text{h})$) | | |
| Max | 30 | 10 |
| Min | <1 | <1 |

The food web structure in the western coastal areas, according to Fonda Umani (1996), has nanophytoplankton as numerically prevailing primary producers, while microphytoplankton (mostly diatoms) has a temporal and spatial distribution highly dependent on the riverine input variability, but in general they have two period of strong abundance (spring and autumn). The nanophytoplankton biomass is mostly grazed by microzooplankton. However, also in this region the role of bacteria as secondary producers and as source of food for microzooplankton is quite important. In the Po delta region Puddu et al. (1998) measured bacterial carbon demand that indicates an organic carbon processing activity by the bacterial compartment comparable (or even larger, in dependence of the riverine dissolved organic carbon input) with the correspondent observed primary production. The Po delta dissolved organic input provides an important carbon source for the microbial food web, whose importance in the northern Adriatic coastal water is further highlighted by the results of the study on the dynamics of the microbial plankton communities carried out by Fonda Umani and Beran (2003) in the Gulf of Trieste. They found that most of the carbon flux in the food web was directed through the microbial compartment through grazing of microzooplankton on heterotrophic nanoflagellates and bacteria.

The occurrence of food web shift mediated by nutrient (phosphate) availability is further highlighted by the results of a one dimensional modelling exercise carried out by Vichi *et al.* (2003) at three different locations in the northern Adriatic Sea (Po river plume, centre of the northern basin, Gulf of Trieste) characterised by different hydrological and environmental conditions. In fig. 36a is shown the ratio between the modelled carbon flow due to herbivorous and to microbial grazers (this ratio has been proposed by Legendre and Rassoulzadegan, 1994, as an index of ecosystem functioning) for each of the three modelled sites. In winter spring the transfer of carbon occur mainly through the herbivorous food chain (ratio > 1), while during the summer season a microbial food web develop (ratio < 1). This shift in the food web structure is matched by a deterioration of the quality of the substrate (dissolved organic matter) for bacteria growth (Fig. 36b), inducing consequently the shift of the microbial community from nutrient remineralizers to competitors for inorganic resources (Fig. 36c).

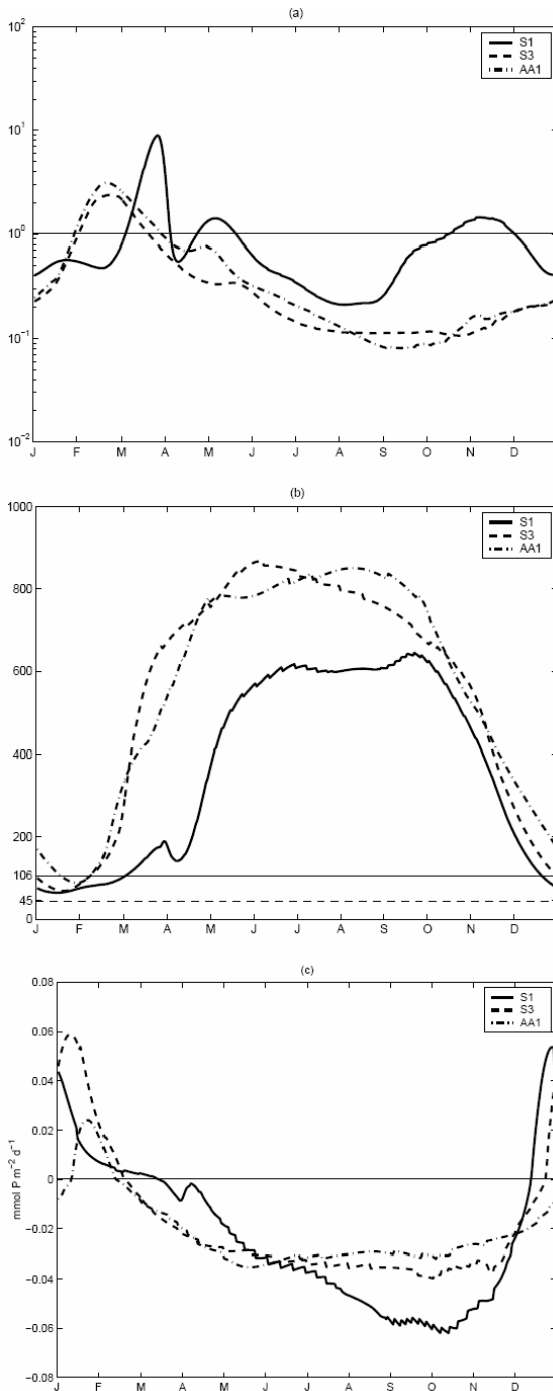


Figure 32.36 Indexes of ecosystem functioning and matter transfer pathways from the one-dimensional modelling of Vichi et al. (2003) at three different locations in the northern Adriatic Sea. S1: Po River plume, S3: Centre of the basin, AA1 Gulf of Trieste. A: ratio between the carbon flow due to herbivorous grazing and the one due to microbial grazing (in semi logarithmic scale). B: ratio between the C- and P-component of the dissolved organic matter. The optimal ratio for phytoplankton (106:1, Redfield et al., 1963) and bacteria (45:1, Goldman et al., 1987) are marked in the plot. C: phosphorus flux between bacteria and phosphate. Positive values indicate active phosphorus remineralization by bacteria. Negative values indicate bacterial phosphate consumption. Reprinted with permission.

6.2.5 The Nile Delta and Israeli shelf areas

Prior to the construction of the Aswan dam the marine ecosystem dynamics of this area was strongly conditioned by the Nile runoff imposing a major phytoplankton bloom in summer-autumn (Sharaf El Din, 1977, Dowidar, 1984) extending from the Egyptian to the Israeli coast (Herut *et al.*, 2000). After the damming the phytoplankton seasonality shifted to a winter bloom period (Berman *et al.*, 1986; Azov, 1986) since the Nile is now regulated to discharge during winter.

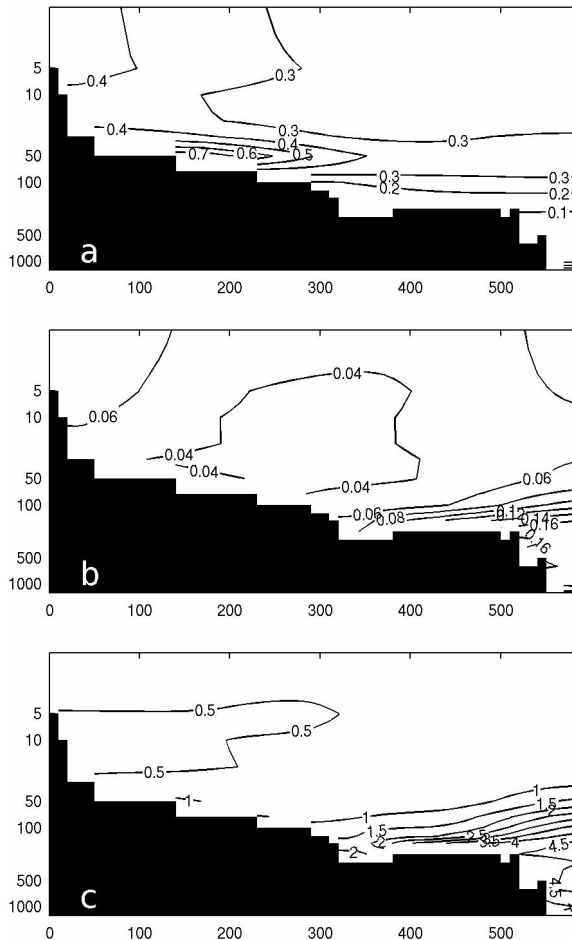


Figure 32.37 annually averaged vertical distribution of: Chlorophyll-a (a), Phosphate and Σ DIN along section 15 of Fig. 32.1a (Nile delta region). Units are mg m^{-3} for Chlorophyll-a and mmol m^{-3} for Σ DIN and Phosphate. Section starts from the Egyptian coast (left) and extends into the eastern Levantine basin. The vertical scale is logarithmic and the horizontal scale is in km. Data are taken from the Medar (2002) database.

The Levantine basin is known to be a severely oligotrophic area (Berman *et al.*, 1984; Krom *et al.*, 1991) controlled by phosphorus limitation. This characteristic

appears to be extended also to the coastal domain (particularly after the Nile damming), as the chlorophyll-a measurements during blooms never exceeded 0.9 mg m^{-3} (Berman *et al.*, 1986; Azov, 1986). This is further confirmed by the annually averaged vertical distributions of Chlorophyll-a, phosphate and ΣDIN along transect 15 of Fig. 1a that are shown in fig. 37, where almost no difference in concentration can be noticed between the coastal and the open sea domain of the transect. Notice also the low values of phosphate and ΣDIN with respect to the western basin transects, almost a factor of two in the deep waters. Notice also the relatively high surface water chlorophyll values extending from the coasts outward, probably connected to the Nile outflow extending far from the coasts. The largest vertical gradients in nutrients starts from the center of the LIW layer, as shown in Fig. 4.12, and located below 100 meters.

The temporal dynamics of the deep phytoplankton bloom is typical of open sea oligotrophic waters with a winter-spring bloom followed by the formation of a deep chlorophyll maximum. No information is available about the bacterial production and it is therefore difficult to assess the main carbon pathways through the trophic web. However the results of Herut *et al.* (2000) seem to indicate for the spring phytoplankton bloom a certain incidence of microphytoplankton (diatoms), but given the extremely oligotrophic conditions of the region it is likely that pico-phytoplankton and the microbial loop play a major role.

7. Exploitation of fisheries resources in the shelf areas

Through history, the coastal area of the Mediterranean Sea has always been very densely populated. It is not surprising that continental shelf areas were and are all subject to intense fishery exploitation. Total marine fishery catches for the Mediterranean are about 1,000,000 tonnes per year (average 1992–2001 GFCM FAO Fishery Statistics Database, (www.fao.org/fi/statist), equivalent to approximately 1% of the total world marine fish catch.

Three main kinds of fisheries resources are exploited in the Mediterranean: demersal and small and large pelagic resources. Small pelagic fish as sardine (*Sardina pilchardus*), anchovy (*Engraulis encrasicolus*), sardinella (*Sardinella* spp.) and mackerels (*Scomber* spp. and *Trachurus* spp.) live in midwater or near the surface in shelf areas and are usually the target of purse seiners and midwater trawlers. Their occurrence is not spread evenly throughout the Mediterranean and is determined by the ecological characteristics of each shelf area. Sardines are predominant in certain areas while in others sardinella or anchovy are more abundant.

Demersal species include fish, cephalopods, crustaceans and bivalves, all living in close proximity to the seabed shelf and slope areas, where they are exploited by bottom trawl fisheries. Up to about 100 demersal species are commercially exploited even if most of the catches comprise a pool of less than 20 species (Papacostantinou and Farrugio, 2000): red mullets (*Mullus barbatus* and *Mullus surmuletus*), sole (*Solea solea*), gurnards (*Trigla* spp.), poor cod (*Trisopterus minutus capelanus*), angler fish (*Lophius* spp.), shrimps (*Penaeus kerathurus* and *Parapenaeus longirostris*), spiny lobster (*Palinurus elephas*), cuttlefish, squids and octopuses (*Sepia* spp., *Loligo* spp., *Eledone* spp. and *Octopus vulgaris*). Some important demersal resources extend their range from the shelf to the slope, such as hake (*Merluccius merluccius*) and Norway lobster (*Nephrops norvegicus*).

Large pelagic fishes include tuna like fishes and pelagic sharks. Their share of the total catch is only about 4% (Leonart and Recasens, 1996) but their economic importance is much higher. They are highly migratory open sea species, which cannot be considered strictly fishery resources of the shelf areas and thus will not be treated here.

Although the Mediterranean is an oligotrophic sea, it sustains some locally very important fisheries, suggesting that there are areas with substantial organic production (Bakun and Agostini, 2001). These areas are mainly shelf areas where river runoff is important, such as the Catalan Coast (Ebro river), the Gulf of Lions (Rhône river), the Adriatic Sea (Po river), the northern Aegean (Thracian rivers and Marmara Sea waters). These northern Mediterranean shelf areas have well developed fisheries, whereas on the southern side of the Mediterranean the situation appears to be quite different.

The main fishery area on the southern side is the Sicilian channel and the north-African shelf off Tunisia and Libya (Charbonnier and Garcia, 1985) where river runoff is absent. The Eastern basin is very oligotrophic and the only important shelf fishery, located on the Egyptian shelf, has been heavily affected by the closure of the Nile outflow by the Aswan Dam (Wadie, 1982). Levi and Troadec (1974) pointed out that fish productivity tends to decrease from west to east and the rate of fishery exploitation is higher along the northern Mediterranean coasts and lower along the southern and eastern coasts. Biodiversity shows the same negative gradient eastwards (Garibaldi and Caddy, 1998).

Research on the links between oceanographic characteristics of the different shelf areas and fishery resources is not particularly advanced in the Mediterranean. Here we shall try to give an overview of the current status of knowledge analysing examples of fisheries exploiting shelf areas with different physical and oceanographic characteristics. Narrow shelf areas with nutrient inputs coming from upwelling and/or by advection from other areas like the Algerian shelf; medium-sized shelf areas where nutrients come from river runoff and upwelling phenomena like the Gulf of Lions; large shelf areas with (Adriatic) and without (Tunisian shelf and Sicilian channel) important river runoff; and finally a shelf area where nutrient input from river runoff has been artificially interrupted by man-induced changes (Egyptian shelf area).

We argue that higher fishery production in the Mediterranean is found in correspondence of substantial river runoff, although upwelling phenomena can be locally important (Bakun and Agostini, 2001). Each area will be briefly described in terms of the main fisheries taking place and the most important species captured. For this purpose, official landings statistics for the Mediterranean (GFCM Statistics database) were used. Specific process studies trying to link fish production to oceanographic features will be reviewed. These are mostly, if not exclusively centred, on small pelagic fish like anchovy (*Engraulis encrasicolus*) and sardine (*Sardina pilchardus*) two species which, due to their abundance and economic importance, have been the object of more detailed ecological research.

7.1 Processes and study cases

7.1.1 Gulf of Lions

The Gulf of Lions is one of the shelf areas with the highest productivity in the Mediterranean thanks to various mechanisms of fertilisation (see sections 4, 5 and 6) such as the permanent front which extends from the Ligurian Sea to Catalonia (associated with the Liguro-Provencal current), the river Rhone runoff, the process of large scale Ekman upwelling associated the prevailing winds and other more localised oceanographic phenomena (Caddy and Oliver, 1996; Bakun and Agostini 2001). This area is exploited mainly by Spanish and French trawlers but also by longliners, gillnetters and purse seiners, and there is a highly developed small scale fishery in inshore waters and lagoons (Papacostantinou and Farrugio, 2000). Average annual total landings in the period 1992–2001 were about 37,000 tonnes. The most important species, or groups of species, account for 80% of the total landings and are reported in Table 11.

TABLE 32.11
Average annual landings (1992–2001) in the Gulf of Lions divided by representative species or group of species (source GFCM Fishery Statistics database).

| species | scientific name | average landings 92–01 | |
|-------------|---|------------------------|----|
| | | tonnes | % |
| sardine | <i>Sardina pilchardus</i> | 12216 | 33 |
| anchovy | <i>Engraulis encrasicolus</i> | 7251 | 20 |
| hake | <i>Merluccius merluccius</i> | 2608 | 7 |
| mackerels | <i>Scomber</i> spp.; <i>Trachurus</i> spp. | 2583 | 7 |
| cephalopods | <i>Octopus</i> spp.; <i>Loligo</i> sp. etc. | 1751 | 5 |
| mulletts | <i>Mugilidae</i> | 817 | 2 |
| poor cod | <i>Trisopterus minutus capelanus</i> | 717 | 2 |
| conger | <i>Conger conger</i> | 601 | 2 |
| angler | <i>Lophius</i> spp. | 403 | 1 |
| sole | <i>Solea</i> spp. | 321 | 1 |
| red mullets | <i>Mullus</i> spp. | 275 | 1 |
| total | | 29541 | 80 |

Small pelagic fishes like sardine and anchovy represent over than 50% of total landings and are caught both by purse seiners and trawlers. Anchovy ranks second in landings but it is by far most sought by fishermen, its price per unit landed being much higher than sardine. Sardine probably is still under exploited.

The peak spawning period for anchovy in this region is June-July (Garcia and Palomera, 1996) and eggs are mostly distributed along the shelf border from 10 to 50 miles offshore (fig. 38). Anchovy eggs are always mainly found in the first 20 m of depth, but larvae are found in day time from 20 down to 40–60 m depth (Olivar et al., 2001). This may be linked to feeding behaviour since during the summer nutrients at the surface are depleted because of the strong thermal stratification, and microzooplankton is concentrated close to the Deep Chlorophyll Maximum at 40–60 m depth (Estrada and Salat, 1989).

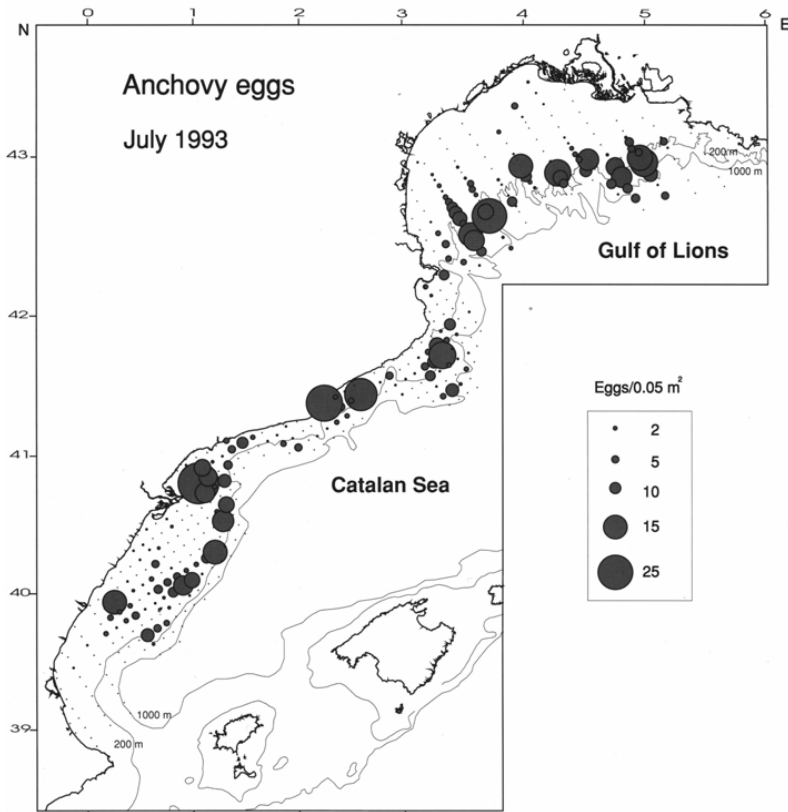


Figure 32.38 Spawning area of anchovy in the Gulf of Lions and Catalan sea (from Garcia and Palomera, 1996). Reprinted with permission.

The presence of the shelf slope front (Sabates 1990) and the corresponding distribution of eggs suggests that the enhanced productivity associated with the front may be exploited by anchovy (Garcia and Palomera, 1996). Agostini and Bakun (2001) proposed that the massive Rhone river outflow enriches the surface waters in the shelf slope front area, where eggs and larvae mostly live (Olivar et al., 2001). The shelf-slope front has here an effect of retention of the nutrients and thus of enhancement of the primary and secondary production which in turn supports larvae growth and survival. In addition, river flow enhances water column stability by stratification and the need for this stability is a general feature of anchovy spawning grounds throughout NW Mediterranean (Palomera, 1992).

Continental, relatively fresh surface waters formed in the Gulf of Lions (*CIW Continental Influence Water*) have higher nutrient and phytoplankton concentrations than adjacent oceanic waters (Cruzado and Velasquez, 1990), as well as higher densities of microzooplankton and copepods (Tudela and Palomera 1995). These waters offer a spawning ground for anchovy, larvae and following the south-westward direction of the Liguro-Provençal current, they could be exported from

the Gulf of Lions to the Catalan coast, where another important fishery for anchovy takes place (Castellon et al., 1985; Sabates et al. 2001).

Sardine is a winter (October to May) spawner in the Mediterranean. In the Gulf of Lions, larvae in November tend to aggregate in the region near the Rhone river delta where water circulation is mainly wind driven (Rasoanarivo et al. 1991). Westerly winds in this season concentrate nutrients of fresh water origin in the coastal areas (Travers and Travers, 1972) promoting phytoplankton production, which is utilised by sardine larvae as a source of food.

In this area, anchovy is more influenced by river runoff in connection with the shelf-slope front in summer while sardine is reliant upon inshore water circulation of freshwater origin in winter. In both cases the nutrient enrichment effect of freshwater inflow seems to be crucial for sustaining these two important commercial fish populations. This has been recently confirmed for the adjacent Ebro river delta area by Lloret et al. (2004) by means of time series analysis of anchovy and sardine landings in relation to river run off and wind mixing.

7.1.2 Algerian shelf

This area of narrow shelf is exploited by purse seiners for small pelagic fish together with some mid-water trawlers fishing the same resources. Demersal species are fished by small scale, fixed gear fleet on rocky areas while trawlers exploit rather heavily the narrow trawlable areas (Caddy and Oliver, 1996). The constant inflow of Atlantic surface waters is an important source of nutrients and thus of fish productivity (Levi and Troadec, 1974). In addition, the Algerian coast is an area of coastal downwelling during the winter season (Bakun and Agostini, 2001). In summer coastal upwelling can take place locally near anticyclones boundaries (see section 4.2.2 and 6.2.2).

TABLE 32.12

Average annual landings (1992–2001) in the Algerian shelf area by representative species or group of species (source GFCM Fishery Statistics database).

| species | scientific name | average landings 92–01 | |
|---------------|---|------------------------|----|
| | | tonnes | % |
| sardine | <i>Sardina pilchardus</i> | 58406 | 58 |
| sardinellas | <i>Sardinella</i> spp. | 11716 | 12 |
| mackerels | <i>Scomber</i> spp.; <i>Trachurus</i> spp. | 6322 | 6 |
| seabreams | <i>Sparidae</i> | 4754 | 5 |
| marine fishes | | 3153 | 3 |
| crustaceans | | 2890 | 3 |
| bogue | <i>Boops boops</i> | 2689 | 3 |
| anchovy | <i>Engraulis encrasicolus</i> | 2645 | 3 |
| clupeoids | <i>Sardina</i> , <i>Sardinella</i> and <i>Engraulis</i> | 2347 | 2 |
| red mullets | <i>Mullus</i> spp. | 1505 | 2 |
| hake | <i>Merluccius merluccius</i> | 1267 | 1 |
| cephalopods | <i>Octopus</i> sp.; <i>Loligo</i> sp. etc. | 998 | 1 |
| total | | 98692 | 98 |

Average annual total landings in the period 1992–2001 were about 100,000 tonnes. The most important species, or groups of species, account for 98% of the total landings and are reported in Table 12.

The relative importance of the small pelagic fishery is evident; sardine, sardinellas, mackerels, anchovy and clupeoids together reach more than 80% of the total landings. Anchovy landings are rather low compared to sardine and sardinellas and this could be due to the lack of low salinity waters in this region, which has no substantial river outflows. The predominance of small pelagic fish catches is a general feature of the Mediterranean; here it is particularly enhanced by the narrow continental shelf, which limits the availability of suitable habitats for demersal species.

In this region there is a lack of studies on the link between environment and resources and, as pointed out by Caddy (1999), there is a difficulty in defining discrete fish stocks inhabiting narrow shelf areas, which can be a thousand kilometres long and only few kilometres wide. The systems of larval concentration and retention that can be observed or postulated on the basis of the water circulation in the Gulf of Lions or the Adriatic are not likely to be the same for the Algerian shelf and other narrow shelf areas in the Mediterranean. There is a possibility of there being some genetic discontinuity along the shelf, with separate fish stocks of the same species along the coast in correspondence of specific spawning grounds, but no data are available. Detailed research on mesoscale oceanography, larval dispersal, and population genetics is needed to improve the management of these stocks (Caddy, 1999).

7.1.3 Tunisian shelf and Sicily channel

The shelf areas of Tunisia and the Sicily channel are the largest and most productive fisheries of the Mediterranean after the Adriatic (Caddy and Oliver, 1996; see Table 13 below for annual landings). This area sustains an important trawl fishery mainly composed of industrial scale Italian vessels, together with a more coastal but equally intensive Tunisian trawl fishery on the southern part, mostly in the Gulf of Gabes (Papacostantinou and Farrugio, 2000).

As shown in Table 13, the pelagic fishery is not predominant in this area. Landings of sardine, sardinellas, anchovy and mackerels are about 27% of the total and stocks of these species are generally believed to be smaller in proportion to other areas (e.g. Adriatic and Gulf of Lions). Although in the past scientific investigations detected important biomasses of small pelagic fish, this was never reflected in the landings, and could be due to overestimation of biomass or lack of an adequate market for this resource (Papacostantinou and Farrugio, 2000).

The productivity of this area seems to be influenced by the modified Atlantic Waters (Maurin, 1997) as well as upwelling and downwelling areas associated with the Atlantic Ionian Stream (AIS). A recent study (Garcia Lafuente et al., 2002) has linked the general circulation pattern of the AIS to the reproductive strategy of anchovy in the Sicilian Channel (Fig. 39). The current is responsible of advection and retention mechanisms for eggs and larvae. Local, wind induced small-scale upwelling phenomena along the Sicilian coast contribute in terms of nutrient enrichment (Agostini and Bakun, 2002).

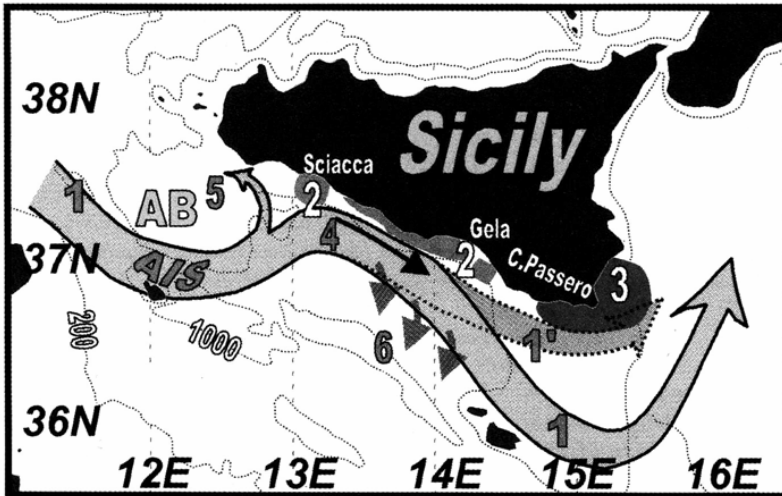


Figure 32.39 Schematic model of the spawning strategy of the Sicilian Channel anchovy (Garcia Lafuente et al., 2002). Main spawning grounds (2), Atlantic Ionian Stream (1 and 1'), eggs and larvae transported downstream (4), main nursery ground of Capo Passero (3), possible offshore advection (5 and 6). Reprinted with permission.

TABLE 32.13

Average annual landings (1992–2001) in the Tunisian shelf and Sicily channel area divided by representative species or group of species (source GFCM Fishery Statistics database). Total landings are about 180,000 tonnes per year.

| Species | scientific name | average landings 92–01 | |
|---------------------|--|------------------------|-----------|
| | | tonnes | % |
| other marine fishes | | 23736 | 13 |
| cephalopods | <i>Octopus</i> sp.; <i>Loligo</i> sp. etc | 21183 | 12 |
| Sardine | <i>Sardina pilchardus</i> | 19611 | 11 |
| Hake | <i>Merluccius merluccius</i> | 16354 | 9 |
| crustaceans | | 15473 | 9 |
| Mackerels | <i>Scomber</i> spp.; <i>Trachurus</i> spp. | 12948 | 7 |
| Seabreams | <i>Sparidae</i> | 9667 | 5 |
| Anchovy | <i>Engraulis encrasicolus</i> | 8881 | 5 |
| Sardinellas | <i>Sardinella</i> spp. | 7855 | 4 |
| red mullets | <i>Mullus</i> spp. | 6808 | 4 |
| sharks and rays | <i>Selachii</i> | 6011 | 3 |
| Bogue | <i>Boops boops</i> | 4321 | 2 |
| Mulletts | <i>Mugilidae</i> | 3975 | 2 |
| Gurnards | <i>Trigla</i> spp. | 2050 | 1 |
| angler fish | <i>Lophius</i> spp. | 1898 | 1 |
| Total | | 160768 | 88 |

The southern area of the Gulf of Sirte and the Gulf of Gabes is rather poor in oceanographic data: high surface values of chlorophyll in the Gulf of Gabes detected by remote sensing have been interpreted as an artefact due to interference from the shallow sea floor (Agostini and Bakun, 2002). On the contrary, we argue that annual Tunisian landings are substantial on a Mediterranean scale (about 70–80,000 tonnes) and mostly come from the Gulf of Gabes and southern areas (Hachemi, 1996). Thus we think that the issue of productivity and nutrients along the Tunisian shelf calls for further research.

Demersal resources are predominant in landings and reflect both the wide continental shelf and the intense trawl fishery that takes place in this area. In Table 13 demersal species comprise 44% of the total, not including the item “other marine fishes” which is probably dominated by demersal species. The presence of sharks and rays in relevant quantity might be considered as an index of lighter exploitation compared to other Mediterranean areas where this group of species has nearly disappeared from landings (Myers and Worm 2003). It is also possible that high yields of demersal species are the result of a lower exploitation compared to other, generally overexploited, Mediterranean shelf areas (Charbonnier and Garcia, 1985). As mentioned before the mechanism sustaining fish productivity in this area is not clear both at pelagic and at demersal species level, and this should be a target for future research in fishery oceanography in the Mediterranean.

7.1.4 Adriatic Sea

The productive Northern and Central Adriatic Sea is characterised by an extended shelf area with muddy or sandy soft bottoms, which are well suited for trawl fishing. The high productivity in this area is a consequence of the strong nutrient outflow from rivers and of an additional input of Mediterranean waters (Papacostantinou and Farrugio, 2000) from the Otranto Strait. The Adriatic has a high productivity of molluscan shellfish (clams and mussels), and a variety of commercial invertebrates and fish (see Table 14). The area is exploited by bottom trawls for demersal resources, pelagic trawls and purse seines for small pelagic fish and an important dredge fishery for clams in the Italian inshore coastal waters.

The clam fishery is perhaps the most valuable monospecific fishery in the Mediterranean and it exploits the area up to one nautical mile offshore (up to a depth of 12–15m), along the Italian coast from Trieste to the Gargano promontory (Frogliia, 1989). The small pelagic fishery is also very important in terms of value and landings, with anchovy being the most sought species. Traditionally anchovy is caught mainly along the more productive, less saline western Adriatic waters by the Italian fleet, and sardine is the main target of eastern Adriatic fishermen and it is generally more abundant in less productive and more saline eastern waters. Demersal resources are exploited all over the continental shelf and species distribution is influenced more by the change in the sediments (mud to sand eastward) than by the very gentle decrease in depth.

TABLE 32.14
Average annual landings (1992–2001) in the Adriatic divided by representative species or group of species (source GFCM Fishery Statistics database). Total landings are about 130,000 tonnes per year.

| Species | scientific name | Average landings 92–01 | |
|---------------------|---|------------------------|----|
| | | tonnes | % |
| Sardine | <i>Sardina pilchardus</i> | 30133 | 22 |
| Clam | <i>Chamelea gallina</i> | 28177 | 21 |
| Anchovy | <i>Engraulis encrasicolus</i> | 25910 | 19 |
| cephalopods | <i>Octopus</i> sp.; <i>Loligo</i> sp. etc | 10435 | 8 |
| crustaceans | | 6656 | 5 |
| other marine fishes | | 6008 | 4 |
| Hake | <i>Merluccius merluccius</i> | 4475 | 3 |
| Mackerels | <i>Scomber</i> spp.; <i>Trachurus</i> spp | 3474 | 3 |
| red mullets | <i>Mullus</i> spp | 2879 | 2 |
| Mulletts | <i>Mugilidae</i> | 2194 | 2 |
| Sole | <i>Solea solea</i> . | 1395 | 1 |
| Seabreams | <i>Sparidae</i> | 1180 | 1 |
| shark and rays | <i>Selachii</i> | 912 | 1 |
| Total | | 123829 | 91 |

The nutrient inputs in the Adriatic are dominated by the Po River and the other northern Italian rivers: these inputs are constrained by the Western Adriatic Coastal Current-WACC to flow along the Italian coast where downwelling motion prevails (see section 4.2.4). On the eastern side of the Adriatic Sea wind induced upwelling prevail due to the climatological wind conditions (Agostini and Bakun, 2001; Cushman-Roisin et al., 2001). These two oceanographic features are linked with the reproductive biology of the two most important small pelagic species, anchovy and sardine.

Anchovy mainly spawns on the western part of the Adriatic (Regner, 1996, fig. 40). This area covers the shallow northern Adriatic waters and the zone along the western coast, down to the Gargano peninsula and corresponds to the area of highest nutrient inputs and primary productivity. There are other spawning areas along the eastern Adriatic coasts but the intensity of spawning is substantially lower (Regner, 1996). Anchovy spawns from April to October with peaks between May and September and, in general, maximum egg production occurs earlier in open waters than in coastal areas. In general little is known about the shifting of spawning centres during the spawning season, the transport of larvae by the circulation of Adriatic surface waters and the various environmental factors, which could affect larval survival. Recently Coombs et al. (2003) studied anchovy spawning and larval distribution associated with the Po river plume, and described the region around the Po river mouth as favourable to survival of anchovy larvae partly because of the additional water column stability caused by the low salinity river outflow. Despite this, a strict relationship between enhanced water column stability and increased survival of anchovy larvae could not be proven. Eggs are released inshore and offshore but late post-larvae and early juveniles are found only along the Italian coast from September to January. The Western Adriatic Coastal Current (WACC, see paragraph 4.2.4) probably plays a major role in the

transport of larvae and post-larvae from spawning to nursery ground but a detailed investigation is needed.

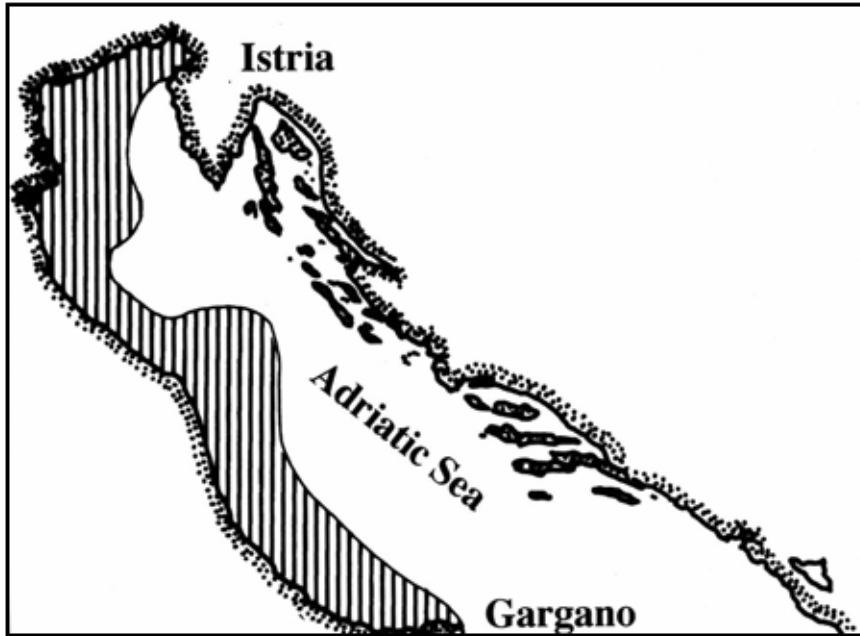


Figure 32.40 The main spawning areas of the Adriatic anchovy (Regner, 1996) shown by dashed areas. Reprinted with permission.

Sardine is a winter spawner in the Mediterranean and in the Adriatic it spawns from Autumn to Spring at temperatures ranging between 9 and 15 °C in the open water zone of the Adriatic (Gamulin and Hure, 1955). Two main spawning centres (see Fig.7.4) exist: a northern one between Ancona and Zadar and a southern one in the area of the Pelagosa Island (Fig. 9, Regner et al. 1987). These main spawning centres are located in oligotrophic areas and, as observed by Regner et al. (1988), temperature might act as a boundary, impeding sardine to spawn in the richer but colder western Adriatic waters in winter. Within the spawning season, the maximum of egg production is in Autumn; immediately along the frontal zone between the western cold waters and the warmer but poorer eastern waters. Sardine tends to spawn at the boundaries of these two zones until temperatures fall below 10 °C; Subsequently sardine moves to the less productive waters along the eastern coast where most intensive spawning has been observed in correspondence with local upwelling phenomena (Regner et al., 1987). On the basis of these observations, Regner et al. (1987) proposed a pattern of spawning and transport of sardine larvae along the eastern side of the Adriatic, which is reported in fig. 41.

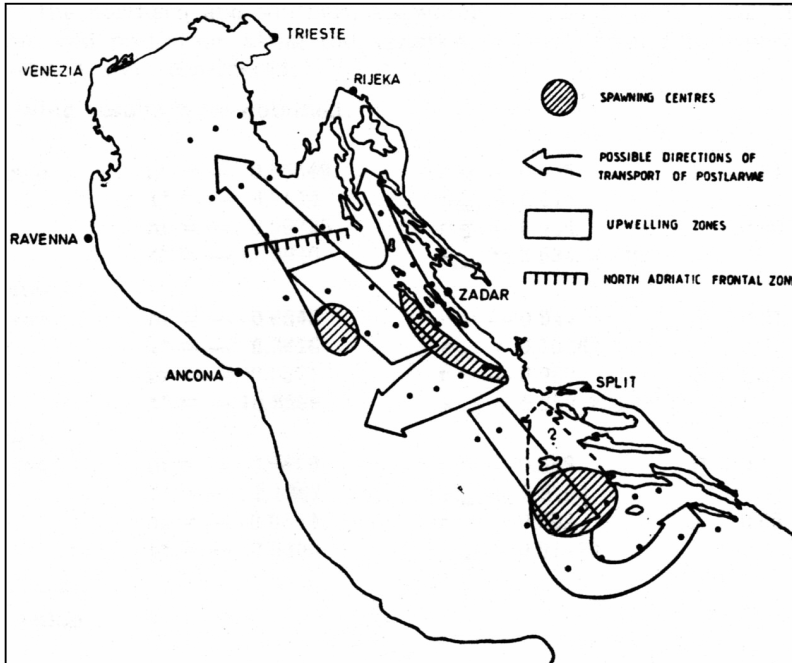


Figure 32.41 Supposed pattern of transport of sardine larvae and post-larvae (Regner et al., 1987). Reprinted with permission.

Spawning centres in fig. 41 should be considered as “main” spawning centres, because sardine eggs are found in most of the Adriatic. The hypothesis is that sardine, within its physiological range of water temperatures, concentrate to spawn in zones enriched either by the mixing of different water masses as frontal areas, or in zones enriched by local upwelling phenomena. Larvae are then transported by the main cyclonic Adriatic circulation or by local gyres that can carry the larvae over the western Adriatic side.

Demersal species are of high economic importance but in general their stock size and landings are not comparable with anchovy and sardine. The Adriatic bottom trawl fishery exploits a pool of species (Table 14) including cephalopods (octopus and cuttlefish), crustaceans (Norway lobster and mantis shrimps), hake, red mullets etc .. The high importance of cephalopods in the catches may be related to the intense exploitation of the demersal resources, with a shift of species composition from long lived (sharks and large ichthyophagous fishes) to fast growing and short lived predators like cephalopods, and planktivorous pelagic fishes (Pauly et al., 1998). For some of the demersal resources of the Adriatic (e.g. Norway lobster, hake and red mullet) general biological parameters, spawning and nursery areas are well known, as well as reproductive periods, although there is a lack (as for most of the Mediterranean) of detailed investigation aimed at clarifying the links between marine environment and population ecology.

7.1.5 Egyptian shelf

This area has a low level of biological productivity due to the low nutrient concentration. The fishing fleet is composed mainly of small-scale vessels, medium size trawlers and purse seiners (Caddy and Oliver, 1996). Before the construction of the Aswan dam the river Nile provided seasonal inflow of sediment and nutrients (see also sections 3.2.1 and 3.2.2). The dramatic reduction of Nile river flow drastically reduced nutrient inflow and had an immediate impact on primary production, small pelagic resources and also demersal resources as shrimps (Bebars and Lasserre, 1983; Wadie and Abdel Razek, 1985).

The small pelagic fishery exploits sardinellas, sardine and round herring (*Dussumieria acuta*) a lessepsian migrant species, which has made its entrance from the Red Sea in the last decades. This fishery uses purse seines (Wassef et al., 1985.) and accounts for about one third of the total landings (Table 15). Shrimps of the family Penaeidae are second only to sardinella in the Egyptian Mediterranean fishery (Wadie and Abdel Razek, 1985).

TABLE 32.15

Average annual landings (1992–2001) in the Egyptian shelf divided by representative species, or groups of species (source GFCM Fishery Statistics database). Total landings are about 54,000 tonnes per year.

| species | scientific name | Average landings 92–01 tonnes | % |
|-------------------|---|----------------------------------|----|
| sardinellas | <i>Sardinellas</i> spp. | 15689 | 29 |
| Marine fishes nei | | 5287 | 10 |
| shrimps | <i>Penaeidae</i> | 4267 | 8 |
| silversides | <i>Atherinidae</i> | 3254 | 6 |
| seabreams | <i>Sparidae</i> | 2537 | 5 |
| mullet | <i>Mugilidae</i> | 2452 | 5 |
| Bogue | <i>Boops boops</i> | 2205 | 4 |
| red mullets | <i>Mullus</i> spp | 1871 | 3 |
| Marine crabs | <i>Portunidae</i> | 1683 | 3 |
| round herring | <i>Dussumieria acuta</i> | 1403 | 3 |
| Sharks and rays | <i>Selachii</i> | 1323 | 2 |
| cephalopods | <i>Octopus</i> sp.; <i>Loligo</i> sp. etc | 1238 | 2 |
| Total | | 43206 | 80 |

The Aswan damming is a good example of the fact that declines in nutrient-rich runoff will reduce the total catch and the proportion of small pelagic fish it contains (De Leiva Moreno et al. 2000). In the period of the Aswan damming catches of Clupeids dropped by 80% in a few years. The change was induced not only by the reduction in quantity but also by the sudden change in the seasonality of the outflow. A recent recovery of catches took place and seems to be associated to the nutrient outflow of drainage waters from the Nile river delta (Papacostantinou and Farrugio, 2000). The role played by nutrient rich runoff in fisheries production is well established for freshwater system and in some cases in marine ecosystems (e.g. Grimes, 2001). The Egyptian shelf case provided a large-scale experimental

evidence of this fact and calls for a detailed scientific reassessment of the present situation in terms of oceanography and fishery.

8. Final remarks

In this chapter we have carried out a first attempt to classify the main characteristics of the Mediterranean shelf areas in terms of physical, sedimentological and ecosystem structures and variability.

First of all we have described the different shelf structures in terms of their morphological and dynamical shelf extension. From a general point of view, the shelf extension increases going from the southern to the northern shores with the noticeable exception of the Sicily Strait. Most of the Mediterranean shelf areas can be defined as 'narrow' (less than 20–30 km from the near shore area to the 200 m isobath). These narrow shelves are dominated by open ocean/shelf exchange processes. On the contrary, most extended shelf areas are dominated by river inputs that interconnect the shelf dynamics to the hydrological cycle of the Mediterranean basin. Shelf extension as well as precipitation regimes have a pronounced positive latitudinal gradient, which produces the first, large scale structural characterization of the Mediterranean shelves. Important exceptions to this north-south rule exist in the Strait of Sicily and the Nile Delta.

The sediment structure and composition of the Mediterranean is mainly connected to the river inflow in the extended shelf areas. The biogenic productivity of surface waters plays a major role both in the extended and narrow shelves. In narrow shelves the sediments arrive also from remote areas carried by the along slope currents. Atmospheric deposition is also very important along the southern shelves of the Mediterranean (Tunisian, Nile Delta and Israeli shelves).

The overall structure of the general circulation of the basin and its atmospheric forcing imposes a dominant downwelling character to the Mediterranean shelf areas, since the circulation is generally cyclonic in the open sea. However, exceptions to this rule occur in wind induced upwelling areas (Sicily Strait, eastern Aegean Sea and Adriatic Sea) and in eddy forced narrow shelves, such as the Algerian and Israeli coasts. The shelf areas account for 20% of the overall net heat flux at the air-sea interface (not including the northern Adriatic Sea): the shelves emerge as a negative heat flux engine, helping the overall basin to lose efficiently the heat stored, thus confirming the prevalent downwelling dynamics of the shelf areas.

The analysis has been carried out by considering examples of shelf regimes throughout the Mediterranean, both for narrow and extended shelves. We have examined the Gulf of Lions and the Algerian shelf in the western Mediterranean, the Adriatic Sea and the Sicily Strait in the Central Mediterranean, the Nile Delta and the Israeli shelves in the Eastern Mediterranean.

The northern extended shelves (Gulf of Lions and Adriatic) have large sedimentation rates, they are ROFI areas and they work as net CO₂ sinks. The ecosystem dynamics at the level of primary and secondary producers is partially dominated, even in these nutrient rich areas, by a microbial food web. The fish resources are large and they can be connected simply to the higher primary productivity of these areas.

The southern shelves are less productive at all levels of the ecosystem due to the absence of substantial river inputs. However, an exception exists for the Sicily Strait that can only be explained in terms of favourable physical conditions connected to the Atlantic water inflow along the shelf break.

It is possible to conclude that the Mediterranean Sea shelf structure and variability is a composite of site-specific dynamic scenarios, involving different open ocean/shelf exchange mechanisms and strong connections with land derived inputs. The possibility that such a system could be highly variable with the low frequency variability of atmospheric regimes and strongly dependent from the river loads makes it difficult to be modified and managed in the long term.

Acknowledgements

This work was partially funded by the EU Project 'Mediterranean Forecasting System Toward Environmental Predictions' and the Italian Ministry of Environment and Territory through the Project 'ADRIatic sea integrated COastal areaS and river basin Management system pilot project- ADRICOSM'. Two authors, Nadia Pinardi and Marco Zavatarelli, thank the skilful technical support of Dr. Luca Giacomelli and Dr. Claudia Fratianni. Another author, Mariangela Ravaoli, would like to thank Dr. Giovanna Orsini (Marine Science Department- Univ. of Urbino) for help in the bibliography search. All authors would like to express their greatest appreciation to Prof. A.R. Robinson for his suggestions and very helpful comments to an earlier version of the manuscript.

Bibliography

- Agostini V.N. and A. Bakun, 2002. 'Ocean triads' in the Mediterranean Sea: physical mechanisms potentially structuring reproductive habitat suitability (with example application to European anchovy, *Engraulis encrasicolus*). *Fish. Oceanogr.* 11 (3): 129–142.
- Alb rola, C., Millot, C., and Font, J., 1995. On the seasonal and mesoscale variabilities of the northern current during the PRIMO-0 experiment in the western Mediterranean. *Oceanologica Acta*, 18, 2, 163–192.
- Almagor, G., 1993. Continental slope processes of northern Israel and southernmost Lebanon and their relation to onshore tectonics. *Marine Geology*, 122, 151–169.
- Alvisi, F., Ravaoli, M., Frignani, M. and Molducci, M., 2000. The study of climate related short time-scale sedimentation pattern in prodelta areas of the northern Adriatic Sea. *Bollettino Geofisico*, a. XXIII, n  3-4, luglio-dicembre 2000.
- Anati, D. A. and J. R. Gat, 1989. Restricted marine basins and marginal sea environments. *Handbook of Environmental Isotope Geochemistry*, Chapter 2, The Marine Environment, A. Elsevier Science, vol. 3: 29–73.
- Antoine, D., A. Morel and J. M. Andr , 1995. Algal pigment distribution and primary production in the eastern Mediterranean as derived from Coastal Zone Colour Scanner observations. *J. Geophys. Res.*, 100(C8), 16193–16209.
- Argnani, A., 1992. Neogene tectonics of the Strait of Sicily, 1992. In: Max, M.D. and Colantoni, P. (Eds.), *Geological Development of the Sicilian-Tunisian Platform*. UNESCO Reports in Marine Science, Proceedings of International Scientific Meeting, Urbino University, Italy, Nov. 1992., pp. 55–60.
- Arnone, R., and P.E. La Violette, 1986: Satellite definition of the bio-optical and thermal variation of coastal eddies associated with the African current. *J. Geophys. Res.*, **91**, 2, 351–2,364

- Artegiani, A., D. Bregant, E. Paschini, N. Pinardi, F. Raicich and A. Russo, 1997a. The Adriatic Sea general circulation. Part I. Air-sea interactions and water mass structure. *J. Phys. Oceanogr.*, **27**, 1492–1514.
- Artegiani, A., D. Bregant, E. Paschini, N. Pinardi, F. Raicich and A. Russo, 1997b. The Adriatic Sea general circulation. Part II. Baroclinic circulation structure. *J. Phys. Oceanogr.*, **27**, 1515–1532.
- Arz, Helge W., F. Lamy, J. Pätzold, P. J. Müller, M. Prins, 2003. Mediterranean Moisture Source for an Early-Holocene Humid Period in the Northern Red Sea. *Science*, **300**, 118–121.
- Astraldi, M. and Gasparini, G.P., 1992. The seasonal characteristics of the circulation in the north Mediterranean basin and their relationships with atmospheric-climatic conditions, *J. Geophys. Res.*, **97** (C6), 9531–9540.
- Astraldi, M., Gasparini, G.P., Sparnocchia, S., Moretti, M., and Sansone, E., 1996. The characteristics of the water masses and the water transport in the Sicily Strait at long time scales the eastern and western Mediterranean through the Strait of Sicily, *Bulletin de l'Institut Oceanographique*, Monaco, CI-ESM Science Series n. 2, 95–115.
- Auclair, F., P. Marsaleix and C. Estournel, 2001. The penetration of the northern current over the Gulf of Lions (Mediterranean Sea) as a downscaling problem. *Oceanol. Acta*, **24**, 529–544.
- Ayoub, N., Le Traon, P.-Y. and De Mey, P., 1998. A description of the Mediterranean surface variable circulation from combined ERS-1 and TOPEX/POSEIDON altimetric data. *J. Mar. Syst.* **18**:3–40.
- Azov, Y., 1986 Seasonal patterns of phytoplankton productivity and abundance in nearshore oligotrophic waters of the Levant basin (Mediterranean). *J. Plankton Res.*, **8**, 41–53.
- Bakun, A. and V. N. Agostini, 2001. Seasonal pattern of wind induced upwelling/downwelling in the Mediterranean Sea. *Sci. Mar.*, **65**, 243–257.
- Bebars, M. I. and G. Laserre, 1983. Analyse des captures des pêcheries marines et lagunaires d'Égypte de 1962 à 1976, en liaison avec la construction du haut barrage d'Assouan achevé en 1969. *Oceanol. Acta*, **6**, 417–426.
- Benninger, L.K., Suayah, I.B. and Stanley, D.J., 1998. Manzala lagoon, Nile delta, Egypt: modern sediment accumulation based on radioactive tracers. *Environmental Geology*, **34** (2/3), 183–193.
- Berland, B. R., D. Bonin, and S. Y. Maestrini, 1980. Azote ou phosphore? Considérations sur le paradoxe nutritionnel de la Méditerranée. *Oceanol. Acta*, **3**, 135–142.
- Berman, T., D. W. Townsend, S. Z. El Sayed, C. C. Trees and Y. Azov, 1984. Optical transparency, chlorophyll and primary productivity in the eastern Mediterranean near the Israeli coast. *Oceanol. Acta*, **7**, 367–371.
- Berman, T., Y. Azov, A. Schellner, P. D. Walline and D. W. Townsend, 1986. Extent, transparency and phytoplankton distribution of the neritic waters overlying the Israeli coastal shelf. *Oceanol. Acta*, **9**, 439–447.
- Bethoux, J. P. .. Budgets of the Mediterranean Sea: their dependence on the local climate and on the characteristics of the Atlantic waters. *Oceanol. Acta*, **2**, 157–163, 1979.
- Bethoux, J. P., L. Prieur, and J. H. Bong, 1988. Le Courante Ligure au large de Nice. *Oceanol. Acta*, **9**, 59–67.
- Bolle, H.-J., 2003. *Mediterranean Climate. Variability and Trends*. Springer, 372 pp.
- Borzelli, G., G. Manzella, S. Marullo, R. Santoleri, 1999, Observation of coastal filaments in the Adriatic Sea. *J. Mar Sys.*, **20**, 187–203.
- Boukthir, M., and B. Barnier. Seasonal and inter-annual variations in the surface freshwater flux in the Mediterranean Sea from ECMWF re-analysis project. *Jour. Marine Systems*, **24**, 343–354, 2000.
- Bowles, F.A., Lambert, D.N. and Richardson, M.D., 1992. In: Max, M.D. and Colantoni, P. (Eds.), *Geological Development of the Sicilian-Tunisian Platform*. UNESCO Reports in Marine Science, Proceedings of International Scientific Meeting, Urbino University, Italy, Nov. 1992., pp. 129–134.

- Brankart, J.M., N. Pinardi, 2001. Abrupt cooling of the Mediterranean Levantine Intermediate Water at the beginning of the eighties: observational evidence and model simulation. *Journal of Physical Oceanography*, Vol. 31, No 8, Part 2, pages 2307–2320.
- Brenner, S., 2003. High-resolution nested model simulations of the climatological circulation in the southeastern Mediterranean Sea. *Annales Geophysicae*, 20: 267–280.
- Brink, K.,N., 1998. Deep-Sea Forcing and exchange processes. In: *The Sea Vol.10*, Brink, K.,N. and A.,R. Robinson (eds.), pg. 151–167, Wiley.
- Bryden, H. L., and T. H. Kinder, 1991. Recent progress in strait dynamics. *Rev. Geophys. (Suppl.)*, 617–631.
- Broche, P., J. L. Devenon, P. Forget, J. C. de Maistre, J. J. Naudin and G. Cauwet, 1998. Experimental study of the Rhone plume. Part I: physics and dynamics. *Oceanologica Acta*, 21(6), 725–738.
- Brunetti, M., M.Maugeri, T.Nanni and A.Navarra, 2000. Droughts and extreme events in regional daily Italian precipitation series. *Int. Jour. Clim.*,
- Buongiorno Nardelli, B., R. Santoleri, S. Marullo, D. Iudicone, and S. Zoffoli. 1999. Altimetric signal and three dimensional structure of the sea in the Channel of Sicily. *J. Geophys. Res.*, 104, C9, 20,585–20,603.
- Buscail, R., Pocklington, R., Dumas, R. and Guidi, L., 1990. Fluxes and budget of organic matter in the benthic boundary layer over the northwestern Mediterranean margin. *Continental Shelf Research*, 10, (9–11), 1089–1122.
- Buscail, R., Pocklington, R. and Germain, C., 1995. Seasonal variability of the organic matter in a sedimentary coastal environment: sources, degradation and accumulation (continental shelf of the Gulf of Lyon – northwestern Mediterranean Sea). *Continental Shelf Research*, 15, n° 7, 843–869.
- Buscail, R. and Germain, C., 1997. Present-day organic matter sedimentation on the NW Mediterranean margin: importance of off-shelf export. *Limnol. Oceanogr.*, 42, 217–229.
- Buscail, R., Foudil-Bouras, A.E. and Pauc, H., 1999. Matière organique et pollution par les hydrocarbures dans les sédiments superficiels du golfe d'Arzew (mer Méditerranée, Algérie). *Oceanologica Acta*, 22, 3, 303–317.
- Caddy, J. F. and P. Oliver, 1996. Some future perspectives for assessment and management of Mediterranean fisheries for demersal and shellfish resources, and small pelagic fish. *Stud. Rev. GFCM*, 66, 19–60.
- Caddy, J. F., 1999. Eléments pour l'aménagement des pêcheries méditerranéennes: unités géographiques et contrôle de l'effort. *Stud. Rev. GFCM*, 70, 1–30.
- Canfield, D.E., 1993. Organic matter oxidation in marine sediments. In: Wollast, R., Mackenzie, F.T., Chou, L. (Eds.), *Interactions of C, N, P and S Biogeochemical Cycles and Global Change*. NATO ASI Ser., 14, 333–363.
- Carter, T.G., Flanagan, J.P., Jones, C.R., Marchant, F.L., Murchison, R.R., Rebman, J.A., Sylvester, J.C. and Whitney, J.C., 1972. A new bathymetric chart and physiography of the Mediterranean Sea. In: *The Mediterranean Sea*, D.J. Stanley editor, Dowden, Hutchinson and Ross, Inc., Stroudsburg, Pennsylvania, 1–23.
- Castellari, S., N. Pinardi, and K.Leaman, 1998. A model study of air-sea interactions in the Mediterranean Sea. *Journal of Marine Systems*, 18, 89–114.
- Castellari, S., N. Pinardi, K. Leaman, 2000. Simulation of water mass formation processes in the Mediterranean Sea: influence of the time frequency of the atmospheric forcing. *Journal of Geophysical Research*, Vol. 105, C10, 24157–24181.
- Castellon, A., J. Salat and M. Masó, 1985. Some observations on Rhone river fresh water plume in the Catalan coast. *Rapp. Comm. int. Mer Médit.*, 29, 119–120.
- Caulet, J.P., 1972. Recent biogenic calcareous sedimentation on the Algerian continental shelf. In: *The Mediterranean Sea*, D.J. Stanley editor, Dowden, Hutchinson and Ross, Inc., Stroudsburg, Pennsylvania, 1–23.

- Charbonnier, D. and S. Garcia, 1985. Atlas of the fisheries of the western and central Mediterranean. FAO, Rome.
- Colantoni, P., Cremona, G., Ligi, M., Borsetti, A.M. and Cati, F., 1985. The Adventure Bank (off Southwestern Sicily): a present day example of carbonate shelf sedimentation. *Giornale di Geologia*, 47/1–2, 165–180.
- Conan, P., M. Pujo-Pay, P. Raimbault and M. Leveau, 1988a. Variabilité hydrologique et biologique du golfe du Lion. I. Transport en Azote et productivité potentielle. *Oceanologica Acta*, 21 (6) 751–765.
- Conan, P., M. Pujo-Pay, P. Raimbault and M. Leveau, 1988b. Variabilité hydrologique et biologique du golfe du Lion. II. Productivité sur le bord interne du courant. *Oceanologica Acta*, 21(6)767782.
- Coombs, S. H., O. Giovanardi, N. C. Halliday, G. Franceschini, D. V. P. Conway, L. Manzueto, C. D. Barrett and I. R. B. Mc Fadden, 2003. Wind mixing, food availability and mortality of anchovy larvae *Engraulis encrasicolus* in the northern Adriatic Sea. *Mar. Ecol. Prog. Ser.*, 248, 221–235.
- Courp, T. and Monaco, A., 1990. Sediment dispersal and accumulation on the continental margin of the Gulf of Lyon. Sedimentary budget. *Continental Shelf Research*, 10, (9–11), 1063–1087.
- Crispi, G. R. Mosetti, C. Solidoro, and A. Crise, 2001. Nutrient cycling in Mediterranean basin: the role of the biological pump in the trophic regime. *Ecological Modelling*, **138**, 101–114.
- Cruzado, A. and Z. R. Velasquez, 1990. Nutrients and phytoplankton in the Gulf of Lyon, northwestern Mediterranean. *Cont. Shelf Res.*, 10, 931–942
- Cushing, D. H., 1989. A difference in structure between ecosystems in strongly stratified waters and in those that are only weakly stratified. *J. Plankton, Res.*, 11, 1–13.
- Cushman-Roisin, B., M. Gacic, P. M. Poulain and A. Artegiani, 2001. Physical Oceanography of the Adriatic Sea. Kluwer Academic Publishers, Dordrecht, The Netherlands, 304 pp.
- Degobbi, D. and M. Gilmartin, 1990. Nitrogen, phosphorus and silicon budget for the northern Adriatic Sea. *Oceanol. Acta*, 13, 31–45.
- De Leiva, M., V. N. Agostini, J. F. Caddy and F. Carocci, 2000. Is the pelagic demersal ratio from fishery landings a useful proxy for nutrient availability? A preliminary data exploration for the semi-enclosed seas around Europe. *ICES J. Mar. Sci.*, 57, 1091–1102.
- Delfanti, R., Frignani, M., Langone, L., Papucci, C. and Ravaioli, M., 1994. The role of the rivers in Chernobyl radiocesium delivery, distribution and accumulation in coastal sediments of northern Adriatic Sea. Seminar on Freshwater Radioecology, Lisbon, March 21–255, 1994.
- Demirov, E. and N. Pinardi, 2002. The Simulation of the Mediterranean Sea circulation from 1979 to 1993. Part I: The interannual variability. *J. Marine Systems*, 33–34, pp. 23–50.
- Diaz, F., P. Raimbault, B. Boudjellal, N. Garcia and T. Moulin, 2001. Early spring phosphorus limitation of primary productivity in a NW Mediterranean coastal zone (Gulf of Lions). *Marine Ecol. Progr. Ser.*, 211, 51–62.
- Dowidar, N. M., 1984. Phytoplankton biomass and primary productivity of the south-eastern Mediterranean. *Deep Sea Res.*, 31, 983–1000.
- Drago, A. F., Sorgente, R., and Ribotti, A., 2003. A high resolution hydrodynamic 3-D model simulation of the Malta shelf area. *Annales Geophysicae*, 21: 323–344.
- Durrieu de Madron, X., Abassi, A., Heussner, S., Monaco, A., Aloisi, J.C., Radakovitch, O., Giresse, P., Buscail, R., and Kerherve, P., 2000. Particulate matter and organic carbon budgets for the Gulf of Lyon (NW Mediterranean). *Oceanologica Acta*, 23, 6, 717–730.
- Echevin, V., Crépon, M., and Mortier, L. Simulation and analysis of the mesoscale circulation in the northwestern Mediterranean Sea. *Annales Geophysicae*, 21: 281–297, 2003.
- Emery, K. O. and Neev, D., 1960. Mediterranean beaches of Israel. *Isr. Geol. Surv. Bull.*, 26, 1–23.
- Estrada, M. and J. Salat, 1989. Phytoplankton of deep and surface water layers in a Mediterranean frontal zone. *Sci. Mar.*, 52, 203–214.
- Estrada, M., 1996. Primary production in the northwestern Mediterranean, *Scientia Marina*, 60 (suppl.), 55–64.

- Fabricius, F. and Schmidt-Thomè, P., 1972. Contribution to recent sedimentation on the shelves of the Southern Adriatic, Ionian, and Syrtis Sea. In: *The Mediterranean Sea*, D.J. Stanley editor, Dowden, Hutchinson and Ross, Inc., Stroudsburg, Pennsylvania, 1–23.
- Faganeli, J., Pedzic, J., Ogorolec, B., Mistic, M. and Naialek, M., 1994. The origin of sedimentary organic matter in the Adriatic Sea. *Continental Shelf Research*, 14, 365–384.
- Flexas, M., Garcia, M. A., Durrieu de Madron, X., Canals, M., and Arnau, P., 2002. Flow variability in the Gulf of Lions during the MATER HFF experiment (March-May 1997). *J. Marine Systems*, 33/34, 197–214.
- Fonda Umani, S., 1996. Pelagic production and biomass in the Adriatic Sea. *Scientia Marina*, 60 (suppl.), 65–77.
- Fonda Umani, S. and A. Beran, 2003. Seasonal variations in the dynamics of microbial plankton communities: first estimates from experiments in the Gulf of Trieste, northern Adriatic Sea. *Mar. Ecol. Progr. Ser.*, 247, 1–16.
- Font, J.,E. Garcia-Ladona,E. Garcia-Gorritz, 1995. The seasonality of the mesoscale motion in the Northern Current of the western Mediterranean, *Oceanologica Acta*, 18, 207–219.
- Fredj G., Bellan-Santini D., Meinardi M., 1992. Etat des connaissances sur la faune marine méditerranéenne. Bulletin de l’Institut océanographique, Monaco, n° spécial 9:133–145.
- Frignani, M., Langone, L., and Ravaioli, M., 1987. Profili e bilancio di massa di ^{137}Cs e ^{210}Pb in alcune carote dell’Adriatico centrale. IV Congresso Nazionale SIRR – S. Teresa (SP), 15–16 September 1987, 17.
- Frignani, M., Langone, L., and Ravaioli, M., 1989. Interpretation of radionuclide activity-depth profiles in three sediment cores from the Middle Adriatic. *Giorn. Geol.*, 51/2, 131–142.
- Frignani, M., Langone, L., Ravaioli, M. and Cadonna, A., 1990. Sediment fluxes on a 100 yr time scale in different environments of the Adriatic Sea (Italy). XXXII Congress CIESM, Perpignan, 15–20 October, 1990.
- Frignani, M. and Langone, L., 1991. Accumulation rates and ^{137}Cs distribution in sediments off the Po River delta and the Emilia-Romagna coast (north-western Adriatic Sea, Italy). *Continental Shelf Research*, 11, 525–542.
- Frignani, M., Langone, L., Beks, J. and Alvisi, F., 1996. Sediment accumulation rates from cores collected in the central and southern Adriatic Sea. In: *Transfer pathways and fluxes of organic matter and related elements in water and sediments of the northern Adriatic Sea and the importance on the eastern Mediterranean Sea*. Final report EUROMARGE-AS Project, EU/MAST2-CT93–0052 Commission of the European Union, 148–156.
- Frihy, O.E., Debes, E.A. and El Sayed, W.R., 2003. Processes reshaping the Nile delta promontories of Egypt: pre- and post-protection. *Geomorphology*, 53, 263–279.
- Frogia, C., 1989. Clam fisheries with hydraulic dredges in the Adriatic Sea. In *Marine invertebrate fisheries: their assessment and management*, J. F. Caddy ed., John Wiley & Sons., New York, pp 507–524.
- Gacic, M., G. Civitarese, L. Ursella. 1999. Spatial and seasonal variability of water and biogeochemical fluxes in the Adriatic Sea. In: *The eastern Mediterranean as a Laboratory Basin for the Assessment of Contrasting Ecosystems*. 335–357, Kluwer.
- Gamulin, T. and J. Hure, 1955. Contribution à la connaissance de l’écologie de la sardine (*Sardina pilchardus* Walb.) dans l’Adriatique. *Acta Adriat.*, 7, 1–23.
- Garcia, A. and I. Palomera, 1996. Anchovy early life history and its relation to its surrounding environment in the Western Mediterranean basin. *Sci. Mar.*, 60 (supl.2), 155–166.
- Garcia Lafuente, J., A. Garcia, S. Mazzola, L. Quintanilla, J. Delgado, A. Cuttita and B. Patti, 2002. Hydrographic phenomena influencing early life stages of the Sicilian Channel anchovy. *Fish. Oceanogr.*, 11, 31–44.
- Garibaldi, L. and J. F. Caddy, 1998. Biogeographic characterization of Mediterranean and Black Sea faunal provinces using GIS procedures. *Ocean Coast. Manage.*, 39, 211–227.

- Garrett, C., Outerbridge, R., Thompson, K., 1993. Interannual variability in Mediterranean heat and buoyancy fluxes. *J. Climate* 6, 900–910.
- Gaudy, R. 1990. Zooplankton feeding on seston in the Rhône River plume area (NW Mediterranean Sea) in May 1988. *Hydrobiologia*, **207**, 241–249.
- Gensous, B., Williamson, D., and Tesson, M., 1993. Late Quaternary transgressive and highstand deposit of a shelf (Rhône delta, France). *Spec. Pub. Ass. Sedim.*, 18, 197–211.
- GFCM FAO Fishery Statistics Database. www.fao.org/fi/statist/statist.asp
- Giordani, P., Hammond, D.E., Bere lson, W.M., Montanari, G., Poletti, R., Milandri, A., Frignani, M., Langone, L., Ravaoli, M., Rovatti, G. and Rabbi, E., 1992. Benthic fluxes and nutrient budgets for sediments in the Northern Adriatic Sea: burial and recycling efficiencies. International Conference Marine Coastal Eutrophication, Bologna, 21–24 March. *The Science of the Total Environment*, Supplement 1992, 251–275.
- Giordani, P., Helder, W., Koning, E., Miserocchi, S., Danovaro, R. and Malaguti, A., 2002. Gradients of benthic-pelagic coupling and carbon budgets in the Adriatic and Northern Ionian Sea. *Journal of Marine System*, 33–34, 365–387.
- Golani D., 1996. The marine ichthyofauna of the eastern Levant-History, inventory, and characterization. *Israel Journal of Zoology*, 42 (1): 15–55.
- Goldman D., J. Caron and M. Dennett, 1987. Regulation of gross growth efficiency and ammonium regeneration in bacteria by substrate C:N ratio. *Limnol Oceanogr.*, 32, 1239–1252.
- Golik, A., 1997. Dynamics and management of sand along the Israeli coastline. *Bull. Instit. Oceanog., Monaco*, n° special 18-Transformation and Evolution of the Mediterranean Coastline, 97–110.
- Got, H. and Aloisi, J.C., 1990. The Holocene sedimentation on the Gulf of Lyon margin: a quantitative approach. *Continental Shelf Research*, 10, (9–11), 841–855.
- Grimes, C. B., 2001. Fishery production and the Mississippi river discharge. *Fisheries*, **26**, 17–26.
- Guerzoni, S., Ravaoli, M., Rovatti, G. and Suman, O.D., 1984. Comparison of 210Pb trace metals (Hg, Pb, Cu, Cr) profiles and river discharge in a core off the Po della Pila river mouth (Italy). *VIIes Journées Etud. Pollutions*, Lucerne, C.I.E.S.M ..
- Hachemi, M., 1996. Les ressources halieutiques de la Méditerranée sud centrale. *FAO Fish. Rep.*, **533** (suppl.), 191–229.
- Hamza, W., P.Ennet, R.Tamsalu and V.Zalensky, 2003. The 3D physical-biological model study in the Egyptian Mediterranean coastal area. *Aquatic Ecology*, (37), 307–324.
- Hecht, A., N.Pinardi, A.R.Robinson, 1988. Currents, Water Masses, Eddies and Jets in the Mediterranean Levantine Basin. *Journal of Physical Oceanography*, Vol. 18, No. 10, pp. 1320–1353.
- Herbaut, C., Mortier, L., and Crépon, M., 1996. A sensitivity study of the general circulation of the western Mediterranean Sea, Part. I: the response to density forcing through the straits, *Journal of Physical Oceanography* 26: 65–84.
- Herbaut, C., Codron, M., Crépon, M., 1998. Separation of a Kelvin front at the entrance of a strait. Example of the Strait of Sicily. *Journal of Physical Oceanography* 28 (7), 1346–1362.
- Herman, Y., 1972. Quaternary Eastern Mediterraneanan sediments: micropaleontology and climatic record. In: *The Mediterranean Sea*, D.J. Stanley editor, Dowden, Hutchinson and Ross, Inc., Stroudsburg, Pennsylvania, 1–23.
- Herut, B., A. Almog-Labin, N. Jannink and I. Gertman, 2000. The seasonal dynamics of nutrients and chlorophyll a concentrations on the SE Mediterranean shelf slope. *Oceanol. Acta*, **23**, 771–781.
- Hill, A.,E.,1998. Buoyancy effects in coastal and shelf seas. In: *The Sea Vol.10*, Brink, K.,N. and A.,R. Robinson (eds.), pg. 21–62, Wiley.
- Hopkins, T. S., 1985, *Physics of the Sea*. In: *Western Mediterranean* (R. Margalef Ed.), Pergamon Press, Oxford, 100–125.
- Hopkins, T.S., Artegiani, A., Bignami, F. and Russo, A., 1999. Watermass modification in the Northern Adriatic. A preliminary assessment from the ELNA data set. In: Hopkins, T.S., Artegiani, A., Cau-

- wet, G., degobbi, D., Malej, A. (Eds.), Ecosystem Res. Report n. 32. The Adriatic Sea (EUR 18834). European Commission Directorate-General for Research, Brussel, 3–23.
- Ignatiades, L., S. Psarra, V. Zervakis, K. Pagou, E. Souvermezoglou, G. Assimakopoulou and O. Gotsis-Cretas, 2002. Phytoplankton size-based dynamics in the Aegean Sea (eastern Mediterranean). *J. Mar. Sys.*, 36, 11–28.
- Jago, C.F. and Barusseau, J.P., 1981. Sediment entrainment on a wave-graded shelf, Roussillon, France. *Marine Geology*, 42, 279–299.
- Josey, Simon A., 2003. Changes in the heat and freshwater forcing of the eastern Mediterranean and their influence on deep water formation. *Journal of Geophysical Research*, Vol. 108, No. C7, 3237, doi:10.1029/2003JC001778.
- Korres, G., N. Pinardi, A. Lascaratos, 2000. The ocean response to low frequency interannual atmospheric variability in the Mediterranean Sea. Part I: Sensitivity experiments and energy analysis. *Journal of Climate*, Vol. 13, No. 4, 705–731.
- Korres, G., N. Pinardi, A. Lascaratos, 2000. The ocean response to low frequency interannual atmospheric variability in the Mediterranean sea. Part II: Empirical Orthogonal Functions Analysis. *Journal of Climate*, Vol. 13, No. 4, 732–745.
- Korres, G., and A. Lascaratos, 2003. A one-way nested eddy resolving model of the Aegean and Levantine basins: implementation and climatological runs. *Annales Geophysicae*, 21: 205–220.
- Krom, M. D., N. Kress, S. Brenner and L. I. Gordon, 1991. Phosphorus limitation of primary productivity in the eastern Mediterranean Sea. *Limnol. Oceanogr.*, 36, 424–432.
- Lefèvre, D., H. J. Minas, M. Minas, C. Robinson, P. J. Le B. Williams and E. M. S. Woodward., 1997. Review of gross community production, primary production, net community production and dark community respiration in the Gulf of Lions. *Deep Sea Res. II*, 44, 801–832.
- Legendre, L. and F. Rassoulzadegan, 1995. Plankton and nutrient dynamics in marine waters. *Sarsia*, 41, 153–172.
- Lermusiaux, P.F.J., A. R. Robinson, 2001. Features of dominant mesoscale variability, circulation patterns and dynamics in the Strait of Sicily. *Deep Sea Res.*, I, 48, 1953–1997.
- Levi, D. and J. P. Troadec, 1974. The fish resources of the Mediterranean and the Black Sea. *Stud. Rev. GFCM*, 54, 29–52.
- Liu, K.K., K. Iseki and S.Y. Chao, 2000. Continental margin carbon fluxes. In: *The Changing Ocean Carbon Cycle*, R.B. Hanson, H.W. Ducklow, & J.G. Field (Eds), pp. 187–239. Cambridge: Cambridge University Press.
- Leonart J. and Recasens L., 1996. Fisheries and the environment in the Mediterranean Sea. *Studies and Reviews GFCM*, 66: 5–18.
- Lloret J., Leonart J., Sole I., Fromentin J., 2001. Fluctuations of landings and environmental conditions in the north-western Mediterranean Sea. *Fisheries Oceanography*, 10 (1): 33–50.
- Leonart, J. and L. Recasens, 1996. Fisheries and the environment in the Mediterranean Sea. *Stud. Rev. GFCM*, 66, 5–18.
- Lloret, J., I. Palomera, J. Salat and I. Sole, 2004. Impact of freshwater input and wind on landings of anchovy (*Engraulis encrasicolus*) and sardine (*Sardina pilchardus*) in shelf waters surrounding the Ebro (Ebro) River delta (north-western Mediterranean). *Fish. Oceanogr.*, 13, 1–9.
- Madec, G., Chartier, M., and Crépon, M., 1991. The effect of thermohaline forcing variability on deep water formation in the western Mediterranean Sea: a high-resolution three-dimensional numerical study, *Dynamics of the Atmosphere and Oceans*, 301–332.
- Manca B., Budillon G., Scarazzato P. and Orsella L., 2003. Evolution of dynamics in the Eastern Mediterranean affecting water mass structures and properties in the Ionian and Adriatic Seas. *Jour. Geophys. Res.*, 108, C9, 101029 – 101046.
- Manzella, G. M. R., Gasparini, G. P., and Astraldi, M., 1988. Water exchange between the eastern and western Mediterranean through the Strait of Sicily, *Deep-Sea Res.* I, 35, 1021–1035.

- Manzella, G., 1992. 'La dinamica degli oceani', pg. 160. Nuova ERI.
- Maouche, S., 1987. Mécanismes hydrosédimentaires en baie d'Alger (Algérie): approche sédimentologique, géochimique et traitement statistiques, thèse de 3e cycle, univ. Perpignan, 214 p.
- Mariotti, A., M.V. Struglia, N. Zeng, K.-M. Lau, 2002. The Hydrological Cycle in the Mediterranean Region and Implications for the Water Budget of the Mediterranean Sea. American Meteorological Society, Journal of Climate, vol. 15: 1674–1690.
- Maurin, C., 1977. Les problème halieutiques en Méditerranée et en Tunisie. *Bull. Off. natn. Pêch. Tunisie*, **1**, 9–16.
- Max, M.D. and Colantoni, P., 1992. Introduction: geomorphological position and geology of the Sicilian-Tunisian Platform. In: Max, M.D. and Colantoni, P. (Eds.), Geological Development of the Sicilian-Tunisian Platform. UNESCO Reports in Marine Science, Proceedings of International Scientific Meeting, Urbino University, Italy, Nov. 1992., pp. 1–2.
- Mc Gill, D. A., 1969. A budget for dissolved nutrient salts in the Mediterranean Sea. *Câh. Océanogr.*, **21**, 543–554.
- MEDAR Group, 2002. Mediterranean and Black Sea database of temperature, salinity and biochemical parameters and climatological atlas 4 CD-ROM and www.ifremer.fr/sismer/program/medar/. European Commission Marine Science and Technology Programme (MAST). Ed. IFREMER.
- Millot, C., 1985. Some features of the Algerian Current. *J. Geophys. Res.*, **90**, 7169–7176.
- Millot C., 1987. Circulation in the Western Mediterranean. *Oceanol. Acta*, **10**, 2: 143–149.
- Millot, C., 1990a. The Gulf of Lions Hydrodynamics. *Continental Shelf Research*, **10**, 9/11, 885–894.
- Millot, C., I. Taupier Letage and I. Benzohra. 1990b. The Algerian eddies. *Earth Sci. Rev.*, **27**, 203–219.
- Millot C., M. Benzohra, I. Taupier-Letage, 1997. Circulation in the Algerian Basin inferred from the MEDIPROD-5 current meters data. *Deep-Sea Res.*, **44**: 1467–1495.
- Minas, M and H. J. Minas, 1991. Hydrological and chemical conditions in the Gulf of Lions and relationships to primary production encountered during CYBELE (First Leg, 12–29 April 1990). *Water Pollution Research Reports*, **28**, 131–144.
- Molcard A., N. Pinardi, M. Iskandarani and D.B. Haidvogel, 2002. Wind driven general circulation of the Mediterranean Sea simulated with a Spectral Element Ocean Model. *Dynamics of Atmospheres and Oceans*, Vol. 35, pp. 97–130.
- Monoley, C.L. and Field, J.G., 1991. Modelling carbon and nitrogen flows in a microbial plankton community. In: Protozoa and their role in marine processes, Springer, P.C. Reid et al editor, 443–474.
- Moran, X. A. G., I. Taupier-Letage, E. Vázquez-Domínguez, R. Ruiz, L. Arin, P. Raimbault and M. Estrada, 2001. Physical-Biological coupling in the Algerian Basin (SW Mediterranean) : Influence of mesoscale instabilities on the biomass and the production of phytoplankton and bacterioplankton. *Deep Sea Res. I*, **48**, 405–437.
- Morel, A and J. M. André, 1991. Pigment distribution and primary production in the Western Mediterranean Sea as derived and modeled from coastal Zone color scanner observations. *J. Geophys. Res.*, **96**(C7), 12685–12698.
- Moutin, T., P. Raimbault, H. L. Golterman and B. Coste, 1998. The input of nutrients by the Rhône river into the Mediterranean Sea: recent observations and comparison with earlier data. *Hydrobiologia*, **373/374**, 237–246.
- Müller, P.J. and Suess, E., 1979. Productivity, sedimentation rate and sedimentary carbon content in the oceans, organic carbon preservation. *Deep-Sea Research*, **26A**, 1347–1362.
- Myers, R. A. and B. Worm, 2003. Rapid worldwide depletion of predatory fish communities. *Nature*, **423**, 280–283.
- Naudin, J. J., G. Cauwet., C. Fajon, L. Oriol, S Terzić J. L. Devenon and P. Broche, 2001. Effect of mixing of microbial communities in the Rhône river Plume. *J. Mar. Sys.*, **28**, 203–227.
- Nittrouer, C.A. and Wright, L.D., 1994. Transport of particles across continental shelves. *Rev. Geophys.*, **32**, 85–113.

- Olivar, M. P., J. Salat and I. Palomera, 2001. Comparative study of spatial distribution patterns of the early stages of anchovy and pilchard in the NW Mediterranean Sea. *Mar. Ecol. Prog. Ser.*, 217, 111–120.
- Owens, N. J. P., A. P. Rees, E. M. S. Woodward and R. F. C. Mantoura, 1989. Size-fractionated primary production and nitrogen assimilation in the north-western Mediterranean Sea during January 1989. *Water Pollution Res. Rep.*, **13**, 126–135.
- Palomera, I., 1992. Spawning of anchovy *Engraulis encrasicolus* in Northwestern Mediterranean relative to hydrographic feature in the region. *Mar. Ecol. Prog. Ser.*, 79, 215–223.
- Papacostantinou C. and Farrugio H., 2000. Fisheries in the Mediterranean. *Mediterranean Marine Science*, 1/1: 5–18.
- Paschini, E., A. Artegiani and N. Pinardi, 1993. The mesoscale eddy field of the middle Adriatic Sea. *Deep Sea Research I*, Vol. 40, No. 7, pp 1365–1377.
- Pauc, H., 1991. La nature minéralogique des apports en suspensions sur la marge algérienne et leur relation avec les sédiments. Actes du 3e Congrès français de sédimentologie, Brest 18–20 novembre 1991, 225–226.
- Pauly, D., V. Christensen, J. Dalsgaard, R. Froese and Jr. F. Torres, 1998. Fishing Down Marine Food Webs. *Science*, 279, 860–863.
- Pedlosky, J., 1987. *Geophysical Fluid Dynamics*. Springer-Verlag, pp. 724,.
- Peixoto, J. P., M. De Almeida, R. D. Rosen, and D. A. Salstein, 1982: Atmospheric moisture transport and the water balance of the Mediterranean Sea. *Water Resour. Res.*, 18, 83–90.
- Phillips, N.A., 1954. Energy transformations and meridional circulations associated with simple baroclinic waves in a two-level quasi-geostrophic model. *Tellus*, 6 273–286.
- Pinardi, N., A. Navarra, 1993. Baroclinic wind adjustment processes in the Mediterranean Sea. *Deep Sea Research II*, Vol. 40, No. 6, 1299–1326.
- Pinardi, N., and E. Masetti, 2000. Variability of the large scale general circulation of the Mediterranean Sea from observations and modelling: a review. *Palaeogeography, palaeoclimatology, palaeoecology*, 158 (2000) 153–173.
- Pinardi, N., I. Allen, E. Demirov, P. De Mey, G. Korres, A. Lascaratos, P.-Y. Le Traon, C. Maillard, G. Manzella, C. Tziavos. The Mediterranean ocean Forecasting System: first phase of implementation (1998–2001). *Annales Geophysicae*, 21: 3–20, 2003.
- The POEM Group. General circulation of the Eastern Mediterranean. *Earth Sciences Review*, 32, pp 285–309, 1992.
- Pomerancblum, M., 1966. The distribution of heavy minerals and hydraulic equivalents in sediments of the Mediterranean continental shelf of Israel. *J. Sediment. Petrol.*, 36, 162–174.
- Poulain, P.-M., 2001. Adriatic Sea surface currents as derived from drifter data between 1990 and 1999. *J. Mar. Syst.*, 29, 3–32.
- Poulain, P.-M., E. Mauri and L. Ursella, 2003 Unusual upwelling event and current reversal off the Italian Adriatic coast in summer, submitted.
- Puddu, A., R. La Ferla, A. Allegra, C. Bacci, M. Lopez, F. Oliva and C. Pienotti, 1998. Seasonal and spatial distribution of bacterial production and biomass along a salinity gradient (northern Adriatic Sea). *Hydrobiologia*, 363, 271–282.
- Pullen, J., J. D. Doyle, R. H. A. Ogston, J. W. Book, H. Perkins, and R. Signell. Coupled ocean-atmosphere nested modeling of the Adriatic Sea during winter and spring 2001. *J. Geophys. Res.*, 108, C10, 3320, doi:10.1029/2003JC001780, 2003
- Raichich, F., 1996. On the fresh water balance of the Adriatic Sea. *J. Mar. Sys.*, 9, 305–319.
- Raichich, F., N. Pinardi, A. Navarra, 2003. Teleconnections between Indian Monsoon and Sahel rainfall and the Mediterranean. *Int. Jour. of Clim.*, 23, 173–186.
- Rasoanarivo, R., J. Folack, G. Champalbert and B. Becker, 1991. Relations entre les communautés phytoplactonique et l'alimentation des larves de *Sardina pilchardus* Walb. Dans le golfe de Fos (Mé-

- diterranée occidentale): influence de la lumière sur l'activité alimentaires des larves. *J. Exp. Mar. Biol. Ecol.*, 151, 83–92.
- Redfield, A., B. Ketchum and F. Richards, 1963. The influence of organisms on the composition of sea water. In: *The Sea* (M. Hill Ed.), Vol 1, 26–77. Interscience New York
- Regner, S., D. Regner, I. Marasović and F. Kršinić, 1987. Spawning of sardine, *Sardina pilchardus* (Walbaum, 1792), in the Adriatic under upwelling conditions. *Acta Adriat.*, 28, 161–198.
- Regner, S., G. Piccinetti-Manfrin and C. Piccinetti, 1988. The spawning of the sardine (*Sardina pilchardus* Walb.) in the Adriatic as related to the distribution of temperature. *FAO Fish. Rep.*, 394, 127–132.
- Regner, S., 1996. Effects of environmental changes on early stages and reproduction of anchovy in the Adriatic sea. *Sci. Mar.*, 60 (Supl.2), 167–177.
- Robinson, A.R., A. Hecht, N. Pinardi, Y. Bishop, W.G. Leslie, Z. Rosentroub, A.J. Mariano, S. Brenner, 1987. Small synoptic/mesoscale eddies: the energetic variability of the Eastern Levantine basin. *Nature*, Vol. 327, No. 6118, pp. 131–134.
- Robinson, A.R., Golnaraghi, M., Leslie, W.G., Artegiani, A., Hecht, A., Lazzone, E., Michelato, A., Sansone, E., Theocharis, A., Unluata, G. The eastern Mediterranean general circulation: Features, structure and variability. *Dynamics of Atmospheres and Oceans* 15 (3–5), pp. 215–240, 1991.
- Robinson, A.R. Physical processes, field estimation and an approach to interdisciplinary ocean modeling. *Earth Science Reviews*, 40, 3–54, 1996.
- Robinson, A.R., Sellschopp, J., Warn-Varnas, A., Anderson, L.A. and Lermusiaux, P.F.J.: The Atlantic Ionian Stream, *J. Marine Systems*, 20, 129–156, 1999.
- Roether, W., B.B. Manca, B. Klein, D. Bregant, D. Georgopoulos, V. Beitzel, V. Kovacevic and A. Lucchetto. 1996. Recent changes in eastern Mediterranean deep waters. *Science*, 271, 333–335.
- Ross, D.A. and Uchupi, E., 1977. Structure and sedimentary history of southeastern Mediterranean Sea-Nile Cone area. *AAPG Bull.*, 61, 872–902.
- Rossignol, M., 1969. Sedimentation palynologique dans le domaine marine quaternaire de Palestine. *Notes mem. Moyen-Orient.*, 10, 1–272.
- Roussenov, V. E. Stanev, V. Artale and N. Pinardi, 1995. A seasonal model of the Mediterranean Sea. *Journal of Geophysical Research*, Vol. 100, C7, 13515–13538.
- Sabates, A., 1990. Distribution pattern of larval fish populations in the Northwestern Mediterranean. *Mar. Ecol. Prog. Ser.*, 59, 75–82.
- Sabates, A., J. Salat and M. P. Olivar, 2001. Advection of continental water as an export mechanism for anchovy, *Engraulis encrasicolus*, larvae. *Sci. Mar.*, 65 (Supl.1), 77–87.
- Sammari, C., Millot, C., Taupier-Letage, I., Stefani, A., Brahim, M., 1999. *Deep-Sea Research I* 46: 1671–1703.
- Sánchez-Arcilla, A., J.H. Simpson, 2002. The narrow shelf concept: couplings and fluxes. *Continental Shelf Research*, 22, 153–172.
- Sandler, A. and Herut, B., 2000. Composition of clays along the continental shelf off Israel: contribution of the Nile versus local sources. *Marine Geology*, 167, 339–354.
- Sassi, R., Souissi, F., Soussi, N., Boukaaba, M. and Belayouni, H., 1998. Organic matter geochemistry to analyse the degradation of the Monastir-Ksibet el Mediouni littoral (Eastern Tunisia) [French]. *Comptes Rendus de l'Académie des Sciences Serie II Fascicule A-Sciences de la Terre et des Planètes*, 327, 303–308.
- Seritti, A., B.B. Manca, C. Santinelli, E. Murru, A. Boldrin, L. Nannicini. 2003. Relationships between dissolved organic carbon (DOC) and water mass structure in the Ionian Sea (winter 1999). *J. Geophys. Res.*, 108(C9), 8112, PBE13.1–13.
- Sharaf El Din, S. H., 1977. Effect of the Aswan high dam on the Nile flood and on the Estuarine and coastal circulation pattern along the Mediterranean Egyptian coast. *Limnol. Oceanogr.*, 22, 194–207.
- Simpson, J.H., 1997. Physical processes in the ROFI regime. *J. Mar. Syst.*, 12, 3–15.

- Smith, S.V. and F. T. Mackenzie., 1987. The ocean as a net heterotrophic system: Implications from the carbon biogeochemical cycle, *Global Biogeochemical Cycles*, 1, 187–198.
- Sorgente, D., Frignani, M., Langone, L. and Ravaoli, M., 1996. 210Pb e 137Cs in sedimenti dell'Adriatico centrale come indicatori dei processi attuali di sedimentazione e accumulo. *Plinius-Supp. Italiano all'European Journal of mineralogy*, 16, 200–201.
- Sorgente D., Frignani, M., Albertazzi, S., Giuliani, S., Ravaoli, M., Langone, L. and Alvisi, F., 2002. 137Cs and 210Pb sediment accumulation in the central Adriatic Sea. *Atti del Convegno "La radioattività nel contesto degli studi ambientali"* Isola del Giglio, 9–10 luglio 2002, pp. 221–228.
- Sorgente, R., Drago A.F., and Ribotti, A., 2003. Seasonal variabilità in the Central Mediterranean Sea circulation. *Annales Geophysicae*, 21: 299–322.
- Sournia, A., 1973. La production primaire en Méditerranée: Essai de mise à jour. *Bulletin de l'étude en commun de la Méditerranée*, 5.
- Stanley, D.J., Mart, Y. and Nir, Y., 1997. Clay mineral distributions to interpret Nile Cell provenance and dispersal: II. Coastal plain from Nile delta to northern Israel. *J. Coast. Res.*, 13, 506–533.
- Stanley, Nir, Y. and Galili, E., 1998. Clay mineral distributions to interpret Nile Cell provenance and dispersal: III. Nile delta shelf to northern Israeli margin. *J. Coast. Res.*, 14, 196–217.
- Struglia, M.V., A.Mariotti, A. Filograsso, 2004. River discharge into the Mediterranean Sea: climatology and aspects of the observed variability. Submitted to *J.Climate*.
- Supić, N., M. Orlić and D. Degobbis, 2000. Istrian coastal countercurrent and its year to year variability. *Est. Coast. Shelf Sci.*, 51, 385–397.
- Tanaka, T. and F. Rassoulzadegan, 2002. Full depth profile of bacteria, heterotrophic nanoflagellates and ciliates in the NW Mediterranean Sea: Vertical partitioning of microbial trophic structures. *Deep Sea Res. II*, 49, 2093–2107.
- Theocharis, A., M.Gacic and H. Kontoyiannis, 1998. Physical and dynamical processes in the coastal and shelf areas of the Mediterranean. In: *The Sea*, Vol. 10, 863–888.
- Thingstad, T. F. and F. Rassoulzadegan, 1995. Nutrient limitations, microbial food web and "biological C-pumps": suggested interactions in a P-limited Mediterranean. *Marine Ecology Progress Series*, 117, 299–306.
- Thingstad, T. F., Å Hagström, and F. Rassoulzadegan, 1997. Accumulation of degradable DOC in surface waters: caused by a "malfunctioning" microbial loop?. *Limnol. Oceanogr.*, 42, 389–404.
- Thingstad, T. F., U. L. Zweifel and F. Rassoulzadegan, 1998. P-limitation of both phytoplankton and heterotrophic bacteria in NW Mediterranean summer surface waters. *Limnol. Oceanogr.*, 43, 89–94.
- Thingstad, T. F. and F. Rassoulzadegan, 1999. Conceptual models for the biogeochemical role of the photic zone microbial food web with particular reference to the Mediterranean Sea. *Progress in Oceanography*, 44, 271–286.
- Tonarelli, B., Turgutcan, F., Max, M.D. and Akal, T., 1992. Shallow sediment composition at four localities on the Sicilian-Tunisian Platform. In: Max, M.D. and Colantoni, P. (Eds.), *Geological Development of the Sicilian-Tunisian Platform*. UNESCO Reports in Marine Science, Proceedings of International Scientific Meeting, Urbino University, Italy, Nov. 1992., pp. 123–128.
- Travers, A. and M. Travers, 1972. Données sur quelque facteur de l'écologie du plancton dans la région de Marseille. 1: Les Vents. *Tethys*, 4, 3–26.
- Tsunogai, S., S. Watanabe, and T. Sato, 1999. Is there a "continental shelf pump" for the absorption of atmospheric CO₂? *Tellus. Ser. B*, 701–712.
- Tudela, S. and I. Palomera, 1995. Microzooplankton and feeding of anchovy larvae in the northwestern Mediterranean. *Rapp. Comm. Int. Mer Médit.*, 34, 259.
- Turley, C. M., M. Bianchi, U. Christaki, P. Conan, J. R. W. Harris, S. Psarra, G. Ruddy, E. D. Stutt., A. Tselepidis and F. Van Wambeke, 2000. Relationship between primary producers and bacteria in an oligotrophic sea – the Mediterranean and biogeochemical implications. *Marine Ecology Progress Series*, 193, 11–18.

- Vichi M., P. Oddo, M. Zavatarelli, A. Coluccelli, G. Coppini, M. Celio, S. Fonda Umani, N. Pinardi, 2003. Calibration and validation of a one-dimensional complex marine biogeochemical flux model in different areas of the northern Adriatic shelf. *Annales Geophysicae*, 21: 413–436.
- Videau, C. and M. Leveau, 1990. Phytoplanktonic biomass and productivity in the Rhône River plume in the spring time. *Compte Rendue Acad. Sci. Paris*, 311(serie III), 219–224.
- Vollenweider, R. A., A. Rinaldi and G. Montanari, 1992. Eutrophication, structure and dynamics of a marine coastal system: results of a ten-year monitoring along the Emilia Romagna coast (North-western Adriatic Sea). *Sci. Tot. Env.*, suppl., 63–106.
- Yoro, S. C., R. Sempère, C. Turley, M. A. Unante, X. Durrieu de Madron and M. Bianchi, 1997. Cross-slope variations of Organic Carbon and Bacteria in the Gulf of Lions in relation to water dynamics (northwestern Mediterranean). *Marine Ecology Progress Series*, 161, 255–264.
- Wadie, W. F., 1982. Observations on the catch of the most important fishes along the Egyptian continental shelf in the South Eastern part of the Mediterranean Sea. *Bull. Inst. Oceanogr. Fish.*, 8, 212–227.
- Wadie, W. F. and F. A. Abdel Razek, 1985. The effect of damming on the shrimp population in the south-eastern part of the Mediterranean sea. *Fish. Res.*, 3, 323–335.
- Wang, X.H. and N. Pinardi, 2002. Modelling the Dynamics of Sediment Transport in the Northern Adriatic Sea. *Journal of Geophysical Research*, vol. 107, N0 C12, 3225 (pp. 23).
- Wassef, E., A. Ezzat, T. Hashem and S. Faltas, 1985. Sardine fishery by purse-seine on the Egyptian Mediterranean coast. *Mar. Ecol. Prog. Ser.*, 26, 11–18.
- Woodward, E. M. S., N. J. P. Owens, A. P. Rees and C. S. Law, 1990. A seasonal survey of nutrient cycling and primary productivity in the Gulf of Lions during 1988 and 1989. *Water Pollution Res. Rep.*, 13, 79–86.
- Zavatarelli, M., F. Raicich, D. Bregant, A. Russo and A. Artegiani, 1998. Climatological biogeochemical characteristics of the Adriatic Sea. *J. Mar. Sys.*, 18, 227–263.
- Zavatarelli, M., Baretta, J.W., Baretta-Bekker, J.G., N. Pinardi, 2000. The Dynamics of the Adriatic Sea ecosystem. Part I: an idealised model study. *Deep Sea Research*, Vol.47, 937–970.
- Zavatarelli, M., N. Pinardi, V.H. Kourafalou, A. Maggiore, 2002. Diagnostic and prognostic model studies of the Adriatic Sea general circulation. Part 1: The seasonal variability. *Journal of Geophysical Research*, vol. 107, (C1): art. n. 3004.
- Zavatarelli M. and N. Pinardi, 2003. The Adriatic Sea modelling system: a nested approach. *Annales Geophysicae*, 21: 345–364.
- Zohary, U. L., and R. D. Robarts, 1998. Experimental study of microbial P limitation in the eastern Mediterranean. *Limnol. Oceanogr.*, 43, 387–395.
- Zuo, Z., Eisma, D., and Berger, G.W., 1991. Determination of sediment accumulation and mixing rates in the Gulf of Lyon, Mediterranean Sea. *Oceanologica Acta*, 14, 253–262.
- Zuo, Z., Eisma, D., Gieles, R. and Beks, J., 1997. Accumulation rates and sediment deposition in the northwestern Mediterranean. *Deep-Sea Research II*, 44, n° 3–4, 597–609.